History of the Black Sea recorded in stalagmites from Northern Turkey

Master's Thesis

Faculty of Science

University of Bern

presented by

Angela Zumbühl

2010

Supervisor:

Prof. Dr. Dominik Fleitmann
Institute of Geological Sciences, University of Bern
and
Oeschger Centre for Climate Change Research

Co-Supervisor:

Prof. Dr. Markus Leuenberger
Physics Institute, University of Bern
and
Oeschger Centre for Climate Change Research

ABSTRACT

Reconstruction of the ancient Black Sea climate is mandatory to predict future climate in this region. However, terrestrial climate proxies covering the last interglacial are very rare in the Black Sea region. In addition during the last few hundred thousand years the hydrologic history of the Black Sea is marked by changes between lake and sea phases. However, this history is only reconstructed back to 30 ka BP by other scientists (Aksu et al., 2002a/b, Kaminski et al., 2002, Bahr et al., 2006, etc). Longer records (e.g., Zubakov, 1988) are not well dated and coarsely resolved. Overall, a distinct lack of terrestrial high-quality records exists in the entire Black Sea region and northern Eastern Mediterranean.

Stalagmites from Sofular Cave at the southern rim of the Black Sea (northern Turkey) capture the oxygen isotopic signature of the Black Sea surface waters and are thus well suited for reconstructing of the Black Sea history (Fleitmann et al., 2009). Furthermore, the isotopic records also allow a reconstruction ancient climate.

The oxygen ($\delta^{18}O$) and carbon ($\delta^{13}C$) isotope profiles of stalagmite So-17A cover the period from ~122.25 ka BP to ~86.190 ka BP and is absolutely dated by 13 U-Th ages. The So-17A record fits into a composite isotopic record of Sofular cave which has already been built up by the group of Prof. Dr. Dominik Fleitmann at the Institute of Geological Sciences at the University of Bern.

With this thesis, a new period of the Black Sea history is revealed. Additionally, the MIS 5e and MIS 5d-b climate can be reconstructed and compared to the already existing climate records from the eastern Mediterranean region.

The results indicate that the MIS 5e climate was warm, moist and relatively stable in the eastern Mediterranean region. However, in comparison with the MIS 1 (Fankhauser et al., 2008), the MIS 5e record indicates higher temperatures and lower amounts of precipitation. In contrast to the MIS 5e, the MIS 5d-a showed more climate variability, with changes between stadial and interstadial conditions and some additional cooling events.

The So-17A isotopic record reveals two periods of sea phase and one period of lake phase in the MIS 5e-b Black Sea history. The sea level fell below the Bosphorus sill (~-35m) about 109.5 ka BP, the two-layer connection between the Mediterranean and the Black Sea was then re-established at an age of 107.5 ka BP. Sea level rises were mainly produced by melt waters and thermal expansion of warming waters (Clark and Huybers, 2009). The final disconnection recorded by stalagmite So-17A happened about 88 ka BP and preceded the MIS 5b. The sea level drops are mainly induced by the building up of ice sheets (Mangerud et al., 1991). As a whole, it can be confirmed that the high-amplitude changes of the isotopes are mainly

produced by the Black sea surface waters, whereas the low-amplitude changes are provoked by temperature or precipitation changes (Fleitmann et al., 2009).

LIST OF CONTENTS

LIST OF FIGURES

LIST OF TABLES

1 CHAPTER ONE – INTRODUCTION

1.1 INTRODUCTION & AIM OF THE PROJECT

The MIS 5e (128-115 ka BP) is the last interglacial preceding the MIS 1 (since 11.7 ka BP; Imbrie et al. 1984). In the current discussion about climate change, it is important to have a look at the conditions during the MIS 5e. The comparison of the MIS 5e and the MIS 1 enables to reveal differences and their possible causes. Moreover, there are controversial discussions on climate variability during the MIS 5e and the MIS 5d-a. For example, some studies claimed that the MIS 5e climate was relatively stable and uninterrupted (Menke and Tynni, 1984; Frenzel, 1991). Some other studies suggested the occurrence of several cold and warm events in the course of the MIS 5 (GRIP members, 1993; Cheddadi et al., 1998; Field et al., 1994; Chapman and Shackleton, 1999 and Boettger et al., 2007; Litt et al., 1996). These inconsistencies occur mainly due to a lack of well dated and highly resolved records covering this time period.

In addition, the stalagmite records of Sofular cave lying at the southern rim of the Black Sea, provide insights into the Black Sea history, which has been conversely discussed in the last few years (Aksu et al., 1999/2002a, Kaminski et al., 2002; Bahr et al., 2006/2008; Major et al., 2002, Ryan et al., 1997/2003). The Black Sea history has mainly been studied back to 30ka BP. The group of Dr. Prof. Dominik Fleitmann built up a climatic record by studying stalagmites from Sofular Caves back to 600 ka BP. However, some temporal gaps prevented the development of a continuous time series. New stalagmites were collected in November 2008 in order to fill some of these temporal gaps. The stalagmite So-17 covers the time period from about 122.96 ka BP to 86.19 ka BP.

First, this period allows reconstructing the climate within the MIS 5, by constructing high-resolution oxygen ($\delta^{18}O$) and carbon ($\delta^{13}C$) isotope records. This opens also the possibility to compare these MIS 5e isotopic records with MIS 1 isotopic profile. Secondly, the stalagmite So-17A is able to fill some temporal gaps within the Black Sea history (Fig. 5.1.). Thirdly, the climate variability of the MIS 5 will be the last subject of this master thesis. The isotopic record of the stalagmite So-17A will show whether climate during the MIS 5 was relatively stable or quite variable. To achieve these objectives a good age-depth model and high temporal resolution are mandatory.

1.2 SPELEOTHEMS

Speleothems are secondary cave deposits formed of calcium carbonate (Hill and Forti, 1997). The word speleothem is made up of two words originating from the Greek language. The term includes two words, ‘Spelaion’ meaning cave and ‘thema’ standing for deposit (Hill and Forti, 1997). The term was established by an American speleologist G. Moore in 1954 (Moore, 1954).

Caves with speleothems are often located below karstic systems consisting of soluble rock (in the majority of cases carbonate bedrock). The downward percolating meteoric water dissolves the host rock and within the cave, the precipitated calcite carbonate accumulates in form of speleothems (Schwarcz, 2007).

Changes in the conditions within the cave or at the Earth surface can lead to alternations in the deposition of stalagmites. The changes in the deposition can be used to reconstruct the ancient environmental conditions (Schwarcz, 2007). The recognition of changes results from the study of growth rates, isotopic composition of the calcium carbonate, fluid inclusions, concentrations of trace elements and mineralogy (Schwarcz, 2007). Speleothems are an appropriate terrestrial alternative to marine sediment cores, ice cores and pollen profiles. In general, caves are extremely stable environments and therefore a good tool to reconstruct the past climate changes (Poulson and White, 1969).

Three principal types of speleothems are used for paleoclimatic research. The three principal types of speleothems are flowstones, stalactites and stalagmites. Flowstones are laminar deposits on the grounds or the walls of caves. The deposit stratigraphy displays the variation of discharge during the previous thousands of years. Stalactites are conical dripstones growing from the ceilings of caves. The internal layering of stalactites is parallel to their surface. Stalagmites are dripstones growing upwards from the cave grounds. The growth of stalagmites depends on the water flow rate, the water supersaturation and the drop fall height. Most scientists with their interest in paleoclimate focus on the analysis of stalagmites (Fairchild et al., 2006a).

2 CHAPTER TWO – STUDY SITE

2.1 GENERAL SETTING OF THE SOFULAR CAVE

The Sofular cave (41°25'N and 31°56'E) lies at the southern rim of the Black Sea at an altitude of ~ 440 meters (m) above sea level (Fleitmann et al., 2009). The cave is situated 15 kilometres (km) eastward of the city Zonguldak and is embedded in the slopes of the Sofular deresi valley (Fig. 2.1.) (Laumanns and Kaufmann, 1988).

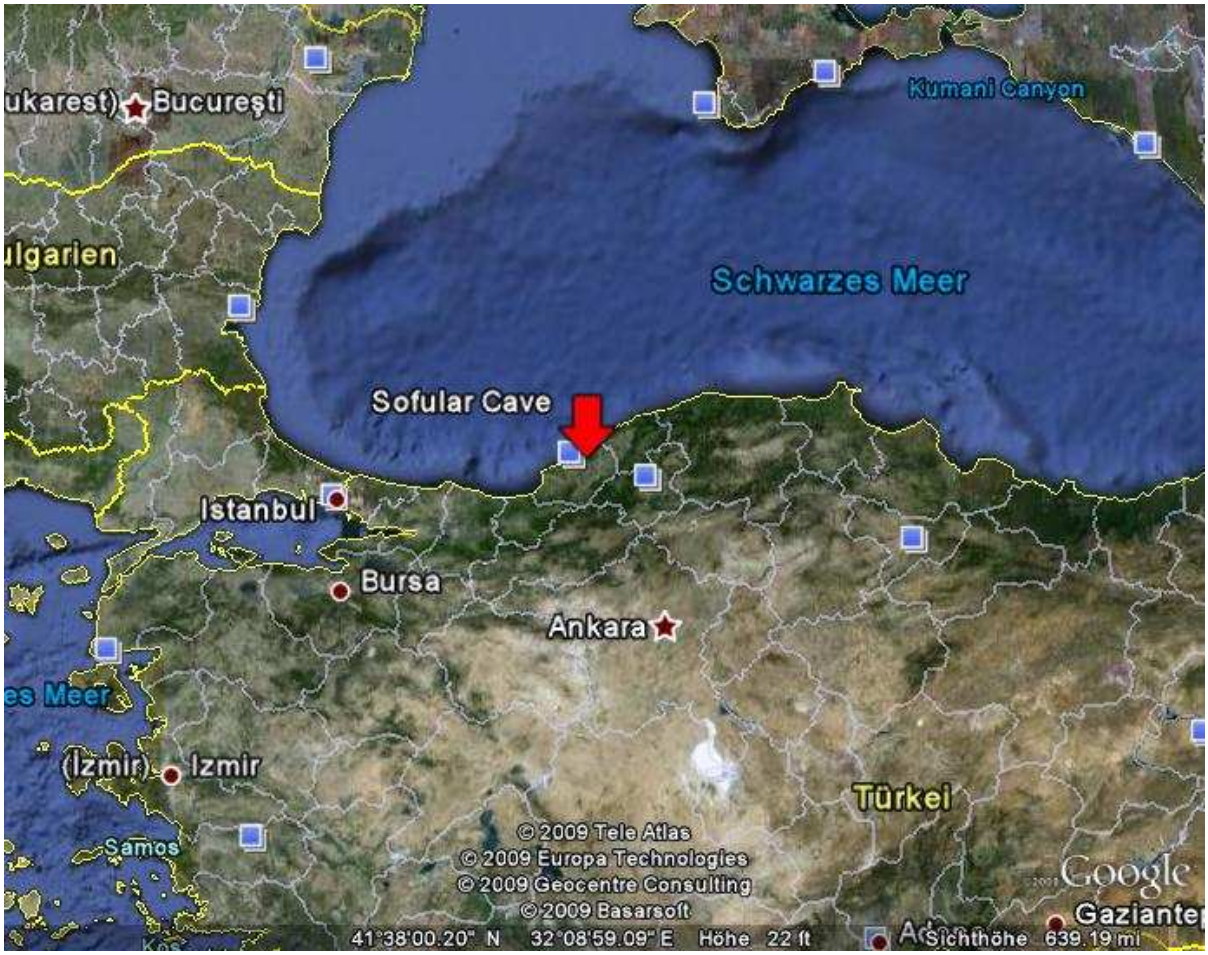

Fig. 2.1. Approximate location of the Sofular cave (red arrow) within the Black Sea region (Source: Google Earth).

Geology

The Black Sea is located within a series of high folded mountain chains of the Alpine system. The Balkanides-Pontides belt is extended to the southern coast of the Black Sea (Panin, 2007). The Black Sea is encircled by the Caucasus in the North, the Crimea in the North-east and the North Dobrogea Mountains in the North-west (Panin, 2007).

Further on, the cave is situated on the northern side of the North Anatolian fault zone (Bozkurt and Mittwede, 2001).

The Sofular cave lies within the Istanbul zone of the Pontides consisting of a pre-Early Palaeozoic crystalline basement and an unconformably Palaeozoic, Mesozoic and Cainozoic (Ordovician to Eocene) sediment succession at the surface (Chen et al., 2002). The basement consists mainly of metasediments, metagranitoids, meta-sedimentary-volcanic succession and metaophiolites (Yilmaz et al., 1995). The Zonguldak basin is filled by lower (clastics and carbonates) and upper (clastics, carbonates and volcanic rocks) cretaceous sediments (Tüysüz, 1999). The cave is situated below a karstified lower cretaceous limestone which is embedded in cretaceous flysch (Laumanns and Kaufmann, 1988).

Sofular Cave

The cave system has a maximum depth of -84 m, and is extended over a length of 490 m and three main grounds (Fankhauser et al., 2008; Turkish Cave Inventory). The first ground is oriented in a west-to-east direction and was built by a drainage system to the East during the Pliocene. The second ground was formed at the end of the Pliocene by the river Sofular which began to drain into the current direction. The Sofular River was also responsible for the formation of the third floor, by reason of erosion and embedding of the former surface (second floor) of the cave (Fig. 2.2.). In the nineties, Sofular cave was explored by the MAD (Turkish Cave Research Community) and the MTA (Mine Research Institution) (Fankhauser et al., 2008; Turkish Cave Inventory). Strong sintering processes prevail in the cave and the lowest parts are filled with muddy sump, due to the oscillation of the karst water-level (Laumanns and Kaufmann, 1988). Tracks of human settlement were found in the form of possible human bones. Bats are the main animals inhabiting the first floor of the Sofular cave (Fankhauser et al., 2008; Turkish Cave Inventory).

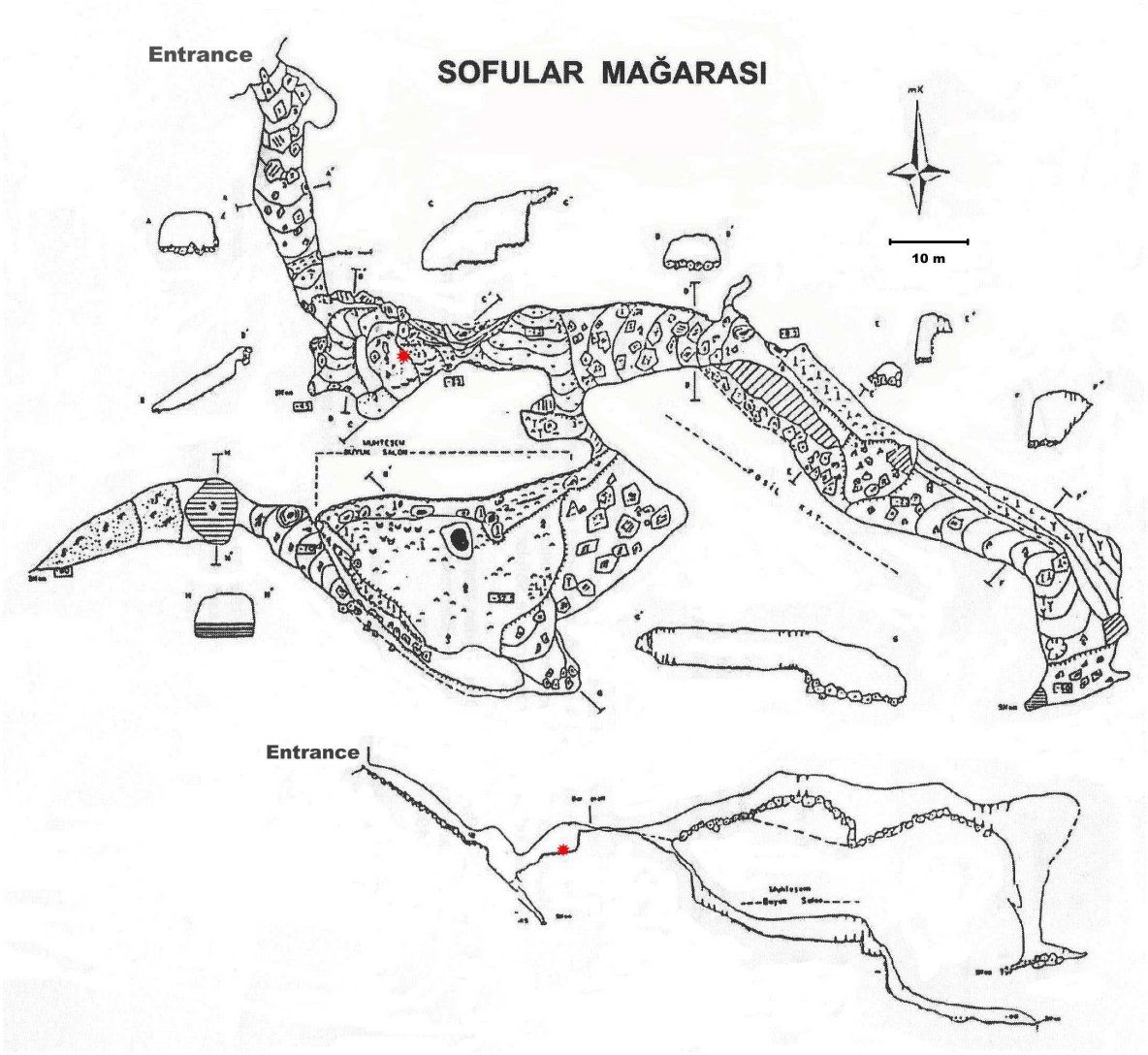

Fig. 2.2. Situation plan of the Sofular cave. Once with the perspective from above (at the top) and with the perspective from the side (below) (Kaufmann and Laumanns, 1988).

2.2 CLIMATE

2.21 Modern Climate

Meteorological information of Sofular in this first section is mainly based on data from the meteorological station of Zonguldak which is situated about 15 km North-west from Sofular cave. Figure 2.3. shows that annual precipitation in the region of Sofular cave is about 1200 millimetre per year (mm/yr). From this total amount, 75% precipitates in the time period between September and April, which produces a seasonal cycle. For example, the total amount of monthly precipitation in December and May is 126 and 47 millimetres (mm) respectively (Fig. 2.3.). Monthly mean temperatures vary between 6 and 22 degrees Celsius (°C) with an annual mean temperature of 13.5°C (Fig. 2.3.). This temperature is approximately equivalent to the prevailing temperature within the cave of about 13°C (Fleitmann et al., 2009).

On the whole, the climate in a region is influenced by three main factors which themselves depend on latitude and topography of a location. These factors are the solar irradiance, the

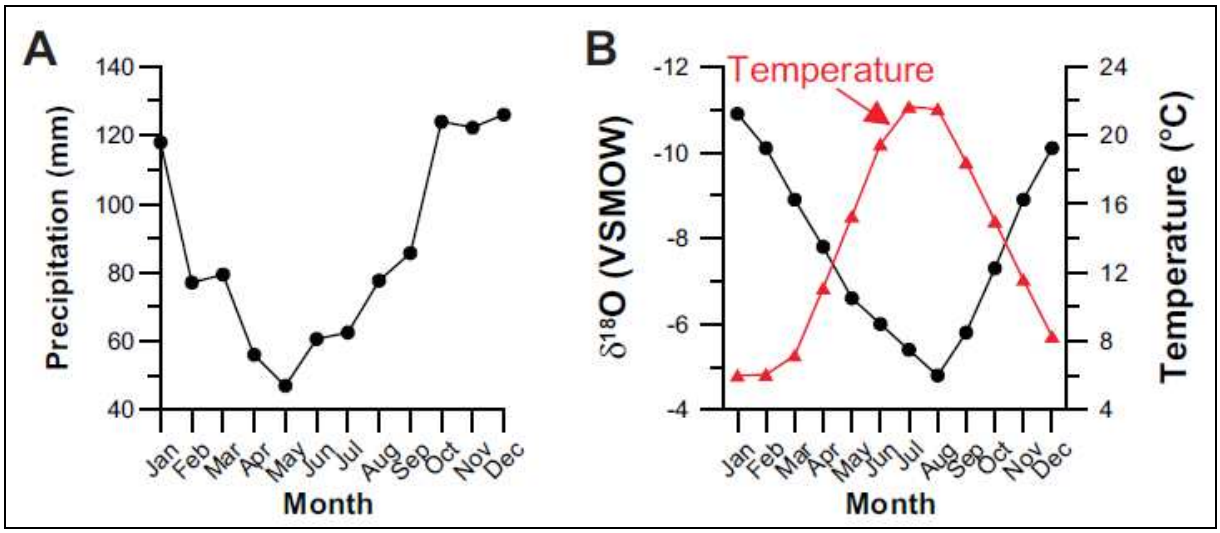

Fig. 2.3. Actual precipitation and temperature values with the corresponding $\delta^{18}O$ precipitation signal at Sofular cave (meteorological station of Zonguldak) in a course of a year (Graph made by Dominik Fleitmann, Sources: GNIP, Turkish Meteorological Service).

character of the underlying surface and the atmospheric circulation. The Black Sea region has a huge supply of solar irradiance due to its southerly position and only a little amount of the downward directed irradiance is reflected (Kosarev et al., 2008).

The atmospheric circulation is the main factor responsible for the distribution of the air masses over a region. The Black Sea is mainly influenced by large-scale atmospheric systems positioned over Eurasia and the North Atlantic. Although the western and eastern parts of the

Black Sea are located in the same latitudinal interval, the climates differ substantial between the two regions (Kosarev et al., 2008).

The air masses penetrating the Black Sea region can be divided into tropical and polar air masses (Sensoy, 2004). These air masses are further separated into maritime polar air masses, continental polar air masses, maritime tropical air masses and continental tropical air masses. Maritime polar air masses originate from the Atlantic Ocean and pass over Europe. They lead to rainfall within the Black Sea region. Continental polar air masses from Sibiria and Russia are cold and dry and catch up some moisture while crossing the Black Sea. This moisture is released as rainfall at the Black Sea coast. Air masses formed over the Azores islands are humid and warm. These tropical maritime air masses lead to higher amounts of precipitation mainly in the western part of the Black Sea region during summer. Continental tropical air masses arrive in the Black Sea region from the North African desert and are therefore hot and dry. They can lead to precipitation events if they pick up enough moisture over the Mediterranean Sea (Sensoy, 2003).

The main wind directions registered in the Black Sea area are northerly, north-easterly or north-westerly winds and to a smaller part, southerly, south-westerly or south-easterly winds (Kosarev et al., 2008). This can be seen on figure 2.4.; the blue arrows denote the prevailing wind system in the region. In wintertime (Fig. 2.4a), the area is mainly influenced by westerly winds deflected by local orography at the surface. These westerly winds occur over the western Black Sea as northerly winds (Raicich et al., 2003). Also south-easterly patterns can influence the Black Sea region during wintertime (Kosarev et al., 2008) The winter is also the season when the amount of regional cyclones created over the Mediterranean Sea increases, but they are often short-lived (Kostopoulou and Jones, 2007).

During the summertime, there is little variability in the atmospheric circulation which is at that time determined by the Atlantic anticyclone and the Asian thermal low (Kostopoulou Jones, 2007). The westerlies registered over the Black Sea region are weaker and therefore, the surface wind regimes are dominated by the meridional wind components. This surface meridional wind regime is also known as the Etesian regime (northerly winds) forming part of the southern Hadley cell (Raicich et al., 2003). The vertical component of the meridional wind regime is known as the local Hadley cell. This circulation system connects the Mediterranean area with the sub-Saharan area. The convective area of the Hadley cell (ascending air) shifts between summer and wintertime from 0-5° latitude band to 15-20° latitude band (Raicich et al., 2003).

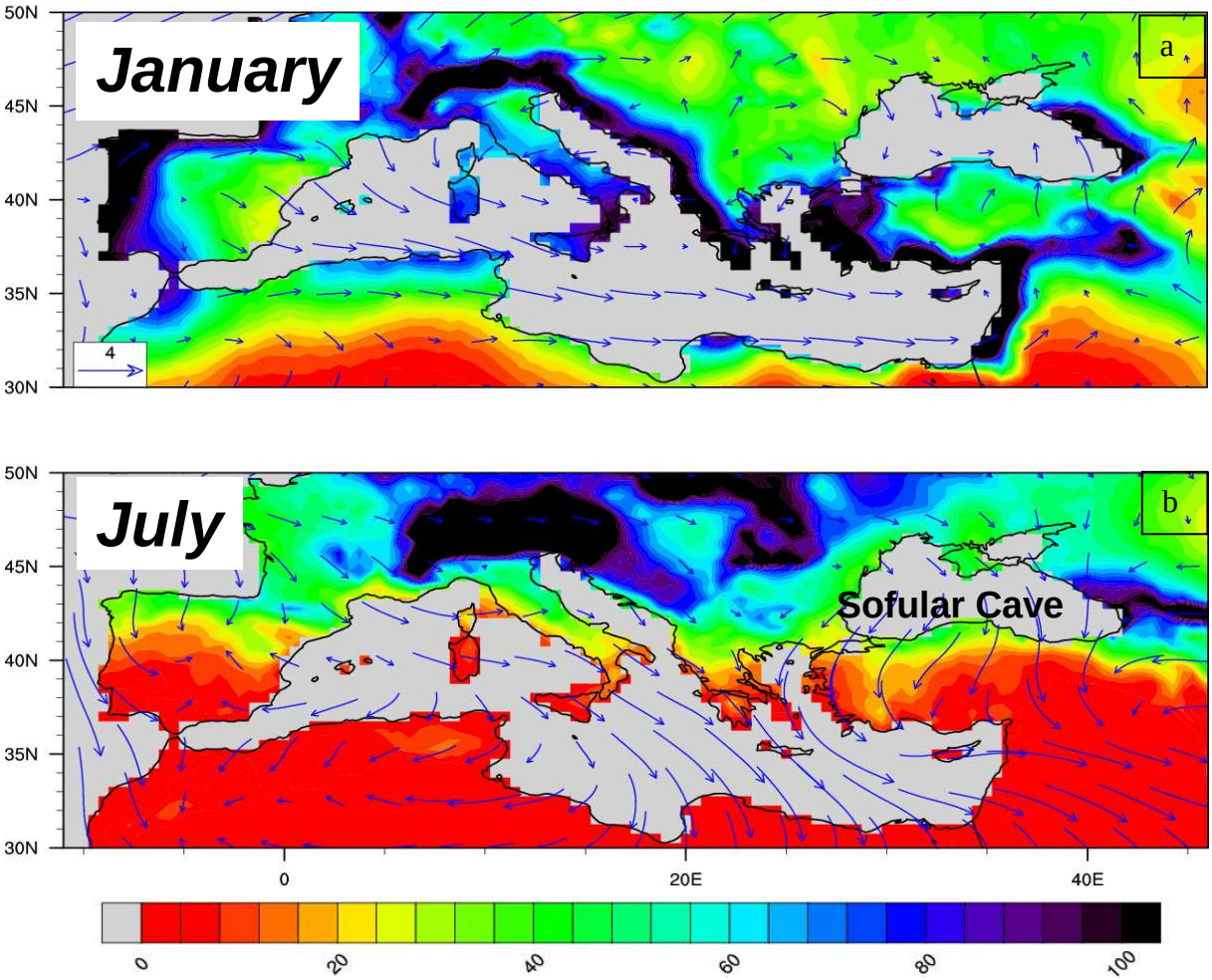

Fig. 2.4. Predominant winds and precipitation (in mm/month) pattern above Sofular cave in January (a) and July (b) (Graph made by Ozan M. Göktürk, Sources: NCEP, CRU).

Also smaller circulation patterns have an influence on the climate at the coasts of the Black Sea region. Especially the land-sea breezes lead to an exchange of air masses between the Black Sea and the coast. The differences in surface temperature induce a circulation of air masses which mainly occurs between March and October. The onshore breezes dominate during the day, while the offshore breezes arise during nighttimes (Kosarev et al., 2008). However, in general the small-scale atmospheric conditions are often dominated by the variability of the large-scale atmospheric systems (Oguz et al., 2006).

The study Fleitmann et al. 2009 shows that there is no significant correlation between temperature and precipitation changes in the region of Sofular. Therefore, different atmospheric circulations are accountable for changes in temperature and precipitation (Fleitmann et al., 2009).

As it was described before, the climate in Turkey differs significantly between the different regions within the country. Reasons are the different landscapes and the mountain belts expanded parallelly to the coast of the Black Sea (Sensoy, 2003). Therefore, the clouds originating from the North cannot overcome the Pontides Mountains and mainly rain out at the coast. As a result, the coastal regions obtain much more precipitation during the year than the inland regions. For example, inland regions and costal regions obtain annual precipitation values of 250-300 mm and 2200 mm, respectively. The Black Sea coast is the only location within the Black Sea region receiving precipitation throughout the year. In contrast, the coasts of the Aegean and Mediterranean Sea have rainy winters but almost no precipitation during summer (Sensoy, 2003).

The main teleconnection-patterns influencing the Black Sea climate are the North Atlantic Oscillation (NAO) and the East Atlantic-West Russia (EAWR) pattern (Oguz et al., 2006). The North Sea-Caspian Pattern index (NCP) established by Kutiel and Benaroch 2002, using 500 hPa geoponential anomaly patterns, shows similar characteristics as the EAWR (Oguz et al., 2006). A positive and a negative NAO-index have a consequence of a relatively cold, dry winter and a mild, wet winter respectively in the Black Sea region (Kazmin and Zatsepin, 2007). The positive NAO is associated with higher pressure gradients between the Icelandic low and the Azores high. This gradient leads to stronger westerly winds which occur over the Black Sea as north westerly winds (Oguz et al., 2006). As a result, the surface temperatures in the Black Sea region decrease. In the case of a negative NAO index, the wind transport over the Black Sea is directed to a north-east direction (Kazmin and Zatsepin, 2007). These patterns do not always dominate the climate over the Black Sea; sometimes other atmospheric systems probably outweigh (Oguz et al., 2006).
The winter EAWR index indicates the distribution of pressure anomaly centers over the Western Europe and the Caspian region (Oguz et al., 2006). This pattern is responsible for the modulation of the NAO-pattern over the Eurasian continent. A positive index is caused by an increasing strength of the North Sea anticyclone and an amplifying of the cyclone over the Caspian Sea. This results in a wind originating in the north-east/north-west of the Black Sea region. In the case of a negative index, the cyclonic anomaly is situated over the North Sea and the anticyclonic anomaly over the Caspian Sea. Consequently, the pressure difference is not that high over Europe and the Black Sea region, which is then influenced by warmer and wetter conditions transported into the region by south-westerly to south-easterly winds (Oguz et al., 2006).

Raicich et al. 2001 revealed an influence of Indian monsoon intensity on the local Hadley cell during summertime. Time periods with lower pressure over Asia lead to higher monsoon precipitation events. During these periods, low pressure is also measured in the eastern Mediterranean area. This pressure disposition has a consequence of an intensification of the northerly, north-easterly winds and therefore the Etesian wind regime (Raicich et al., 2001).

2.22 Global climate history

Past global climate is an important framework to understand the climate at the regional scale. The regional climate is often influenced by global patterns, which are further modified by regional patterns. Therefore, the past global climate is also worth to be looked at. In the following section, only the MIS 1 (~ since 12 ka BP) and the MIS 5e-b (128 – 87 ka BP) climate are covered, because only they are of particular interest for this master's thesis. An overview of the climate at Sofular cave of the last 50 kilo years before present (ka BP) is provided by the master thesis of Fankhauser et al. 2008.

End of MIS 6

During the end of the MIS 6 (~135 ka BP), the general climatic conditions were colder and drier than the present-day conditions. These conditions were more pronounced in the northern regions of Europe. Mainly continental climate regimes predominated in the European area, due to a reduction of the heat transport by the Gulf Stream (Brewer et al., 2008). During the glacial periods, the climatic belts shifted into the southern direction (Frumkin et al., 1999).
This climatic continentality was weakened in the oceanic regions (Brewer et al., 2008).

Eemian (MIS 5e)

The term 'Eemian' originates from Harting et al. 1874. Harting named some sediment from a warm period after a river in the area of Amersfoort (Netherlands). First, this term was only used for marine sediments. Later, the word Eemian was also applied to the field of isochronous terrestrial sediments (Kühl and Litt, 2007).
The MIS 5e is mainly thought to have been warmer than the MIS 1. The ice cover was reduced and the sea level was up to 12 m higher compared to modern sea levels. At the time of maximal insolation (~125 ka BP), summer temperatures were about 4°C higher than modern temperatures in the middle and high latitudes. In the Arctic region, simulated winter temperatures showed values of about 2-8°C higher than modern values. These findings are mainly confirmed in the region of northern Scandinavia (Van Andel and Tzedakis, 1996).
The Eemian interglacial period in Europe lasted from approximately 128 to 115 ka BP (Brewer et al., 2008) and is synonymous with the MIS 5e (Shackleton et al., 2003). However, Kukla et al. 1997 came to the position that the Eemian extended into the ice growth phase of the MIS 5d (Kukla et al., 1997). Triggers for the MIS 5e climate were maybe modifications in solar activity amplified by changes in the North Atlantic Ocean current or by the North Atlantic Oscillation (Müller et al., 2005).

The early MIS 5e was characterized by a climate with a strongly heterogeneous characteristic in Europe. A steep increase in temperature and a slower rise in precipitation took place across Europe (Chedaddi et al., 1998). Especially, the summer temperatures rose with a gradual increase from Western to Eastern Europe. A winter-warming pattern was principally revealed in Central and North-Eastern Europe (Brewer et al., 2008, Velichko et al., 2007). A probable reason for this warming is an increased advection of warm air from the Atlantic by westerlies (Velichko et al., 2007). The rise in winter temperatures led to a decrease in the seasonal contrasts (Chedaddi et al., 1998). The previously predominant continental climate of Eastern Europe was being modified and became a Mediterranean climate regime (Sanchez-Goni et al., 1999). In general, the conditions during the mid-MIS 5e were relatively stable compared to the beginning of the MIS 5e which was the warmest and wettest period during the whole MIS 5e (Kühl and Litt, 2003; Chedaddi et al., 1998). Despite the assumption of a relative stable MIS 5e (Brewer et al., 2008), a number of abrupt, weak, cold and/or arid events led to some climate variation during the MIS 5e (Maslin and Tzedakis, 1996; Cheddadi et al., 1998). An analysis of Müller et al. 2005 suggests that these events occurred in intervals of approximately 1370 years (Müller et al., 2005).

In the final part of the MIS 5e, the decrease in temperatures and the dry conditions continued and accelerated (Brewer et al., 2008). Winter temperatures decreased by a larger amount than summer temperatures. Therefore, an increase in seasonality was registered during this period, especially in the northern parts of the world (Chedaddi et al., 1998). The transition to glacial conditions took longer, than the transition to interglacial conditions, probably due to more complex forcing factors (Brewer et al., 2008).

During the MIS 5e period (128ka-115ka BP), the sea level of the Eemian Sea reached its highest water level (Streif, 1991) and occupied the whole Baltic basin. However, on the North Sea coast, only the main river beds were flooded. Furthermore, the Eemian Sea covered the whole area between the North Sea, the White Sea and the Arctic Ocean. Consequently, Fennoscandia was an island during the high stand of the Eemian Sea. At the end of the MIS 5e, the sea level regressed before 110 ka BP (Zans, 1936; Gross, 1967).

Sites across whole Europe showed an interglacial vegetation succession (Van Andel and Tzedakis, 1996). The presence of the Eemian Sea probably led to a uniform climate on the bordering continents, and therefore to an expansion of uniform vegetation and the settlement of temperate forests (Tzedakis, 2007).

The period of 115-71 ka BP is divided into periods of different stadials and interstadials MIS 5a-5d (Fig.2.5.). During this phase, the climate deteriorated and changed afterwards into the MIS 4 with a first major advance of the glaciers in Europe. The main conditions during

stadials were cold and dry climates. The interstadials were more continental than the phases of the MIS 5e (Van Andel and Tzedakis, 1996). The first stadial was the Herning/Melisey I stadial (MIS 5d; ~107 ka BP) directly following the MIS 5e. The sea level dropped to a value of -50 m compared to present sea levels (0 m). At that time, the Scandinavian ice-sheets had not yet been extensive (Mangerud et al., 1991) and therefore had most likely not reached the coast of Norway yet. This stadial is thought to have had a shorter duration than the previous/following warm phases (Van Andel and Tzedakis, 1996).

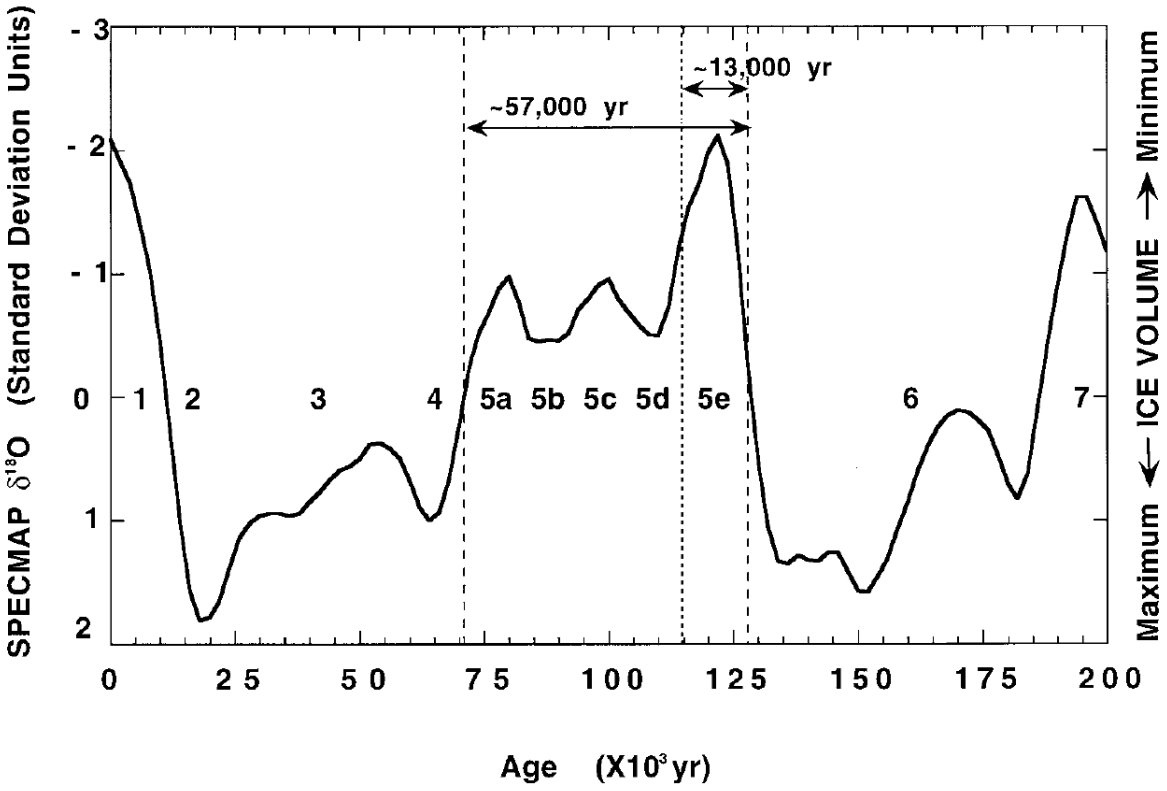

Fig. 2.5. The MIS 7-1 defined by the foraminiferal $\delta^{18}O$ time series of SPECMAP Imbrie et al., 1984). The curve was supplemented by Winograd et al. 1997 with the Marine $\delta^{18}O$ isotope stages 1-7 defined by Shackleton 1969. The periods of 57 ka and 13 ka within the dotted lines display the entire MIS 5.

A quite warm phase followed with the Brørup/St. Germaint interstadial (MIS 5c; 99 ka BP). A huge part of the ice-sheet which was formed in the previous stadial melted during this interstadial (Mangerud et al., 1991). The sea level rose to a level of -20 m (Bard et al., 1990) and the vegetation state was in a situation comparable to the late MIS 5e. A next sea level dropping took place during the Rederstall/Melisey II stadial, also called MIS 5b (~87 ka BP). This event was associated with a modest increase of the ice volume (Mangerud et al., 1991) and a sea level of -25 m (Van Andel and Tzedakis, 1996). The mechanisms of starting ice sheet formations are not yet clear (Van Andel andTzedakis, 1996). Lambeck et al. 2002

suggested that the ice sheets can build up without a decrease in temperature if there is enough air moisture available (Lambeck et al., 2002). The transitions between stadials and interstadials revealed in pollen sequences are mainly showed as alternations between open and closed forest conditions. Each interstadial was characterized by a fast expansion of the original vegetation which is thought to have taken place due to the near refugees. Van Andel and Tzedakis 1996 suggested that the conditions during the MIS 5d were not that harsh as they were during the MIS 5b (Van Andel and Tzedakis, 1996). According to Lambeck et al. 2002, the oscillation between interglacial and glacial climates is mainly caused by a transfer of waters between the two largest water-reservoirs, the ice sheets and the World Ocean (Lambeck et al., 2002).

MIS 1

A substantial warming was recorded during the transition from the MIS 2 to the MIS 1 in several paleoclimate archives (Solomina et al., 2008). The beginning of the MIS 1 was marked by an increase of temperature of about 7°C (Lemke and Harff, 2005). Depending on the location, this warming was delayed because of the large ice sheets which influenced the climate in the high northern latitudes (Solomina et al., 2008). Models show that temperatures at 9ka BP were about 5°C higher than present temperatures on northern continent inlands (Kutzbach and Webb, 1993). At 8.2 ka BP a short cooling event occurred with about 2°C lower temperatures than before. Afterwards, the phase known as the climatic optimum followed with higher temperatures and more rainfall than today. After about 4.5ka BP, the temperatures/precipitation began to fluctuate around present values (Lemke and Harff, 2005).

The vegetation in the European region changed from steppe or tundra flora to mixed, deciduous forests at the beginning of the MIS 1. During the MIS 1 optimum, thermophile plants began to dominate the countryside (Lemke and Harff, 2005).

A MIS 1 climate reconstruction of Mayewski et al. 2004 shows six periods of rapid climate changes since approximately 11,500 ka BP. Mayewski gained this evidence from 50 globally distributed paleoclimate records. These rapid events occurred in quasi-periodic intervals (~2000 years), with a higher frequency after the middle part of the MIS 1. The paleoclimate records showed an occurrence of these events ~9000-8000, ~6000-5000, ~4200-3800, ~3500-2500, ~1200-1000 and 600-150 cal yr. BP. These events were climatically characterized by polar coolings, North-Atlantic ice rafting events, alpine glacial advances, tropical aridity, strengthened westerlies and major atmospheric climate changes. Causes for these abrupt events are mainly ascribed to changes in solar insolation produced by Earth orbital variations or solar variability (Mayewski et al., 2004).

2.23 Eastern Mediterranean climate history

Frogley et al. 1999 has evidence from a lacustrine sequence in north-western Greece for possible duration and course of the MIS 5e in Greece. In the time span of 130-127.5 ka BP, the data showed an increase in the Precipitation/Evaporation (P/E) ratio, indicating an increase in precipitation (Frogley et al., 1999). The start of the full MIS 5e was characterized by wetter conditions. After 126.8 ka BP, the climate in Greece was dominated by Mediterranean climate with warm temperatures, mild winters and dry conditions (Frogley et al., 1999). MIS 5e optimum temperatures (~125 ka BP) were about 2° C higher than modern values. The MIS 1 temperatures showed only a deviation by 1°C compared to modern values (Zelikson et al., 1998). From 126.1 ka to 124.7 ka BP, $\delta^{18}O$ values rose, indicating increased aridity. After that, a stepwise decrease in $\delta^{18}O$ showed a higher availability of moisture, higher summer precipitation and lower winter temperatures (Frogley et al., 1999). Mediterranean elements disappeared about 122.6 ka BP and in the meantime, the winter and summer temperatures dropped. At 118.1ka BP, a period of higher aridity led to higher $\delta^{18}O$. After 116.7 ka BP, the MIS 5e was characterized by a more oscillatory climate. Frogley et al. 1999 suggested that there were smaller changes of the $\delta^{18}O$ within the full MIS 5e than during the late-glacial interval and the transition to the stadial (Frogley et al., 1999). The instabilities at the end of climate states could have taken place due to non-linear reactions to changes in solar forcings and transitions between preferred climate states (Frogley et al., 1999).

In the eastern Mediterranean region, the vegetation pattern showed the following succession; climate favourable for cold and dry steppe alternated with Mediterranean evergreen plants. In general, the interstadial vegetation was more open than the vegetation during the MIS 5e (Van Andel and Tzedakis, 1996).

The MIS 2 climate can be described with cold winters, intense winter precipitation and summer droughts. However, the MIS 2 was drier than the climate regime dominating today. The temperatures varied between 12-16°C and the annual rainfall fluctuated in an interval of 300-450 mm. Afterwards, the climate became more humid, with an increase in precipitation during the transition from the late MIS 2 to the MIS 1 approximately 12 ka BP (Bar-Matthews et al., 1997).

In the time period of 10-7 ka BP, a high amount of precipitation was recorded in different paleoclimate archives. Afterwards, the climate parameters become constant and turned into present climatic conditions with higher temperatures and less rainfall than the preceding period (Bar-Matthews et al., 1997).

2.24 Orbital parameters

To achieve a reasonable comparison between different interglacials, the prevailing solar and orbital forcings have to be understood. The orbital parameters have an influence on the angle under which irradiance strikes the earth surface. Eccentricity, obliquity and precession are the factors controlling this angle. The eccentricity indicates the shape of the Earth's orbit around the sun, variations occur at the time scale of about 100 ka. Furthermore, the Earth's orbit around the sun has an elliptical form. In the aphelion and perihelion position, the distance between the earth and the sun is the largest and smallest respectively.

Obliquity can be described as the tilt of the Earth's rotational axis relative to the ellipse of the Earth's orbit. Repetitions of equal conditions occur in a cycle of about 41 ka. An increase in the tilt leads to a higher (smaller) amount of insolation in the respective hemispheric summer (winter).

Precession is driven by the variations of eccentricity and quantifies the distance between the Earth and the sun at a fixed time in the year. The equal conditions repeat in a cycle of about 21 ka (chapter based on Berger et al., 1993). The situation of the parameters during the MIS 1 and the MIS 5e will be discussed under the chapter 5.3.

2.3 BLACK SEA SETTING

The Black Sea is the largest permanently anoxic, semi-enclosed basin with a volume of 537,000 cubic kilometres (km^3) (Bahr et al., 2008) (Fig. 2.6.). It is connected to the Marmara Sea through the Bosphorus Strait which has an approximate depth of - 35 m. The ocean connection continues with the connection from the Marmara Sea to the Aegean Sea by the Dardanelles Strait (Strait of Canakkale, ~ depth = -70 m). The Dardanelles Strait has a length of 74 km and a width of 1.3-7.5 km (Gökaşan, 2008). The properties of the Bosphorus Strait are a length of 31 km and a width between 0.7 and 3.5 km (Gökaşan, 1997).

Fig. 2.6. The location of the Black Sea with its connections to the Marmara and Aegean Sea in the south-western direction (Source: Google Earth).

Today, the exchange of waters through these straits is ensured by a two-layer flow. The cooler, less saline surface waters originating from the Black Sea flow with a velocity of 10-30 centimetres per second (cm/s) in a southerly/south-westerly direction. The surface waters have temperatures of 5-15°C, a salinity of 17-20l (= 17-20 gram/litre, 17-20‰), and form a layer of 25-100m in the Aegean and Marmara Sea. In the Black Sea, the less saline water forms a 100-200m thick layer, which is also the upper part of the stable pycnocline (Öszoy and Ünlüata, 1997). The warmer water from the Mediterranean flows along the Aegean Sea

and descends near the Dardanelles Strait below the cold-water surface layer. Subsequently, the waters with a temperature of 15-20°C and a salinity of 38-39l (= 38-39 gram/litre, 38-39‰) penetrate into the Dardanelles Strait with a transport velocity of 5-25 cm/s in a north-easterly direction (Aksu et al., 2002b).

The circulation can be maintained because of height differences between the basins, the Black Sea sea level is located 40 cm above the Marmara Sea and the sea level of the Marmara Sea itself lies 30 cm above the Aegean Sea sea level. The sea levels of the basins can fluctuate up to 50cm in the course of one year due to seasonal variations in the river discharges (Aksu et al., 2002b).

The water balance of the Black Sea is made up of different parts like precipitation, freshwater input, outflow through the Bosphorus and evaporation (Fig. 5.5) (Swart, 1991). The Black Sea has a positive hydrological balance, with higher influxes from precipitation and rivers, than outflux by evaporation (Aksu et al., 2002b). A possible disequilibrium generated by these factors is regulated by the net-export of water into the connected basins (Özsoy and Ünlüata, 1997). The water balance is built up in the following way; the water input is formed by excess precipitation and riverine freshwater input with a transport amount of 300 cubic kilometre per year (km^3/yr) and 350km^3/yr, respectively. Evaporation is one factor acting into the other direction, with an export of water of 350km^3/yr (Özsoy and Ünülata, 1997). Therefore, the Black Sea has to export a certain amount of water to maintain its sea level. Without this export, the sea level of the Black Sea would rise by ~94 cm per year. The main freshwater sources of the Black Sea are the rivers Danube, Dniester, Dnieper, Southern Bug and Don Rivers (Aksu et al., 2002b). The freshwater input from the Danube accounts for approximately 50% of the total river input (Özsoy and Ünülata, 1997). The drainage zone has an approximate area of two million of km^2 (Mudie et al., 2002).

The circulation within the Black Sea is mainly dominated by two central cyclonic gyres and several smaller anticyclonic costal eddies (Oguz et al., 1993). The gyres are separated by a narrow cyclonic peripheral rim current (Aksu et al., 2002a). A mixing of the surface waters exists to a depth of 200m induced by winds and winter circulation. The bottom water circulation is generated by the penetration of Mediterranean water into the Black Sea (Özsoy and Ünlüata, 1997). The turnover rate of the deep waters in the Black Sea is approximately 2000 years (Östlund and Dyrssen, 1986).

The isotopic values of the Black Sea waters are controlled by different parts which are involved in the water balance of the Black Sea. These parts have different isotopic signatures. Swart 1991 suggested that the surface water isotopic signature lies between the meteoric water line (MWL) and a mixing line.

H. Craig established an average relationship between oxygen and hydrogen ratios in terrestrial waters named global meteoric water line (GMWL). The relationship is: $\delta D = 8.0 * \delta 18O + 10$ ‰. This equation can be adapted for different locations (MWL) (Craig, 1961). The mixing line is defined by two extremes, the bottom water Mediterranean Sea ($\delta^{18}O = 1.8$‰ (SMOW)) and the river input with a $\delta^{18}O$ value of -10 to -8‰ (SMOW; Swart, 1991). The isotopic signatures of the river inputs are not that precisely known. However, the Danube draining the highest amount of water, into the Black Sea has an isotopic signature of at least -6‰. The other rivers arise from a region farther north than the Danube and are therefore probably even more depleted in $\delta^{18}O$ isotopic composition (Swart, 1991). Concerning the MWL, the precipitation falling in the Black Sea region has a $\delta^{18}O$ isotopic signature between -4 and -8‰ (SMOW). The atmospheric water vapour is supposed to be in balance with the local precipitation (Swart, 1991).

The salinity of the Black Sea is mostly influenced by the strait depth and the global sea level. But some additional factors like climate, amount of water exchange and the upward mixing of saltwater within the Black Sea also have a substantial effect on the salt-composition of the Black Sea. The climate controls the freshwater fluvial input and the balance between evaporation and precipitation (Mudie et al., 2002).

2.4 BLACK SEA HISTORY

The history of the Black Sea is fairly well known for the last 30 ka BP. Most of the research has been conducted by multiproxy studies including micropaleontological and palynological data (Bahr et al., 2006/2008, Aksu et al., 1999/2002a, Kaminski et al., 2002, Mudie et al., 2002, Ryan et al., 1997, etc).

Generally, the Black Sea was a lake during glacial periods when sea levels were below the sill depths of the Bosphorus and the Dardanelles. During interglacial periods, however, a connection to the Mediterranean Sea could have been established (Aksu et al., 2002b). During the MIS 2, sea level of the Black Sea dropped to a value of -110 m due to the formation of glaciers (Aksu et al., 2002a). As a result, the sea level of the Black Sea water body was below the sill depth of the Bosphorus and was a fresh, brackish water lake (Mudie et al., 2002). The data of Bahr et al., (2006) indicate stable isotopic compositions of the Black Sea water body during the interval from 30 ka to 18.5 ka, with values between -5 and -6 ‰ (VPDB) (Bahr et al., 2006).

The post MIS 2 interval started about 18ka BP with the deglaciation of the Eurasian, Scandinavian and Siberian ice sheets (Bahr et al., 2006). Figure 2.8. illustrates the history of the connections between the basins since 18ka BP (Kaminski et al., 2002, Fig. 2.8.). The river Volga discharged isotopically depleted melt waters from the Scandinavian ice sheet to the Caspian Sea area (Mangerud et al., 2004). The following sea level rise in the Caspian Sea led to an outflow of the waters through the Manych-Kerch spillway into the Black Sea (Chepalyga, 2007). Besides the melt water inputs, there were also other factors leading to an overflow of the Caspian Sea: Permafrost melting, a higher runoff coefficient, an increased catchment area, lower evaporation and superfloods in spring because of long winters with large snow masses (Chepalyga, 2007). Furthermore, the warmer climate induced a large amount of melt water discharge from the Eurasian glaciers into the Black Sea. The main part of this discharge was formed by the big rivers draining into the Black Sea. Thereby, the $\delta^{18}O$ in Black Sea ostracods decreased to a value of -6.5‰ (Bahr et al., 2006) which is in good accordance with the results from Fankhauser et al. 2008 and Fleitmann et al., 2009. Therefore, decrease in $\delta^{18}O$ of So-1 at 15.49 ka BP (Figure 2.7.) is not a result of a temperature effect, but due to the inflow of isotopically depleted water (Fleitmann et al., 2009; Fankhauser et al., 2008; Bahr et al., 2006). Afterwards, the period of the Bølling/Allerød (14-12.9 ka BP) led to a stepwise increase in $\delta^{18}O$ of the ostracods from -5 to -1.95‰ (Bahr et al., 2006). The main factors responsible for this ascent are an increase in $\delta^{18}O$ of atmospheric precipitation (temperature effect), increasing runoff and evaporation (Bahr et al., 2008).

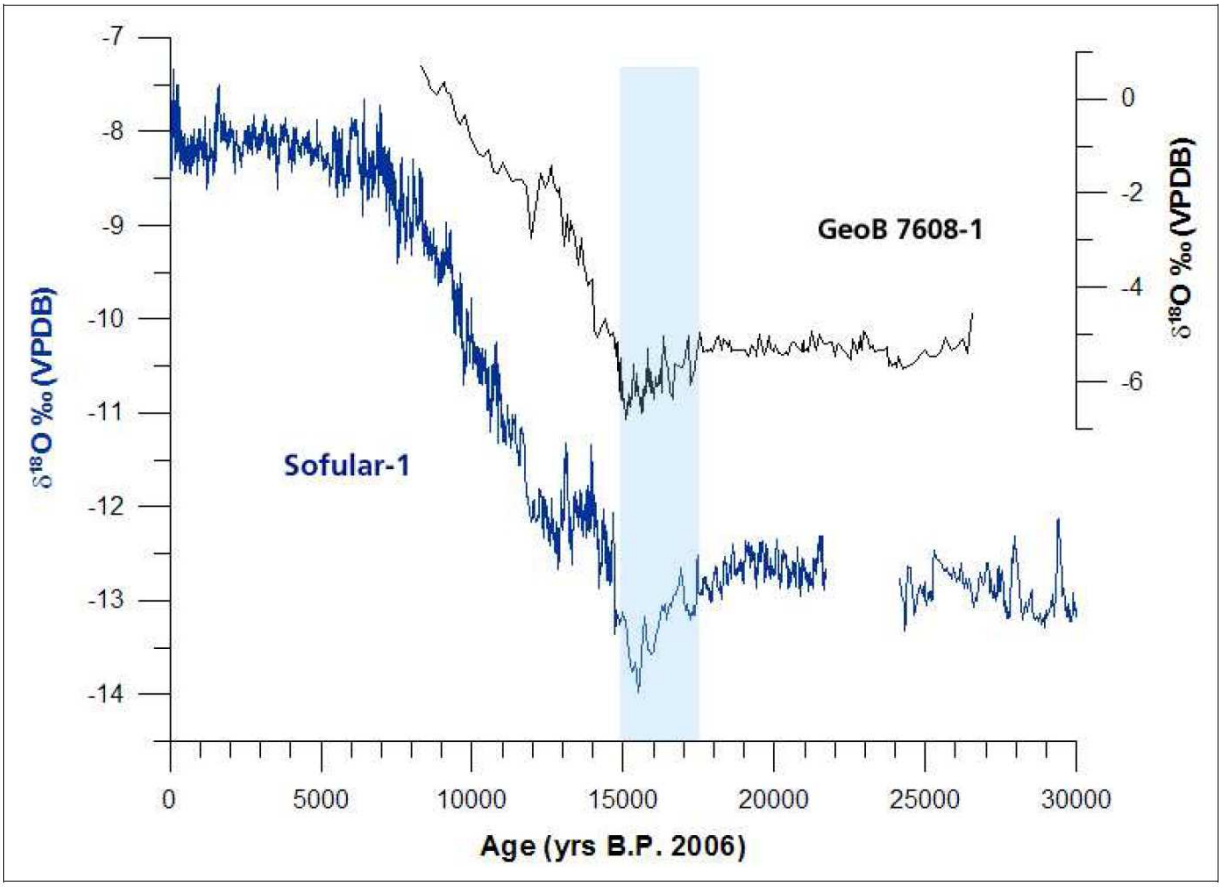

Fig. 2.7. The Black Sea $\delta^{18}O$ signature of the last 30 ka BP with the melt water inundation at 15.49 (Graph made by A. Fankhauser).

After 17ka BP, the enhanced melt water input into the Black Sea led to a sea level rise as well as a refill of the Black Sea basin to a level of -20m. The excess water spilled through the Bosphorus Strait into the Marmara Sea (Yanko-Hombach et al., 2007).

The Aegean Sea reached the Dardanelles sill (-77 m below present sea level) at about 12ka BP. Afterwards, the Aegean water masses penetrated into the deeper parts of the Marmara Sea (Kaminski et al., 2002). In the time period of 12-9.5ka BP, the sea level of the Aegean sea rose from -77 m to -40 m (Aksu et al., 2002a), with a short standstill between 12.9 and 11.7 ka BP (Rasmussen et al., 2006) because of the cold excursion of the Younger Dryas (Aksu et al., 2002a).

At the time of 10 ka BP, a sapropel layer was deposited in the Mediterranean Sea, one responsible factor could have been the low-salinity surface lid produced by the Black Sea outflow (Çağatay et al., 2000; Aksu et al., 2002a). The inflow of saline Mediterranean water through the Bosphorus Strait into the Black Sea started at around 9.5ka BP, when the Mediterranean sea level reached the sill depth (Yanko-Hombach et al., 2007). But the waters could not penetrate into the Bosphorus until 9.1ka BP due to the strong outflow of Black Sea

water originating (Lane-Serff et al., 1997; Kaminski et al. 2002). Kaminski et al. 2002 gained evidence for this theory in a study about foraminifera at the southern end of the Bosphorus. The foraminifera increased in their abundance, as a result of a reduced outflow from the Black Sea (Kaminski et al., 2002). Furthermore, hydrological models suggest that the rising sea level in the Mediterranean Sea had to reach a critical height before a two-layer exchange could be established (Lane-Serff et al., 1997). Thus, during the early MIS 1 the conditions for a penetration of saline waters into the Black Sea were guaranteed (Kaminski et al., 2002, Lane-Serff et al., 1997). The denser Mediterranean water replaced the bottom water of the Black Sea, which has never returned to a fully oxygenated state since then (Kaminski et al., 2002). This distinct hydrological change is also recorded in ostracods which show a more positive $\delta^{18}O$ of +0.68‰ at around 8ka BP (Bahr et al., 2006). In general, the Black Sea isotopic composition changes slowly because of its large volume (Bahr et al., 2006). The present-day two-layer flow through the Bosphorus was well established by 6ka BP (McHugh et al., 2008).

However, the nature of the reconnection of the Black and Mediterranean Sea is subject of controversial discussions. Based on faunal and sedimentological evidence, Ryan et al. (1997) argues that the reconnection of the basins resulted from a catastrophic inundation of the Black Sea by Mediterranean waters. In accordance with the data, Ryan et al. 1997 came to an age of approximately 7.15 ka BP for the inundation. These arguments are also known as the Noah's Flood hypothesis (Ryan et al., 1997). But there are some findings of other studies which contradict this hypothesis. Some points which have to be fulfilled for the accuracy of the hypothesis are a Black Sea level lower than -40m (~-100 to -40m), a breakdown of the stable stratification and a decrease in the strength of the outflow from the Black Sea. Furthermore, the Black Sea has to be colonized by Mediterranean species at that time. However, there was no support found in other studies showing the occurrence of such a situation at about 7.15 ka BP (Aksu et al., 2002a; Kaminski et al., 2002; McHugh et al., 2008; Yanko-Hombach et al., 2007). Also, there still exist discussions about the timing and the way of the water exchange between the Mediterranean and Black Sea (Aksu et al., 1999/2002a; Kaminski et al., 2002; Mudie et al., 2002a; Ryan et al., 1997/2003; Major et al., 2002/2006).

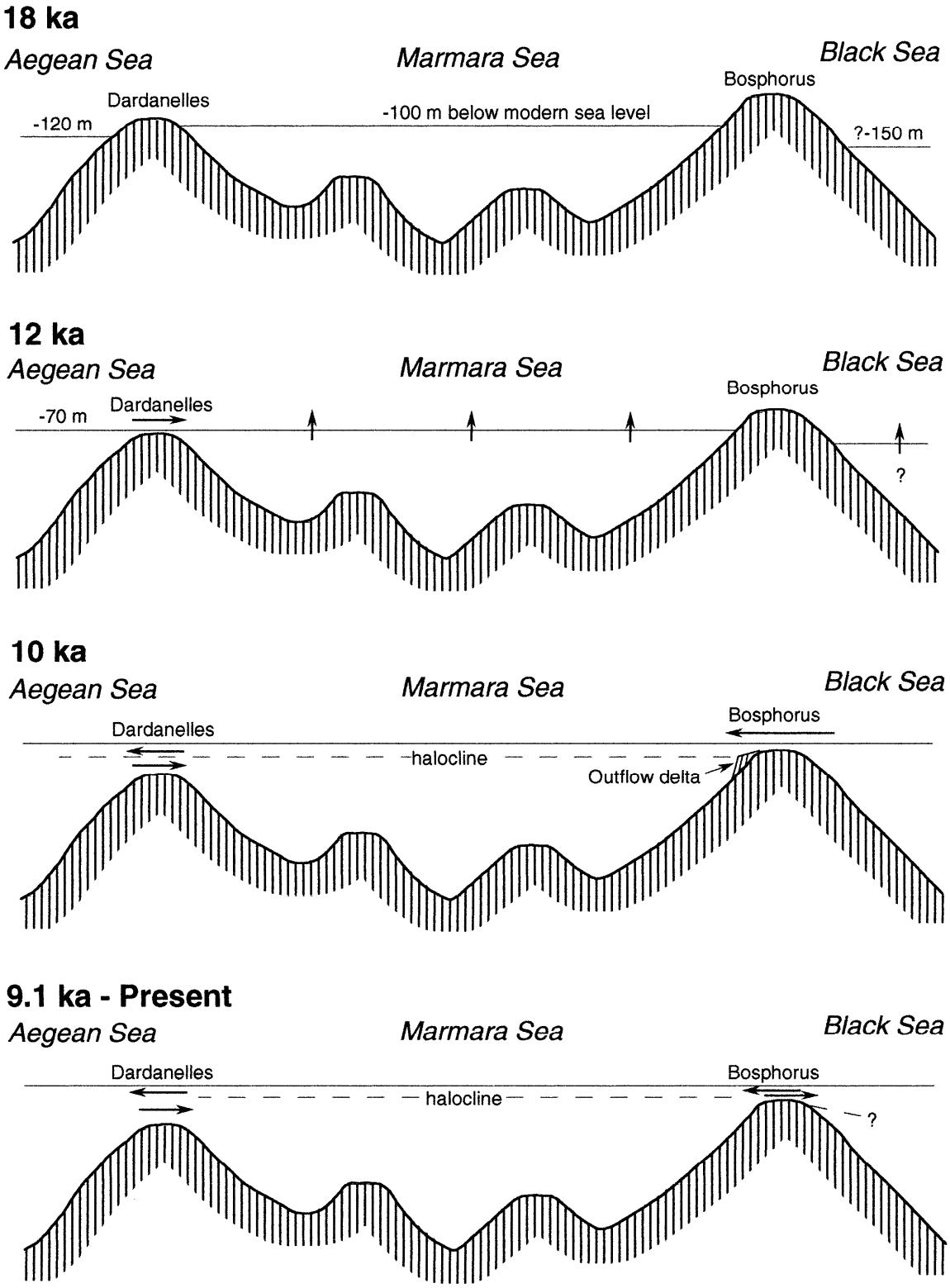

Fig. 2.8. The exchange history between the Aegean Sea, the Marmara Sea and the Black Sea basin of the last 18 ka BP (Kaminski et al., 2002)

3 CHAPTER THREE – METHODS AND MATERIAL

3.1 SPELEOTHEMS

3.11 Formation of speleothems

A speleothem is a secondary mineral deposit formed in caves. Caves are a product of karstification of relatively soluble host rocks (limestones). Speleothems are secondary deposits, because they differ from the primary mineral bodies. Examples for primary mineral bodies are the bedrock enclosing the cave, mineral veins within the bedrock and sediment loads accumulated in the cave. These mineral bodies work as important sources for the formation of new secondary bodies through the dissolution of material during physical and chemical processes (Self and Hill, 2003).

The formation of stalagmites often takes place below karstified host rocks (epikarst), with enhanced permeability, where major conduits and lower transmissivity fissures feed the drip water zones in the cave (Fairchild et al., 2006a). The water recharge of the aquifer is driven by several parameters such as surface topography, the nature of soils, other superficial depositions and the degree/style of karstification of the aquifer (Fairchild et al., 2006b).

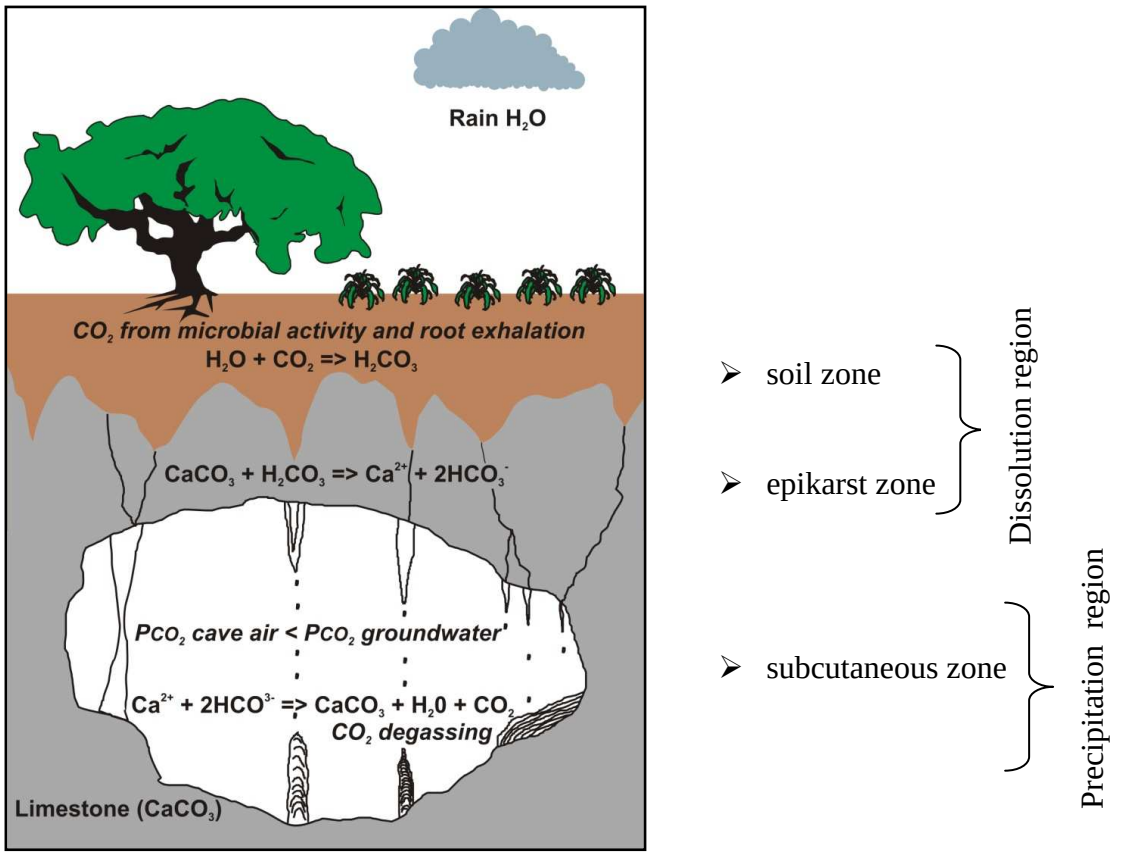

Fig. 3.1. The formation of speleothems takes place in several steps (Figure made by Fleitmann).

Generally, the recharge is focused in doline depressions which are fed by lateral flows (Fairchild et al., 2006b).

The aquifer is divided into 2 parts, the dissolution region (soil, upper epikarst) and the precipitation region (Fig. 3.1.). The upper part includes processes of limestone dissolution, circulation of waters with a high partial pressure of CO_2 (due to plant respiration and soil microbial activity) and decays of organic matter. In the precipitation region within the cave, the formation of speleothems is taking place (Fairchild et al., 2006a).

As illustrated in Figure 3.1., the formation of speleothems operates in the following way: Water (H_2O) infiltrates into the soil, mainly through rainfall or surface runoff events. In the soil, it reacts with CO_2 to carbonate acid (H_2CO_3) (Fairchild et al., 2006a). When the water percolates through the soil, which is enriched with organic compounds, the CO_2 concentration of the water may rise up to 10% (White, 2007). This carbonate acid has the ability to dissolve limestone rocks. If the acid encounters limestone, the dissolution takes place and the groundwater with the dissolved calcite (Ca^{2+}, $2HCO_3^-$) percolates farther down to the cave. Within the cave, the CO_2 partial pressure of the groundwater exceeds the CO_2 partial pressure of the cave environment. Consequently, CO_2 degasses to the cave environment and calcite minerals are deposited in the form of speleothems (Fairchild et al., 2006a). This process occurs due to super saturation of the water with respect to calcium carbonate (Harmon et al., 2004). Each drop of the cave drip water deposits its small load of $CaCO_3$ (White, 2007). The calcium carbonate concentration in the drip water is dependent on the porosity/permeability of limestone, soil pCO_2-levels, moisture and temperature (Richards and Dorale, 2003).

Three different ways of calcite precipitation from the drip-waters are observed. Precipitation of calcite occurs due to slow degassing of CO_2 from the solution, due to fast degassing of CO_2 and due to evaporation (Baker et al., 1997). Slow degassing of CO_2 leads to a deposition of calcite in isotopic equilibrium with the seepage water (Harmon et al., 2004).

The deposition of speleothems is controlled by several factors like distribution, quantity and chemistry (calcium concentration of drip waters) of the percolating water (Fairchild et al., 2006b). But also the nature of the water flow has an influence on the precipitation of calcite minerals. Turbulent flows rise the rate of precipitation, whereas stagnant/laminar conditions lead to lower precipitation rates (Dreybrodt, 1999). The water flow through the aquifer can last from a couple of days to up to several years, depending on the karst system and the availability of water (Fairchild et al., 2006b). Additional factors controlling the formation of speleothems are the cave microclimate (cave geometry), aquifer properties and the external microclimate (Fairchild et al., 2006b). For example, the cave ventilation removes the CO_2 and holds up the partial pressure gradient between the CO_2 in the groundwater and the cave air.

Consequently, this process enables the stalagmite to continue its growth. The better the ventilation within the cave, the lower the pCO_2 and therefore enhanced speleothem growth rate is possible. The main factors influencing cave ventilation are the geometry of the cave (e.g., one or several entrances), the wind direction and the pressure differences between the cave interior and the external atmosphere (Fairchild et al., 2006b).

The maximal theoretical growth rate of a stalagmite varies between 70-100 micrometer per year (µm/yr) (at a temperature of 6°C) and 1000 µm/yr (at a temperature of 13°C) (Fairchild et al., 2006b). In reality, growth rates of stalagmites in the cool, temperate zone and the subtropical zone are 10-100 µm/yr and 300-1000 µm respectively. Consequently, a stalagmite of a temperate zone, with a height of one meter provides a temporal record of 10-100 ka. Speleothems can grow continuously for $10^3 - 10^5$ years (Fairchild et al., 2006a). Possible events which can interrupt the deposition of stalagmites are the absence of water (due to dry or glacial phases (Spötl et al., 2002; Burns et al., 2001)), clastic sedimentation (Sasowski and Myltorie, 2004), a breakdown of deposits, seismicity and archaeological disturbances (Fairchild et al., 2006b).

Shape / Mineralogy of stalagmites

The shape and the diameter of a stalagmite depend on the drop fall height (splash effects), the water super saturation and the water flow rate. For example, the width of a stalagmite increases with increasing fall height of the drip waters (Fairchild et al., 2006a). With an increase of the super saturation of water with respect to calcium (Richards and Dorale, 2003), the solution tends to precipitate more calcite minerals resulting in a higher growth rate of the stalagmite. The smaller a flow rate, the smaller the resulting height of a speleothem (Fairchild et al., 2006b). A uniform growth of a stalagmite implies rather stable drip rates and drip water chemistry (White, 2007).

Hiatuses in speleothems are phases of no deposition of calcite minerals; consequently, the speleothems are inactive. A hiatus can have its cause in the change of drip locations, the absence of water (due to dry or glacial phases (Spötl et al., 2002; Burns et al., 2001)) and other long term evolutionary changes in the cave environment (Fairchild et al., 2006a). In the case of stalagmites situated in the northern regions, hiatuses occur through glacial periods, caused by a lack of available drip waters (e.g., Spoetl et al., 2002). In semi-arid regions, hiatuses are mainly induced by the absence of drip waters during arid periods (Burns et al., 2001).

The speleothem crystal morphology depends on several factors like drip rate, chemistry of drip waters, capillary and gravitational supply of ions to growth sites and rates of CO_2 outgassing (Fairchild et al., 2006b).

The mineralogy of stalagmites varies between compact to porous compositions. The minerals may contain impurities of 0-10% of the weight mass. These impurities are particularly clay minerals and organic matter (Fairchild et al., 2006). Most stalagmites are built out of calcite minerals but occasionally in association with high magnesium- or dolomite-host rocks, deposits can also consist of aragonite crystals (McDermott, 2004). Calcite stalagmites often contain large crystals which lay parallel to the growth direction and a lot of component crystallites. Conversely, aragonite stalagmites often contain fibrous crystals which are oriented parallel to the growth direction (Farichild et al., 2006b).

A study of Gascoyne (1992) shows that in cool, temperate regions, where fairly slow growth dominates, the stalagmites mainly consist of massive macro-crystalline minerals, whereas in tropical regions, porous and sugary textured mineral deposits with a higher content of detritus dominate. This detritus mainly originates from occasionally occurring flooding events or dust within the cave (Gascoyne, 1992). Variations in crystal textures lead to fine laminations and large-scale banding (Fairchild et al., 2006a).

3.12 Registration of environmental and climate signals in speleothems

Speleothems are an ideal paleoclimate archive. There are several properties of speleothems which support this statement: a well-defined internal stratigraphy, an accurate age-dating method and variations in the internal chemical, isotopical compositions which are determined by environmental conditions at deposition (Fig 3.2.; Fairchild et al., 2006b).

The measurement of isotopic ratios is the most popular type of geochemical investigations performed on speleothems (Fairchild et al., 2006b). Furthermore, speleothems capture surface-derived dust, pollen and organic acids which are sequentially deposited. These properties of speleothems allow for the correlation with events on the land surface above the cave (White, 2007). Formerly, paleoclimate scientists tried to use speleothems for reconstructing paleotemperature. Today, speleothems are mainly used to estimate the timing and duration of major O- or C-isotope defined climate and environmental events (McDermott, 2004). In terms of paleoclimate reconstructions, various

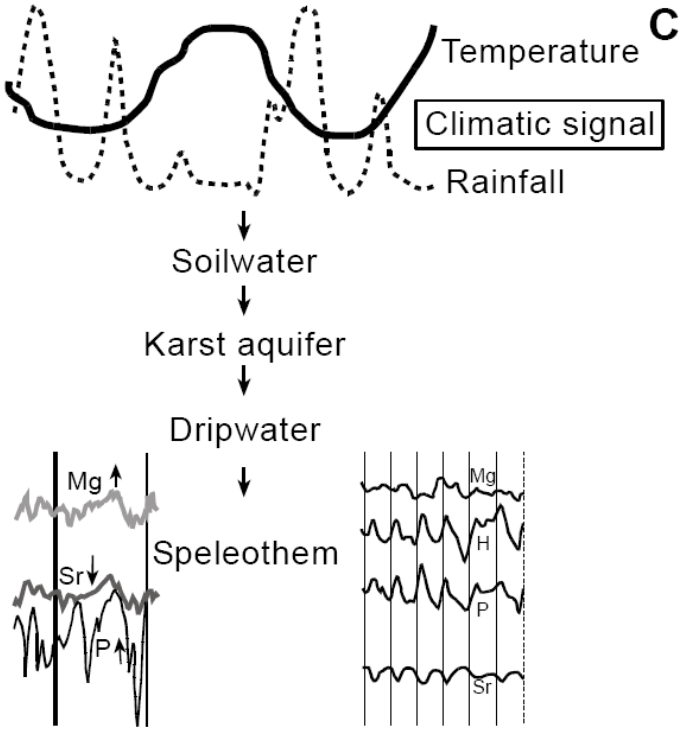

Fig. 3.2. Transfer of climate and environmental signals and their registration in the speleothems (Fairchild et al., 2006b).

aspects of speleothem growth can be considered. Paleoclimatic information can be extracted by measuring the thickness of annual growth lamina, growth-rate changes, presence/absence of speleothem growth, stable isotope ratios and variations in trace element ratios, colour banding and luminescence banding. The analysis of these different aspects provides scientists with an insight into different climate-driven processes in the past (White, 2007).

The following climatic features can be captured by speleothems: changes in mean annual temperature, rainfall variability, atmospheric circulation changes and vegetation responses (McDermott, 2004). The soil water is responsible for the transport of the dissolved carbonate to the speleothems and can be affected by external or internal forcings (Fairchild et al., 2006a).

Besides the external forcing, there are also sources of internal modifications induced by the ecosystem, soil, karst aquifer and cave environment (Fairchild et al., 2006a). For example, the soil influences the amount of discharge to the cave and the geochemical properties of the soil water. The soil water is only one fraction of the total annual precipitation. The other fraction of precipitation is lost due to evaporation, surface runoff, transpiration and canopy interception (Fetter, 1994). Modifications induced by the karst aquifer and the cave environment can have an influence on the water flow behaviour (Fairchild et al., 2006a). Different transit times of the waters through the karst system arise because of the complex build-up of the karst body with three different appearing flow systems. The water flows through the body using conduits, fractures or the pervasive matrix, leading to a mixing of recharged waters and therefore to a smoothing of the $\delta^{18}O$ signal of soilwater (Fairchild et al., 2006a). Thus, waters undergo individual mixing histories on their way to the cave; consequently, the climate signal is smoothened and contains probably an isotopic mixture of different climatic events (Fairchild et al., 2006a). The precipitation of carbonates within the cave is associated with an isotope fractionation between the gaseous and the liquid phase, which is temperature-dependent. The lighter oxygen isotopes prefer the gaseous phase and this leads to last an enrichment of the heavier isotopes in the carbonates (Hendy, 1971). The fractionation between the water and the calcite averages -0.22‰/°C (Epstein et al., 1953).

To improve the understanding of the processes influencing the original climate signal, studies of the cave-specific processes of infiltration, flow routing, drip seasonality, saturation state and cave microclimate have to be carried out (Lachniet, 2009).

3.13 Stalagmite So-17A

Prof. Dr. Dominik Fleitmann and his group from the Institute of Geological Sciences, University of Bern, collected new stalagmites from Sofular Cave during a field trip in the end of the year 2008. Stalagmite So-17 was one of several samples and showed an interesting growth history. So-17A forms one part of a three-part stalagmite (Fig. 3.3). The growth of So-17 was possibly interrupted by several seismic events (Fig. 3.3.).

Fig. 3.3. Stalagmite So-17A in is original position within the Sofular cave (left; picture mady by Fleitmann) and its cross-section (right).

Stalagmite So-17A began to grow approximately 122.96 ka BP and was probably overthrown by the impact of a seismic event at around 86 ka BP. Afterwards, stalagmite So-17B was formed on the backside part of the fallen stalagmite So-17A. A next seismic event may also have interrupted the growth of So-17B (upper part is missing). The growth of stalagmite So-17B extended from 82.23 to 77.15 ka BP. However, the drip water source remained constant and led to a continuation of stalagmite growth in the form of stalagmite So-17C. This stalagmite was also formed on the tail of So-17A and continued its growth up to the year 65 ka BP. However, this age is not very certain, because of some age dating problems.

The stalagmite So-17A has a height of 100.4 cm and a diameter of approximately 10 cm. The diameter is nearly constant over the whole height of the stalagmite. (Fig. 3.3.). The stalagmite

is built up of dense calcite minerals. The overall form is cylindrical with a possible dislocation of the drip source in the span of approximately 98 -90 ka BP.

3.2 URANIUM-THORIUM DATING

3.21 Theory

The growing interest in speleothems as climate archives was mainly encouraged due to the positive progresses in the field of the uranium-dating method (U-Th hereinafter). The advantages gained from these progresses are a higher accuracy of ages (uncertainty of 0.1-0.4%) and a use of smaller sample sizes. The sample sizes were reduced from a weight of 10-100 grams (g) to 10-500 milligrams (mg) (Goldstein and Stirling, 2003). The U-Th dating method produces absolute ages and therefore no age calibration is required. Furthermore, this method is applicable for samples back to 500 ka BP. This is considerably further back in time compared to the ^{14}C method (Richards and Dorale, 2003).

The U-Th dating method is based on the decay of the reactive, long-living parent isotopes ^{238}U and ^{234}U to stable daughter isotopes ^{206}Pb, ^{207}Pb and ^{208}Pb. The stable lead conditions are achieved by 6, 7 and 8 α- decays respectively and several intermediate β- and γ-decays (Fig. 3.4) (Van Calsteren and Thomas, 2006).

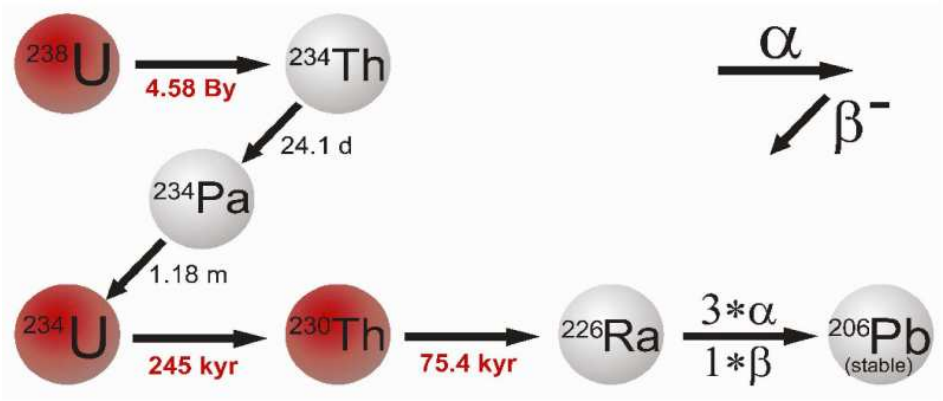

Fig. 3.4. The decay chain of uranium (from Fankhauser et al., 2008)

Most of the isotopes in this decay chain are short-lived species. However, there are two long-living isotopes, ^{234}U and ^{230}Th with half-life times of 248 ka and 75.2 ka respectively (White, 2007). Several ratios from the uranium decay series are used for dating purposes. The ratio $^{231}Pa/^{235}U$ can be applied to time periods of 0-200 ka (Edwards et al., 1997), U-Pb dating is appropriate for calcite samples with high uranium and minimal lead content (Richards et al., 1998) and $^{234}U/^{238}U$ disequilibrium dating is used for low-precision ages > 500ka (Ludwig et al., 1992). The main calcite-dating method which has been used in the last decades is mainly based on the ratio between ^{234}U and ^{230}Th (Gascoyne, 1992).

The decay of parent isotopes into daughter isotopes can be described by the following equation:

$$N = Pe^{-t\lambda}$$

N = number of parent isotopes today, P = number of parent isotopes present at the time of formation, t = time since the formation, λ = decay constant, e = base of the natural logarithmus (Van Calsteren and Thomas, 2006).

After about six half-lives, the decay-system reaches a secular equilibrium (activity (decay per unit time) ratio = 1). The six half-lives are calculated from an intermediate isotope in a decay chain with the longest half-life (Bourdon et al., 2003). In a recently deposited calcite mineral the activity ratio between the parent and the daughter nuclide is zero, due to the initial absence of daughter nuclides (Van Calsteren and Thomas, 2006). This equilibrium is defined by an equal decay rate of all nuclides within a chain. In this equilibrium phase, the isotopic ratios of the nuclides are equal to the ratios of their decay constants (Van Calsteren and Thomas, 2006). The U-Th dating method is dependent on a fractionation process separating the parent uranium isotopes from the long-lived daughter isotopes ^{231}Pa and ^{230}Th (Richards and Dorale, 2003). The separation process is started by weathering of rocks and minerals. The uranium within these rocks and minerals is leached and transported in the form of the aqueous species $UO_2(CO_3)_3^{4-}$ (Fairchild et al., 2006b). In many cases, the UO_2^{2+}- ion is attached to carbonic or humic acid complexes during its transport (Van Calsteren and Thomas, 2006). In the case of speleothems, the water with the dissolved uranium reaches cave environments where precipitation of carbonates takes place. The uranium is then incorporated into the $CaCO_3$ of stalagmites. Conversely, thorium is very particle-reactive. The dissolution of a small amount of thorium in water is directly followed by its re-precipitation of certain particulate matters (Van Calsteren and Thomas, 2006). Therefore, the advantage of this dating method is that the daughter product Th is not soluble in water and is therefore incorporated in speleothems in not-carbonate phases only (Fairchild et al., 2006b). The calcite contains several tens to hundreds of parts per million of uranium, but no thorium (Fairchild et al., 2006a). It is also important, that there is no accumulation or loss of parent/daughter nuclides after the formation (Richards and Dorale, 2003). The radiometric clock effectively starts at time point zero (Van Calsteren and Thomas, 2006). Consequently, the thorium that accumulates within the calcite carbonate allows a direct derivation of the ages passed since the deposition of the calcite (White, 2007). If there is a contamination of the sample with initial Th, this can be corrected with knowledge of the initial ^{230}Th/^{232}Th ratio. If the concentration of ^{232}Th is high, a contamination with initial ^{230}Th has to be assumed (Richards and Dorale, 2003).

Landscapes are divided into uranium-rich and uranium-poor reservoirs formed by uranium-rich rocks and young strata respectively (Gascoyne, 1992). The average uranium content in sedimentary rocks varies between 2 and 4-10 microgram per gram (μg/g). Normally, the uranium content of the soil is lower than the uranium content of the host rock. However, this also depends on the soil type and its maturity (Van Calsteren and Thomas, 2006). The average abundances of uranium and thorium in the earth continental crust are 1.7 μg/g and 8.5 μg/g respectively (Richards and Dorale, 2003). Generally, the concentration of uranium in meteoric water lies between 0.01-100 microgram per litre (μg/l) and depends on the following factors: ionization potential, pH of water, uranium concentration and solubility of mineral phases in host rocks, interaction time of water and rock and the abundance of complex ligands (Richards and Dorale, 2003).

The accuracy of the U-Th dating method is dependent on the amount of uranium incorporated in stalagmites. The upper age limit which can be achieved with this dating method is 500 ka. The obtained ages should be in chronology with the structure of the stalagmite. Otherwise, it should be assumed, that a remineralisation or a contamination by nuclides has taken place during the growth of the stalagmite (Gasgoyne, 1992).

3.22 Sample preparation

The process of U-Th dating method was carried out in several steps: drilling of the samples, chemical separation of the elements of interest and finally the determination of the elements in the mass spectrometer.

The U-Th dating method begins with drilling a sample of 100 – 400 mg, whereas sample size depends on the uranium content. The samples are mainly drilled at the centre of the stalagmite and along the orientation of a lamina, because one lamina over the width of the stalagmite is often deposited at the same time. The drilling of So-17A was performed with a dentist drill.

In a next step, chemical separation is performed to separate the elements of interest (in this case U and Th) and to remove matrix elements (mainly Ca) of the probe (Goldstein and Stirling, 2003). Therefore, the samples have to be separated into a uranium and thorium fraction for subsequent analysis in the multi-collector inductively coupled plasma mass spectrometer (MC-ICP-MS).

First, the powdered samples are spiked with mixed ^{229}Th- ^{236}U, this spike works as a standard for the analysis and can be also used to evaluate the effectiveness of the chemical separation. Subsequently, the sample is dissolved in 6.4 M HCl, evaporated to dryness and again dissolved in 7.5 M HNO_3. Then, the sample is again taken to dryness. Afterwards, the samples are loaded on conditioned (with 0.5 and 7M HNO_3) columns filled with anion exchanging resin (450 µl U-TEVA and 120 µl DOWEX). If present, the organic material is removed by rinsing of the columns with 7M HNO_3. In a first separation, a pure Th fraction and an impure U fraction are produced by flushing the sample within the column with 2 times 2ml 5M HNO_3. In the same column, the impure U fraction is purified with 2 times 2ml 0.5M HCl. Then, the sample is again dried on a heating element. At the end, organic impurities from the resins are removed from the samples by a treatment in a low pressure oxygen plasma (further details provided by Fleitmann et al., 2007; Fankhauser et al., 2008).

3.23 Measurement and Calculations

Measurement

The U-Th dating method was carried out with a Nu Instruments® multi-collector inductively coupled plasma- mass spectrometer (MC-ICP-MS).

Mass spectrometers are mainly used to quantitatively detect the contents of interest in a sample (Brand, 2004). The results of the analysis are relative masses/abundances of different isotopes. A mass spectrometer consists of the following parts: an inlet system, an ion source, an analyzer for ion separation and a detector for ion registration (Fig 3.5.; Goldstein and Stirling, 2003).

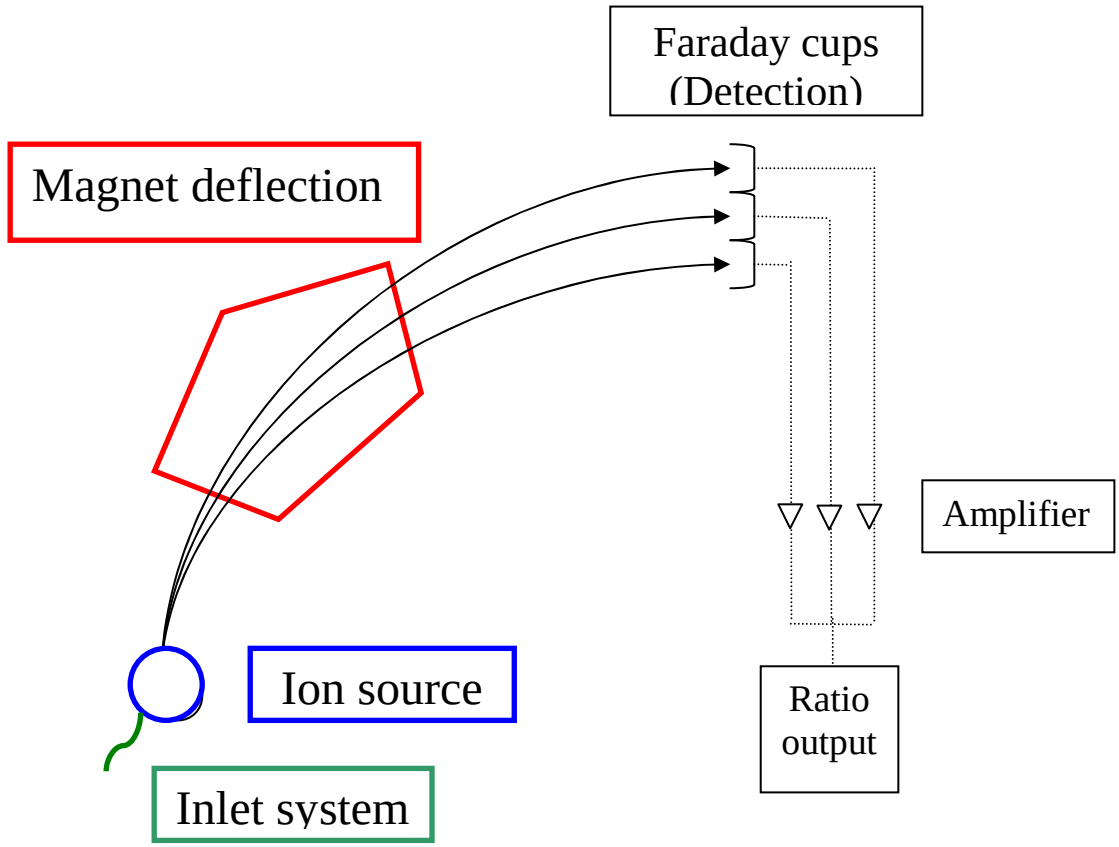

Fig. 3.5. Basic construction of a mass spectrometer (adapted from Revesz et al., 2001).

The MC-ICP-MS combines the ionisation efficiency of an ICP with a magnetic sector and multiple faraday cups (Rehkämper et al., 2001). With the high temperatures achieved in the plasma source, nearly all elements can be ionized (measured). The sample solutions are transported by a carrier gas (eg. Ar), pass through the inlet system and are then ionized in the plasma (Rehkämper et al., 2001). Further on, the ionized components are accelerated by the conductive potential of the plasma and transferred to the magnetic sector of the mass spectrometer. The magnetic sector separates the arriving beam into several beams (Rehkämper et al., 2001). The isotopes are separated by variable magnetic deflection of

isotopes due to differences in mass and charges (Brand, 2004). At the end, the different isotopes are detected by faraday cups or ion counters in accordance to their different masses (Goldstein and Stirling, 2003). Isotope ratios are mainly declared as deviations from the reference gas, to which the sample gas is compared all the time during the measuring procedure (Brand, 2004). The today's mass spectrometers are equipped at least with three faraday cups. The ratios need some corrections at the end, because of memory, background and other effects (Brand, 2004). Details about the U-Th dating method on a Nu Instruments® MC-ICP-MS can be found in the studies of Fleitmann et al., (2007/2009).

Calculation

The age calculations are carried out in the way as Fankhauser et al. 2008 mentioned in her master thesis. The calculations are made with a computer program working with an equation from Kaufman and Broecker 1965. The equation is arranged in the following way:

$$^{230}Th/^{234}U = [1-e-\lambda 230t/(^{234}U/^{238}U)] + [1- 1/(^{234}U/^{238}U)]*\lambda 230/(\lambda 230 - \lambda 234)*[1-e-(\lambda 230-\lambda 234)t]$$

In the case of a contamination of the sample by initial ^{230}Th, an additional term has to be added to get a reasonable age.

$$^{230}Th/^{234}U = (^{230}Th/^{234}U)_{init}\ e-\lambda 230t + [above]$$

The initial $^{230}Th/^{234}U$ content can be estimated with the measured $^{232}Th/^{238}U$ ratio and an assumed $^{232}Th/^{238}U$ ratio of the source material (mean value from lithosphere). The λ-value is the decay constant of the individual isotopes, and t stands for time (see also Fig. 3.4).

To obtain an adequate age from the equation, t can be replaced with different ages and the resulting ratios can be compared with the data. Another possibility is to use the graph of Schwarcz 1979 (Fankhauser et al., 2008).

The age uncertainties lie in a range of 0.25-2 % of the absolute age and the main error sources are inhomogeneity of the sample, the cleanliness of the sample preparation and the precision of the mass spectrometer measurement (Spötl, 2001/2002 and references therein). Furthermore, the accuracy depends also on the U concentration of the sample. The age uncertainty for a young speleothem with low U content can be in a range of 5-10% of the absolute age, because the Th concentration is close to the detection limit (Fleitmann et al., 2008).

3.3 STABLE ISOTOPES

3.31 Theory

General Characteristic

The term ‘isotope’ originates from the Greek language and means ‘equal places’. This term refers to the periodic table where two isotopes occupy the same position. Isotopes are atoms which contain the same number of protons in their nuclei but a different number of neutrons. Isotopes are often written in the form ${}^{m}_{n}\mathrm{E}$ where ‘m’ declares the mass number (the sum of the weight of protons and neutrons) and ‘n’ indicates the average weight of an element of all contributing isotopes (and the position in the periodic table). As the name of stable isotopes indicates, the isotopes remain stable during their lifetime and do not show any radioactive decay (following chapters based on Hoefs, 2009).

Isotope effects

Isotope effects can be initiated by differences in physical properties caused by variations in the atomic mass of an element. The chemical and physical properties of an element are often regulated by its electronic structure and the nucleus respectively. Consequently, the chemical behaviour of an element remains more or less stable because all isotopes of an element have a constant number of electrons. Physical separations can occur due to differences in physical properties of isotopes. The achieved energy level of the molecule depends on the vibrational frequency of the atoms with respect to another. The fundamental vibrational frequency of a molecule is a function of the mass of its isotopes. Heavy isotopes have a smaller vibrational frequency than lighter isotopes and therefore a smaller zero-point energy. As a result, bonds including lighter isotopes are much weaker, than bonds built up by heavier isotopes. In other words, for a dissociation of a bond, a smaller amount of energy is needed in the case of light isotopes. Among all elements, especially the light ones are affected by mass differences, which are induced by changes in the isotopical composition (Hoefs, 2009).

Isotope Fractionation Processes

An isotope fractionation is produced by change of isotopic ratios due physical isotopic effects (Hoefs, 2009). The result is depletion or accumulation of isotopes relative to others in a sample (Spötl, 2001/2002 and references therein). Different intense chemical bonds within a molecule lead to a diversity of reactions of isotopes in physical processes. Consequently, the redistribution of isotopes is dependent on their internal energies. These energies are translation energy, rotation energy and vibrational energy. Vibrational energy is the most

important one, having inverse proportionality to its mass (Spötl, 2001/2002 and references therein).

The fundamental processes for the incidence of isotope fractionations are equilibrium isotope distributions and kinetic processes (Hoefs, 2009).

Equilibrium isotope distribution

Equilibrium processes (for example condensation of water vapour) are defined as processes during which no net reaction of isotope exchange between different phases (A,B) takes place (Hoefs, 2009). Velocities of such reactions are equal in both direction of the reaction equation, with only small isotopic fractionations (Spötl, 2001/2002 and references therein). Consequently, the ratio of two proportions of isotopes (1,2, molar ratios) in the different phases remains stable during the exchange reactions (equilibrium constant = K, following equation). In geology, the equilibrium constant mainly depends on temperature (Hoefs, 2009).

$$K = \frac{\left(\frac{A_2}{A_1}\right)^{\mathrm{a}}}{\left(\frac{B_2}{B_1}\right)^{\mathrm{b}}},$$

Equilibrium fractionation in relation to deposition of speleothems occurs most likely under conditions far from the entrance of a cave where humidity and CO_2-content of cave air are high (Fairchild et al., 2006b).

As a control for equilibrium deposition of the stalagmite, the 'Hendy-test' is applied (Hendy, 1971). The test acts in the following way. It is checked whether the $\delta^{18}O$ stays constant and the $\delta^{13}C$ varies along a single growth layer of a stalagmite. It is important, that there is no correlation between these two isotope ratios. If these two conditions are fulfilled, it can be assumed that the speleothem was deposited under equilibrium circumstances (McDermott, 2004). An alternative control of equilibrium deposition is the analysis of several stalagmites from the same cave. The kinetic fractionation can be neglected, if a good reproducibility is realized (pers. communication Dominik Fleitmann).

Disequilibrium fractionation (Kinetic processes)

A second type of isotope effects is produced by kinetic processes. These processes are fast, unidirectional and incomplete (Spötl, 2001/2002 and references therein). If isotopes do not reach an equilibrium state, the lighter isotopes accumulate in the product phase. The reason for this behaviour is, as it was described before, that the lighter isotopes are more reactive due

to their weaker bonds and higher vibrational energy (Spötl, 2001/2002 and references therein). Consequently, the educts are enriched with heavier isotopes. Examples of these processes are diffusion, evaporation and biologically mediated reactions (Hoefs, 2009). Diffusion is an exchange of isotopes forced by concentration differences. Isotopes have different velocities due to mass differences and thus produce a fractionation (Spötl, 2001/2002 and references therein).

Evaporation is a process of transferring substances from fluidic to gaseous phases. During this process, the lighter isotopes favourably change the phase and thus are enriched in the gaseous phase. Alternatively, the heavier isotopes accumulate in the fluid (Spötl, 2001/2002 and references therein).

Organisms produce biologically mediated reactions inducing disequilibrium isotope redistributions. This holds true for the isotopes involved in metabolic processes. For example, plants prefer to take up $^{12}CO_2$ instead of $^{13}CO_2$ and induce a fractionation of the C-isotopes (Spötl, 2001/2002 and references therein).

Fractionation Factor

The equilibrium constant K is often substituted by the fractionation factor α, which is displayed in the following equation. The equation shows the general fractionation factor and its application to the fractionation between water and calcium carbonate. The values of R_A and R_B denote the isotopic ratios of any two isotopes in two different phases (A,B) (Hoefs, 2009).

$$\alpha_{A-B} = \frac{R_A}{R_B}. \qquad \alpha CaCO_3 - H_2O = \frac{\left(\frac{^{18}O}{^{16}O}\right)_{CaCO_3}}{\left(\frac{^{18}O}{^{16}O}\right)_{H_2O}}$$

The Delta Value (δ)

Isotopic ratios are mainly indicated in the form of delta-(δ) values. The advantage of this notation is the indication of isotopes in their relative abundance. The resulting values are in a ‰-form (per mil, parts per thousand). The delta notation is calculated by the comparison of an isotope ratio to a standard (Spötl, 2001/2002 and references therein). These delta-values are also attained from stable isotope measurements carried out in the mass spectrometer and are defined in the following way (Hoefs, 2009):

$$\delta_B = \left(\frac{R_B}{R_{st}} - 1 \right) 10^3 \, (\%)$$

A higher delta-value shows that the fraction of the heavier isotope in the sample is higher compared to the standard ratio (Hoefs, 2009).

3.32 Stable isotope measurement

The isotope measurements were all performed at the Institute of Geological Sciences, University of Berne. The stable isotope laboratory is equipped with a Thermo Finnigan Delta V Advantage mass spectrometer with an automated carbonate preparation system (Gas-Bench-II) (Fleitmann et al., 2009).

Prior to the isotope measurement, samples were prepared the following way: First, the stalagmite, which has been broken into a few pieces of about 25-30cm length, was sliced and polished. To obtain the carbonate samples (150-200 μg weight) for the stable isotope analysis, the stalagmite was drilled along its growth axis in intervals of 0.75 mm. The drilling resolution is primarily dependent on possible sampling throughput in the laboratory. The resulting carbonate samples are measured by using a gas source mass spectrometer. During the measurement process, the samples were flushed with helium to remove the ambient CO_2 and water and thereby to avoid any background effects. Then, one needle injects orthophosphoric acid which reacts with the carbonate sample in the tube. This step is necessary to release the CO_2 of the sample (Spötl, 2001/2002 and references therein). The resulting gas mixture is then taken up by the sampling needle and transferred to the mass spectrometer. After the process of separating the CO_2 (measured gas) from the other gases, the final step is the measurement of the isotope ratios of $\delta^{18}O$ and $\delta^{13}C$. The measured CO_2 has the same $\delta^{13}C$ signature as the calcite of the sample (Spötl, 2001/2002 and references therein). From the three O-atoms of the calcite, only two of them are transferred with the CO_2 to the measuring device. Consequently, a fractionation is taking place; with a constant temperature, however, the fractionation factor remains stable. The fractionation factor from CO_2 to calcite is: $\alpha_{CO2\text{-}calcite} 5.60 * 102 * T (°K)^{-2} + 1.003943$. This equation varies between different carbonate minerals. The calibration of the mass spectrometer is often done by internal standards (reference materials; Spötl, 2001/2002 and references therein).

The analytical accuracy of the isotopes is dependent on the homogeneity of the sample, the cleanliness of the preparation and the precision of the MS-measurement (Spötl, 2001/2002 and references therein).

The key information which is desired to be extracted from the isotope measurements is the ratios of $^{18}O/^{16}O$ and $^{13}C/^{12}C$ compared to an international standard (Lachniet, 2009). For carbonate samples, the standard used for the comparison is the Vienna PeeDee Belemnite (VPDB), a Belemnite of the Pee Dee Formation. The scientists who are interested in water samples use the Vienna Standard Mean Ocean Waters (VSMOW) for the isotope analysis (Lachniet, 2009). The $\delta^{18}O$ values of the VSMOW- and VPDB- standards are defined by

convention to be zero. Therefore, all the $\delta^{18}O$ sample-values are declared as deviations from the standards. Consequently, higher values show an accumulation of ^{18}O isotopes in the sample. The conversion between the two standards can be calculated by using the following formula (Lachniet, 2009):

$$\delta^{18}O_{SMOW} = 1.03091(\delta^{18}O_{PDB}) + 30.91$$

$$\delta^{18}O_{PDB} = 0.97002(\delta^{18}O_{VSMOW}) - 29.98$$

3.33 $\delta^{18}O$ and $\delta^{13}C$ signals in Paleoclimate

$\delta^{18}O$ signal

Variations in $\delta^{18}O$ of speleothem calcite are the result of complex interactions of different environmental factors. These complex controls can arise from processes in the following parts of the environment: ocean, atmosphere, soil zone, epikarst and cave system (Lachniet, 2009). Some of these processes are described in detail hereinafter.

The equilibrium fractionation processes are based on the Rayleigh distillation law. It explains the change in the isotopic composition between two phases (e.g., vapour and liquid phase) if one phase is continuously removed from the system. For example, during rainout processes, the ^{18}O isotopes preferentially change into the condensation phase, whereas the vapour phase is depleted in heavier isotopes (Clark and Fritz, 1997).

Under equilibrium conditions the $\delta^{18}O$ of speleothems only depend on the $\delta^{18}O$ of the dripwater and the cave temperature (Epstein et al., 1953). The cave temperature at the time of deposition influences the oxygen fractionation between the water and the calcite with a gradient of -0.22‰/°C at 20°C (Epstein et al., 1953). The $\delta^{18}O$ of the dripwater is influenced by the different effects of the global water cycle (Rozanski et al., 1993). These effects predominate the temperature-dependent fractionation during calcite precipitation in magnitude (Lachniet, 2009). There are a lot of processes altering the original climate signal on its way to the stalagmite. The $\delta^{18}O$ signal of water is in the hydrological cycle mainly controlled by phase changes, due to kinetic and equilibrium processes (Dansgaard, 1954). The starting point of the hydrological cycle of the Earth is the ocean, also termed as the ‘bulk of the earth evaporation’. For the interpretation of the paleoclimatic signal, information about the local and regional hydrology and climatology are necessary (Lachniet, 2009).

Temperature effect

Largest variations in the isotopic composition of precipitation are related to evaporation and condensation processes of the atmospheric air masses (Gat, 1996). If the condensation process runs as equilibrium fractionation, air temperature (cloud base temperature) is the dominant factor influencing the isotopic fractionation process between the cloud and the raindrop (Gat, 1996). Consequently, the isotopic composition of precipitation at a specific location can be correlated to the surface air temperature (Gat, 1996). For example, the heavier isotopes preferentially accumulate in the raindrops leaving the cloud. The lighter isotopes remain in the vapour phase (Gat, 1996).

The mean annual temperature at a given location is positively correlated with the mean $\delta^{18}O$ value of the local precipitation. This correlation is approximately +0.59‰ ±0.09‰ per °C for mid- to high-latitude locations (Rozanski et al., 1993). Consequently, a higher mean temperature leads to a higher $\delta^{18}O$ value in the local precipitation. This can also be supported by rainfall measurements above Sofular cave. Figure 3.6. shows that highest $\delta^{18}O$ in precipitation is achieved during summertime, when highest temperatures are expected in the Black Sea region (Fig. 3.6.).

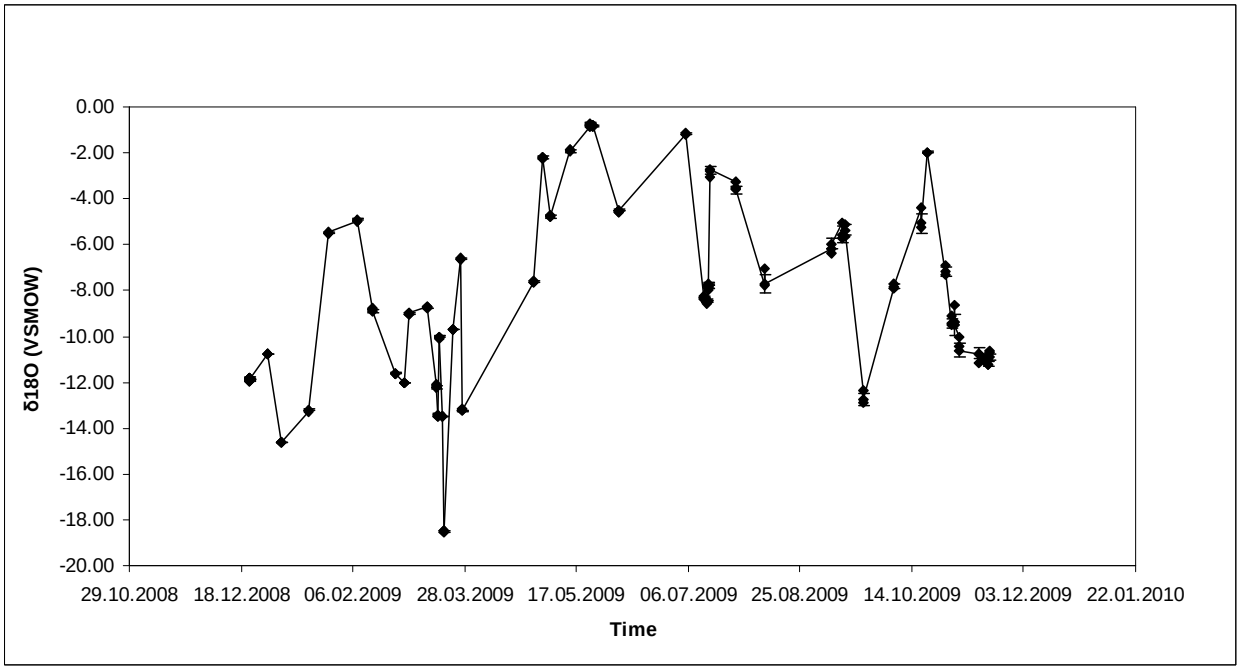

Fig. 3.6. $\delta^{18}O$ (VSMOW) rainfall measurements in a one year cycle above Sofular cave (modified after Göktürk, unpubl. data).

The exact correlation coefficient between temperature and the $\delta^{18}O$ of precipitation is location-dependent (Lachniet, 2009).

Altitude effect

The $\delta^{18}O$ of water vapour decreases with increasing altitude. Air masses approaching an orographic ridge are forced to rise and rain out as orographic rain. The heavier oxygen isotopes are, according to the law of the Rayleigh distillation, the first ones leaving the cloud. The remaining air masses are therefore depleted in heavier isotopes (Clark and Fritz, 1997). The altitude effect has a gradient of -0.2 to -0.3‰ $\delta^{18}O$ per 100m (McDermott et al., 1999).
A reinforcement of this effect occurs, if raindrops have to fall from a high altitude through a warmer air mass-column. These raindrops are re-evaporated in the air-column. For this reason, the longer falling rain is enriched with heavy isotopes (Rozanski et al., 1993).

Latitude effect

The main reservoirs for moisture are located in the equatorial region, where the air masses are transported by atmospheric circulation systems into several directions. The air masses travelling in poleward directions are increasingly depleted in heavier isotopes with growing distance to the equator. This is because of the repeating rainout events of the air masses on their way over the continents. These rainouts follow the law of the Rayleigh distillation. Consequently, the rain composition changes with increasing latitude (Clark and Fritz, 1997). The ice sheets on the poles are mainly built up of ice containing light oxygen isotopes, whereas the isotopic composition of precipitation at the equator is equal to the isotopic composition of the Sea (Spötl, 2001/2002 and references therein).

Continental effect

The continental effect describes the decrease of heavier isotopes within the air masses with the increasing distance from the ocean. This phenomenon occurs for the reason that air masses cool progressively towards the interior of the continent. The raindrops composed of heavier isotopes leave the cloud earlier by raining events (Clark and Fritz, 1997).

Amount effect

This effect mainly arises in the lower mid-latitudes and tropical monsoon-regions (Gat, 2001). During light rains raindrops are favourably evaporated below the cloud base and consequently the rain arriving at the surface is enriched in ^{18}O-isotopes (Lykoudis et al., 2009). Conversely, heavy rains are less affected by evaporation effects within the air column and therefore to a decreasing influence on the amount effect (Lykoudis et al., 2009).

The amount effect describes a decrease of the $\delta^{18}O$ of rainfall with an increase in the amount of rainfall. This phenomenon occurs mainly in the tropical regions, where deep convective systems often prevail (Lachniet, 2009). $\delta^{18}O$ values of different records rise with a gradient of -2- -3‰ per 100 millimetre increase in monthly amount of rain in Barbados (Jones et al., 2000).

Source effect

Air masses originating from different moisture sources may have different $\delta^{18}O$ signatures. The reason for this is that air masses from different directions are controlled by different air mass histories. This effect can also occur in case of direction changes of storm tracks (Rozanski et al., 1993).

Seasonal effect

In general, winter precipitation is isotopically lighter than summer precipitation, due to the above mentioned temperature effect. As an example, continental regions show higher seasonal variations in temperatures than other regions do. This consequently also leads to higher seasonal isotopic amplitudes (Clark and Fritz, 1997).

Ice volume effect

On glacial timescales, the ice volume effect has an influence on the $\delta^{18}O$ composition of oceans. The formation of the ice sheets results in isotopically heavier ocean water, because the ^{16}O-isotopes are evaporating faster and accumulate in continental ice sheets (Jex et al., 2009). The melting of ice sheets leads to a decrease in the $\delta^{18}O$ of seas by a value of -1.2‰ (Frumkin et al., 1999).

Additional factors influencing the $\delta^{18}O$ of water vapour on its way to the cave are air moisture differences, evaporative enrichment at the surface/epikarst zone, complex mixing histories (McDermott, 2004).

Within the soil aquifer, further modifications of the isotopic signal take place. These processes were already discussed in this master thesis in the section 3.12.

$\delta^{18}O$ signal of Sofular cave

From a previous study of Fleitmann et al. 2009, there is evidence that the decadal/centennial (for example: DO-cycles) variations in the $\delta^{18}O$ of stalagmites from Sofular cave are mainly induced by changes in air temperature and seasonality of precipitation (Fleitmann et al., 2009). On longer time-scales, the $\delta^{18}O$ of Sofular stalagmites are principally controlled by changes in the Black Sea surface waters. This is proven by a comparison between data of stalagmites and marine cores from the Black Sea (Fleitmann et al., 2009)

$\delta^{13}C$ profile

The $\delta^{13}C$ of stalagmite calcite mainly depends on the $\delta^{13}C$ of dissolved inorganic carbon (DIC) of drip water, growth rates of plants (Turner, 1982), exchanges with the gaseous phase and the supersaturation state of the water with respect to calcium carbonate (Richards and Dorale, 2003). The carbon dissolved in drip waters consists of atmospheric CO_2, soil CO_2 and dissolution of the karstic host rock (Fairchild et al., 2006b). The $\delta^{13}C$ of calcite is isotopically heavier than the gaseous CO_2 by approximately 10‰, due to several fractionation processes (eg. during the dissolution of CO_2, dissociation in HCO_3^- or CO_3^{2-} and precipitation of

$CaCO_3$). The main fractionation takes place during the dissolution of the carbonate host rock (Clark and Fritz, 1997). Compared to the atmosphere CO_2 concentrations are considerably higher. There are two sources of soil CO_2, root respiration and microbial decomposition of organic substances (soil organic matter (SOM)). The pCO_2 changes seasonally due to fluctuations in soil activity (Clark and Fritz, 1997). For example, if the pCO_2 of soil decreases in winter due to a smaller soil activity, the $\delta^{13}C$ values increase and vice versa (Spötl, 2001/2002 and therein). The $\delta^{13}C$ of soil CO_2 is closely related to the type (photosynthetic pathway) and density of vegetation above. C3 –vegetation (Calvin cycle) is mainly built up of trees and plants growing in the higher and middle latitudes (McDermott, 2004). Their $\delta^{13}C$ signature varies between -26 - -20‰ (VPDB). In stalagmites below a C3-plant community, the $\delta^{13}C$ fluctuates between -14 to -6 ‰ (VPDB) (McDermott, 2004). In order not to misinterpret the data, all the possible fractionation processes have to be carefully observed (McDermott et al., 2006).

C4-vegetation (grasses, sedges; Hatch-Slack cycle) is specialised to survive in dry and open ecosystems like tropical and temperate grasslands (more information about C4/C3-plants is provided by Clark and Fritz, 1997). Big maize, sorghum and sugarcane belong to the group of C4-plants with a $\delta^{13}C$ between -13 to -12‰ (VPDB) (Spötl, 2001/2002 and therein). Stalagmites under a C4-plant dominated plant community have a $\delta^{13}C$ signature between -6 to +2 ‰ (VPDB). After the wilting of the plants, their $\delta^{13}C$ signature gets into the soil and ground water (McDermott, 2004).

In general, the lighter C-isotopes in speleothems originate from soil CO_2, whereas the heavier carbon isotopes are dissolved from limestone bedrock (McDermott et al., 2006).

The $\delta^{13}C$ profile of stalagmites from Sofular cave is mainly controlled by the type of vegetation, the density of vegetation and the soil microbial activity (Fleitmann et al., 2009). For example, warmer and wetter climatic conditions would lead to a higher proportion of C3-plants within the vegetation, to more dense vegetation, and to enhanced soil productivity. Consequently, the $\delta^{13}C$ in deposited stalagmites decreases (Fleitmann et al., 2009). These factors themselves depend on the effective moisture and the ambient temperature.

The $\delta^{13}C$ for C3 and C4-plants in the Sofular stalagmites are -12‰ and -6‰ (VPDB) respectively. Today, the $\delta^{13}C$ signature varies around a value of about -10‰ (VPDB) (Fleitmann et al., 2009).

4 CHAPTER FOUR - RESULTS

4.1 URANIUM-THORIUM DATING

Thirteen U-Th dates were performed along the growth axis of stalagmite So-17A (Table 4.1.). The stalagmite grew continuously from an age of ± 122.96 ka BP to ± 86.19 ka BP. Age uncertainties lie in a range of 230 to 420 years, leading to an uncertainty of only 0.22 – 0.34%. The measurements were all performed at the Department of Geology and Geophysics, University of Minnesota, USA. All ages are in chronological order (Tab. 4.1.), indicating that an alteration after the deposition can be excluded. Based on the results of the U-Th dating, a precise age model could be constructed, which is based on a linear interpolation of the ages between the measurements. The aim of this age model is to achieve an attribution of environmental events to a certain age (Fankhauser et al. 2008).

The age-depth profile of the stalagmite So-17A is displayed in Fig. 4.1.. The growth history of the stalagmite So-17A reveals 13 periods of changing growth velocities.

For example, the interval between the two age-datings M5 and M6 includes a span of about 15 ka. However, the distance covered by this time period is the shortest on the stalagmite; this can be explained by a slow growth-rate during this phase. Afterwards, the growth rate

Sample Name	Depth [mm]	Age [ka]	± Uncertainty [ka]	± Uncertainty [%]	Growth rate in the Age model [mm yr^{-1}]
So-17A M1	16.1	86.46	0.238	0.28	0.057
So-17A M2	267.3	90.81	0.230	0.25	0.034
So-17A M7	396	94.65	0.208	0.22	0.031
So-17A M3	533.9	98.99	0.299	0.30	0.037
So-17A M8	580	100.25	0.246	0.25	0.033
So-17A M9	650	102.37	0.230	0.22	0.036
So-17A M10	757	105.31	0.268	0.25	0.025
So-17A M4	822.7	107.88	0.369	0.34	0.011
So-17A M5	831.9	108.72	0.299	0.28	0.020
So-17A M11	862	110.23	0.266	0.24	0.009
So-17A M12	916	116.40	0.320	0.27	0.045
So-17A M13	922	116.54	0.321	0.28	0.012
So-17A M6	995.1	122.26	0.416	0.34	0.012

Tab. 4.1. Summary of the obtained U-Th ages.

increased. The growth rates are determined by the number of performed age measurements. Therefore, real growth rates cannot be established on the basis of 13 U-Th dates. The growth history can only be divided into different time steps.

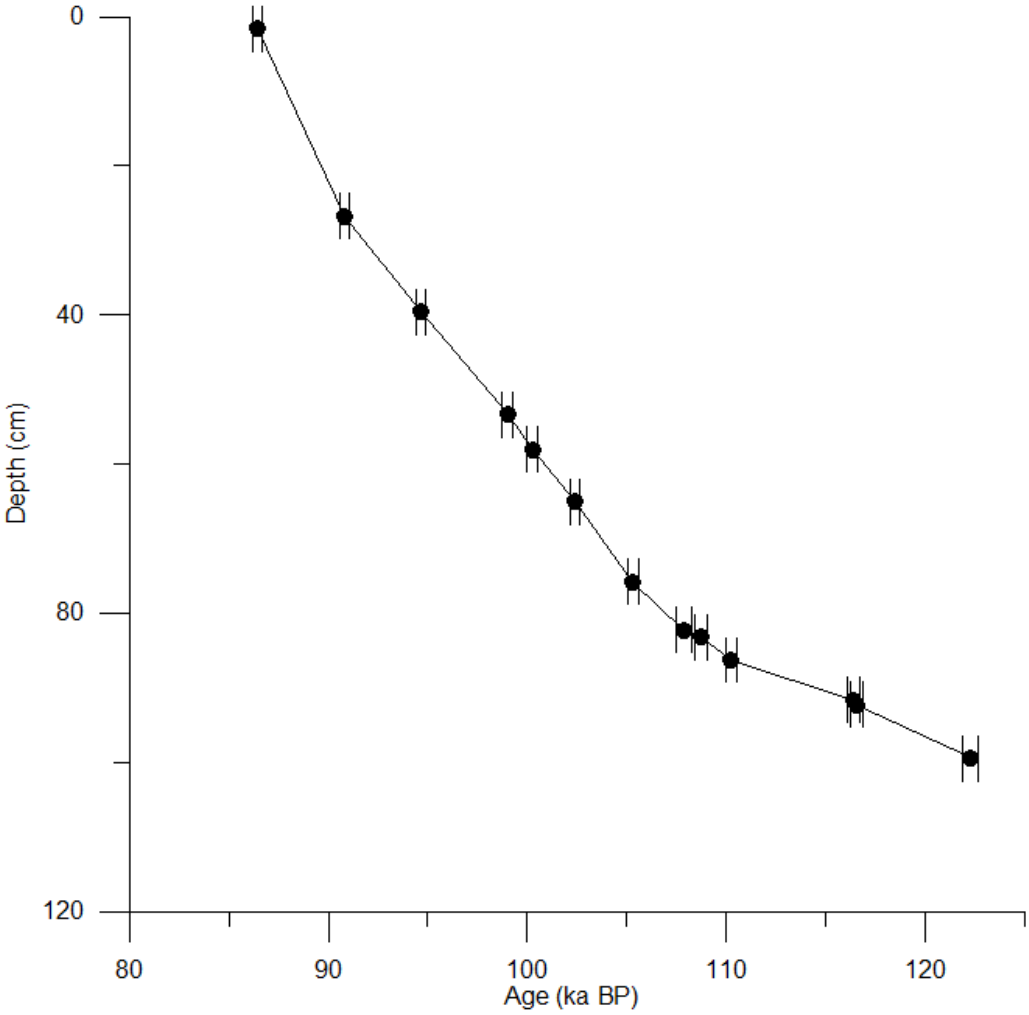

Fig. 4.1. Age-depth model: Growth history of stalagmite So-17A with its U-Th ages and the calculated growth rates.

4.2. STABLE ISOTOPES

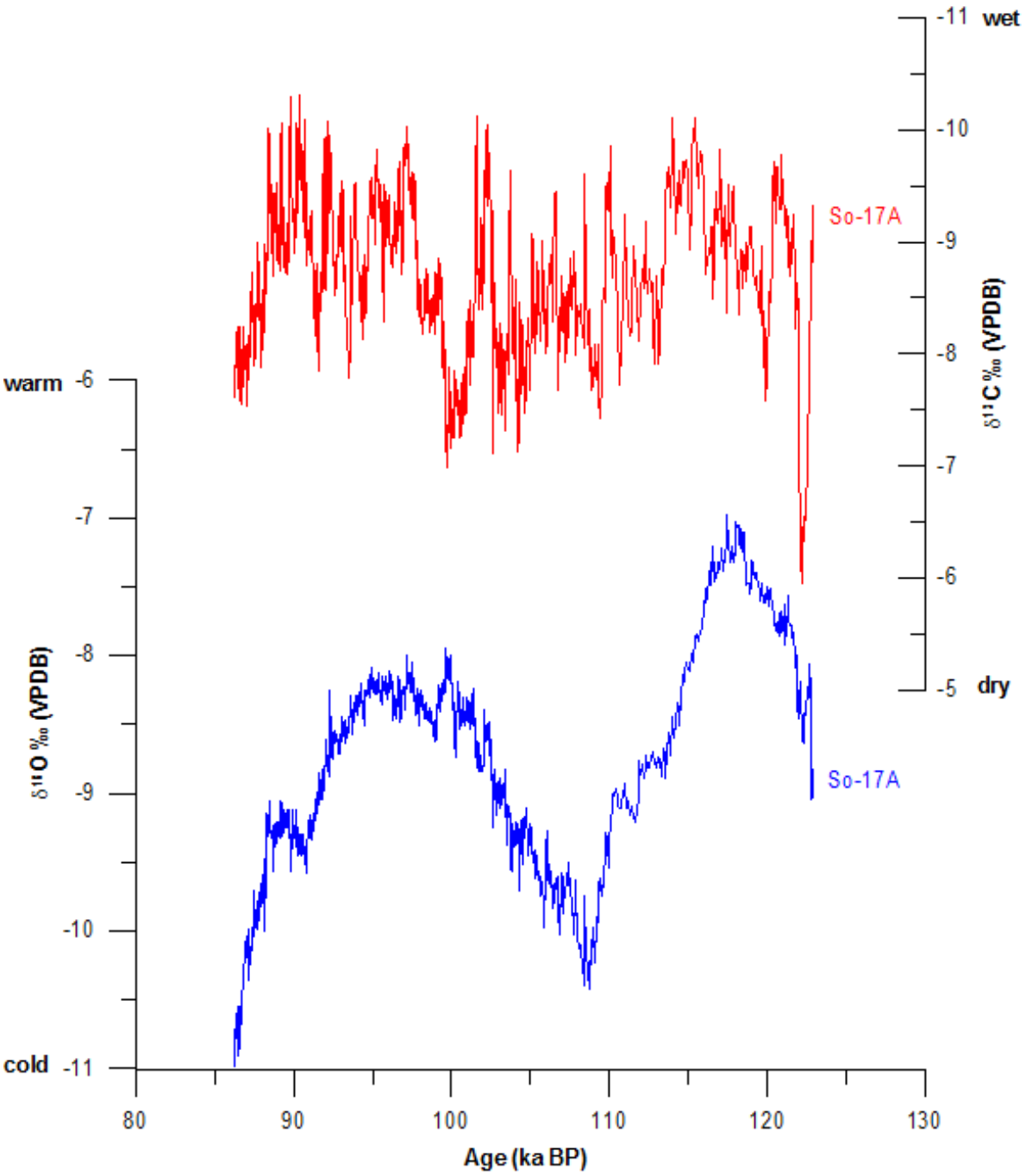

Fig. 4.2. Resulting $\delta^{18}O$ and $\delta^{13}C$ values of the stable isotope measurements

A total of 1306 samples have been drilled from stalagmite So-17A for stable isotope analysis. The drilling has been carried out with a continuous resolution of 0.75mm. The figure 4.2 shows the result of the stable isotope measurements which were performed by using a gas source mass spectrometer (see chapter 3.32 for further details). All isotope values are denoted relative to the VPDB standard. The average temporal resolution of the So-17A isotope profile

is 28.2 years. Depending on the growth rate, the temporal resolution of stalagmite So-17A lies within a range of 13.2 and 88.16 years. The $\delta^{18}O$ of stalagmite So-17A varies between a minimal value of -11.04‰ and a maximal value of -6.98‰. This adds up to an overall variation of the $\delta^{18}O$ in the range of 4.06‰ during the observed period. Overall, the main pattern produced by the data is a two-fold undulating distribution of $\delta^{18}O$ values.

The results of the $\delta^{13}C$ measurement do not show such a clear pattern. The $\delta^{13}C$ of So-17A lies within a maximal value of -5.95‰ and a minimal value of -10.3‰. This leads to a variation in the range of 4‰ which is approximately the same overall variance as in the $\delta^{18}O$ profile (Fig. 4.2.). However, the $\delta^{13}C$ shows faster changes over short time spans whereas the $\delta^{18}O$ varies within a small range looking at short periods.

The first peak in the $\delta^{18}O$ of So-17A is located between 122.90 ka BP and approximately 110 ka BP. The culmination point of this first peak lies around 117 ka BP. After this point, a decrease in $\delta^{18}O$ of ~-3.2‰ takes place in a period ~8 ka with the trough at the age of about 108.7 ka BP. Within this decrease, two small increases in the $\delta^{18}O$ can be recognized. These excursions take place about 113.5 ka BP and 111.7 ka BP.

Simultaneously, the $\delta^{13}C$ values of So-17A reach their peak just at the beginning of the record. Afterwards, they show an abrupt decrease at about 120 ka BP, before they again achieve a higher value of approximately -7.5‰ at 119 ka BP.

After the trough centered at 108.5 ka BP, $\delta^{18}O$ of So-17A increases over a span of approximately 9 ka until a next maximum is reached at around 99.7 ka BP with a value of 7.95‰. A small trough at ~99 ka BP follows directly this maximum with a decrease in the $\delta^{18}O$ of about 0.5‰. After that, the curve fluctuates around a certain value, before the values continuously sink after 93 ka BP. A third smaller culmination point is recognized around 88.5 ka BP where the $\delta^{18}O$ again reaches the -9‰ threshold. Subsequently, the values decrease to the end of the record.

At about 114 ka BP, a steady increase of the $\delta^{13}C$ of So-17A starts, with the culmination point at about 100 ka BP. During this period, one striking event was recorded at approximately 102ka BP, with a decrease of the $\delta^{13}C$ by nearly 3‰ in a short period. Furthermore, the short-term variation in this increase fluctuates in a range of approximately 2‰. Afterwards, a decrease in the $\delta^{13}C$ can be recognized, before the values again increase at the end of the record, approximately 88 ka BP.

The curve of the So-17A $\delta^{18}O$ shows less variation in the region of the first culmination point than it does in the second part. Especially the values after the first peak continue almost in a straight line, whereas the $\delta^{18}O$ following the trough show higher variation. The two steepest

declining parts within the $\delta^{18}O$ record can be found from about 117 ka BP to 114 ka BP, and later on, from about 88.5 ka BP to the end. The steepest increase can be detected at the beginning of the measured period from 123 ka BP to the culmination point at 117 ka BP.

The $\delta^{13}C$ mostly shows a uniform range of variation over the whole record. Probably, a smaller amount of variation can be recognized at the beginning and in the end of the record, with the highest variability from about 115 ka BP to 95 ka BP. These results will be discussed in the following chapters of this thesis.

5 CHAPTER FIVE - DISCUSSION

5.1 PALEOCLIMATIC INTERPRETATION OF THE $\delta^{13}C$ AND $\delta^{18}O$ PROFILES

To use isotopic signals for the reconstruction of environmental and climate history, their main controlling factors need to be revealed. The following chapter is dedicated to the estimation of these factors.

The isotopic record of stalagmite So-17A covers almost the entire marine isotope stage (MIS) 5. The term MIS originates from $\delta^{18}O$ sequences of marine sediments (Imbrie et al., 1984). Variations in these sequences are mainly caused by changes in $\delta^{18}O$ of the global ocean water (Shackleton et al., 2003). These $\delta^{18}O$ values were then used as the definition of several global ocean states. The MIS 5 lasted from approximately 128 ka BP to 71 ka BP (Imbrie et al., 1984) and is characterized by a minimal to low ice volume (Sanchez-Goni et al., 2007). MIS 5 can be divided into MIS 5e (Eemian interglacial; 128-115 ka BP), MIS 5d (Herning stadial; peaked 107 ka BP), MIS 5c (Brørup interstadial; peaked 99 ka BP), MIS 5b (Rederstall stadial; peaked 87 ka BP) and the MIS 5a (Odderade interstadial; peaked 80 ka BP) (Imbrie et al., 1984). As a whole, the stalagmite So-17A covers the period from the middle MIS 5e to the first part of the MIS 5b.

5.11 $\delta^{18}O$

The So-17A-record can be integrated into the stacked Sofular cave isotopic record of the last 600 ka (Fig. 5.1.), which has already been reconstructed by the group of Dominik Fleitmann. A comparison of So-17A $\delta^{18}O$ record with other time periods shows that the MIS 5e exhibits the most positive $\delta^{18}O$ of the whole record. Similar values were only recorded at the age of 215 to 205 ka BP during the MIS 7 (chronology from Imbrie et al., 1984). The isotopic level of the MIS 5d can be compared with a cold phase approximately 280 ka BP. The achieved $\delta^{18}O$ values during MIS 5c are comparable with the ones of MIS 1.

Long-term changes

The long-term variation in the $\delta^{18}O$ of So-17A covers a range of 4‰ (Fig. 5.2.). This isotopic variance has to be explained to achieve a reasonable interpretation of the paleoclimate during the MIS 5 in the Black Sea region.

The main factors influencing the $\delta^{18}O$ of stalagmites are the climate-controlled variation in the $\delta^{18}O$ of precipitation and temperature-controlled fractionation during calcite precipitation

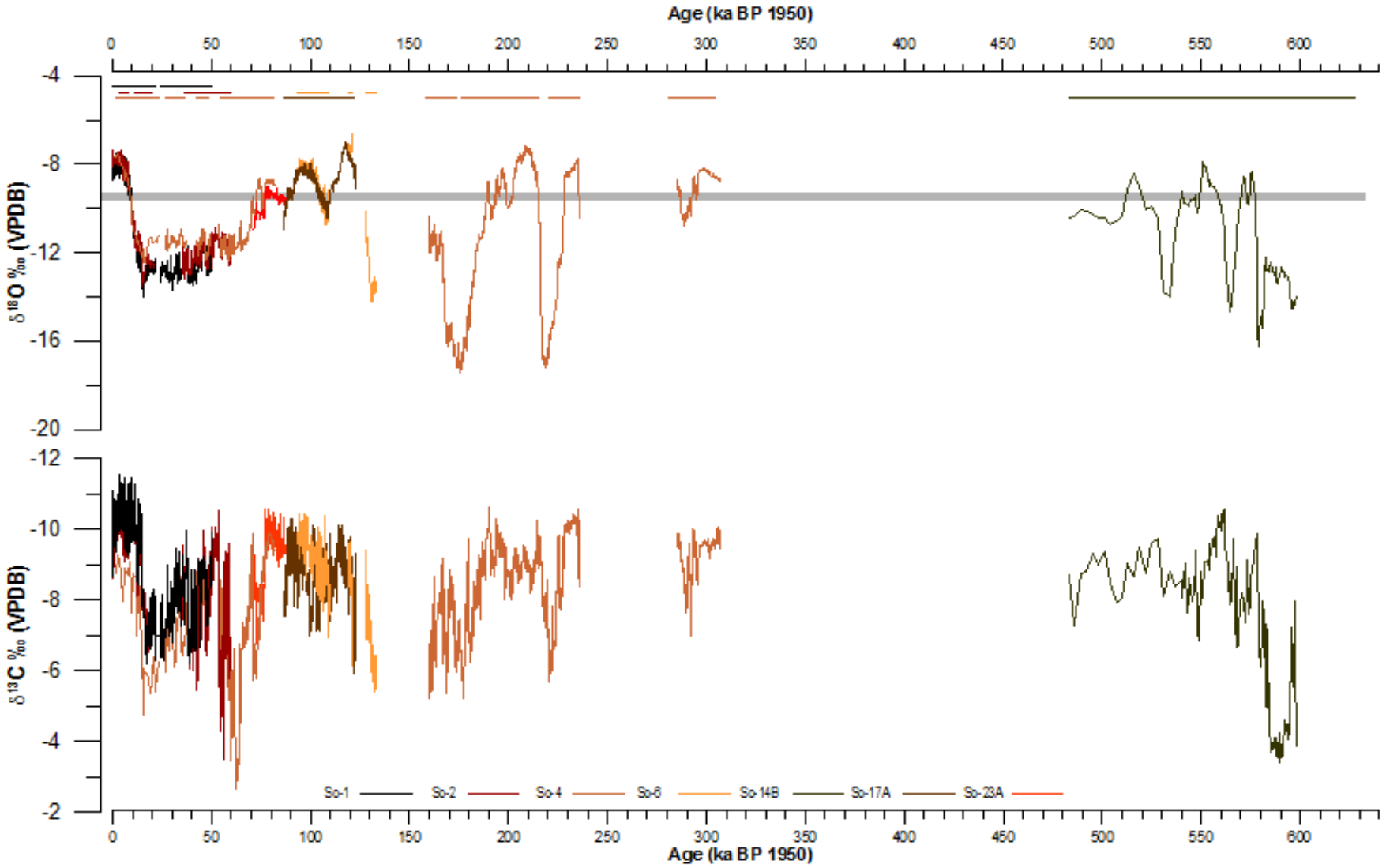

Fig. 5.1. Composite Sofular record over the last 600 ka BP (adopted from Badertscher in prep). The grey bar represents the depth of the Bosphorus.

(see chapter 3.3 for further details). It has to be checked if these factors are also responsible for the long-term change in the $\delta^{18}O$ of So-17A. The fractionation during the process of calcite precipitation is temperature-dependent. This temperature dependence is ~0.22‰/°C (Epstein et al., 1953).

The $\delta^{18}O$ difference between the MIS 5e and MIS 5d in So-17A is about -3.5‰. If this decrease after the MIS 5e had been completely induced by the fractionation process during the calcite precipitation, the temperature should have declined about 16°C within the cave. This is not realistic, because the temperature within the cave would then have fallen below the freezing point and these circumstances would have prevented stalagmite growth during MIS 5d. Consequently, the factor of calcite precipitation played only a minor role in the long-term $\delta^{18}O$ changes of So-17A. The second main factor inducing changes in the $\delta^{18}O$ of stalagmites is the climate-controlled variation in $\delta^{18}O$ of precipitation. For mid-latitude locations, the correlation coefficient is approximately 0.59‰/°C (see chapter 3.3 for further details; Rozanski et al., 1993). For an explanation of the 4‰ variation within the $\delta^{18}O$ profile of So-17A, the mean temperature should have changed by 6.8°C during MIS 5. A temperature change of about 6°C was suggested by Guiot et al. 1989 for central Europe, the eastern Mediterranean could have been exposed to less temperature variability due to the more southern position. Therefore, an additional factor has to be responsible for the first-order changes in the So-17A record. Bar-Matthews et al. 2003 has already suggested a relation between an Eastern Mediterranean marine isotope record and isotopic records of stalagmites from caves in Israel (Bar-Matthews et al., 2003). They argued that the Eastern Mediterranean surface waters served as a source for the precipitation falling above the Peqiin/Soreq caves (Bar-Matthews et al., 2003). A similar source effect can also be established between the Black Sea surface waters and the precipitation falling above Sofular cave. The predominating wind regimes lead a southward transport of air masses over the Black Sea, where they take up moisture. Later on, this moisture is precipitated above Sofular cave at the southern rim of the Black Sea. Thus, any changes in the isotopic signal of Black Sea surface waters will also induce a change in the $\delta^{18}O$ of local precipitation and thus in stalagmite $\delta^{18}O$ (Fleitmann et al., 2009).

Conclusively, we suggest that long-term variations of $\delta^{18}O$ in Sofular stalagmites relate to changes in the Black Sea surface waters (source-effect; Fleitmann et al., 2009). This argument will be discussed in more detail in the chapter 5.2.

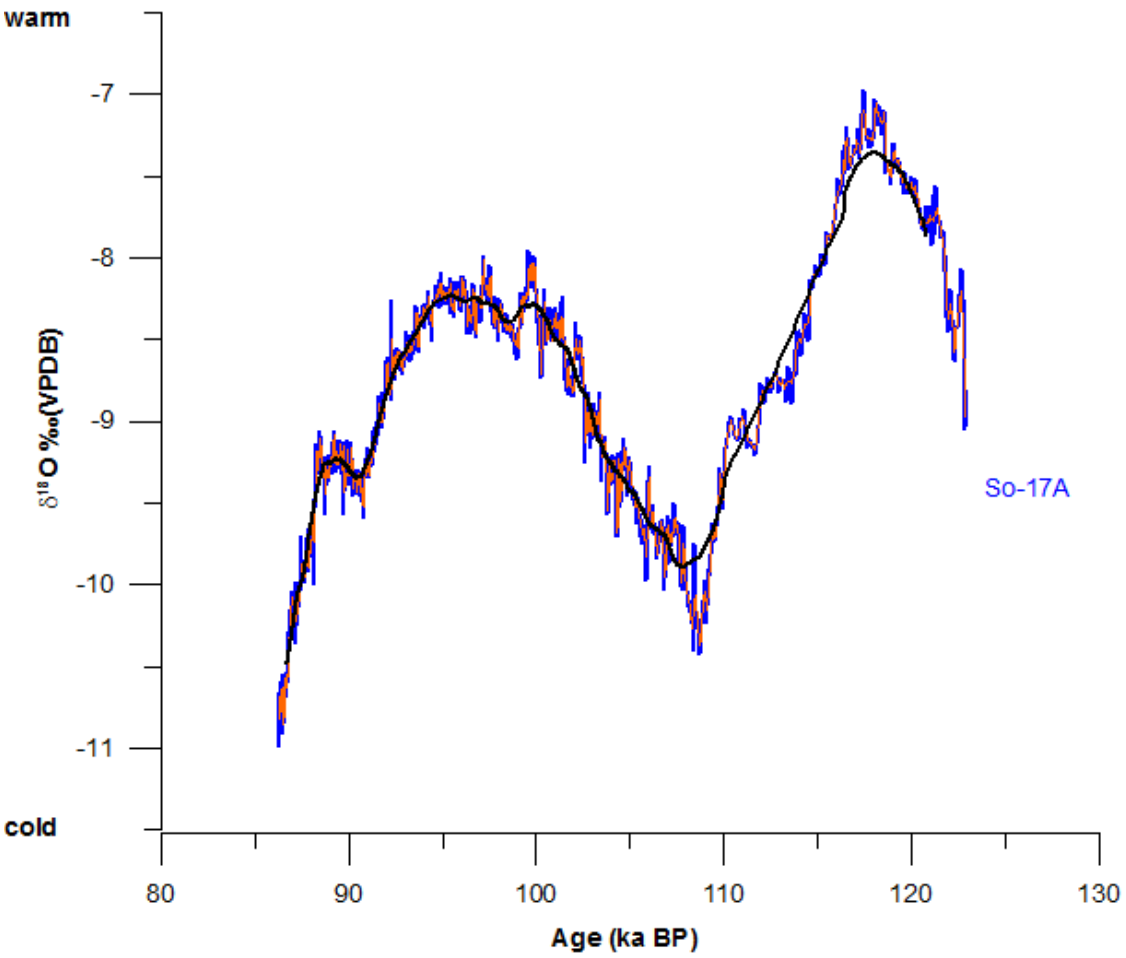

Fig. 5.2. Original $\delta^{18}O$ record of So-17A (blue), the long-term changes (moving average = 71 points, because of main resolution: 28 years and a turnover time of the Black Sea deep waters of ~2000 years (Östlund and Dryssen, 1986); black) and the short-term changes of the $\delta^{18}O$ record (moving average = 3 points; ~decadal variation; orange).

Short-term changes

The short-term changes within the $\delta^{18}O$ of So-17A extend over a range of 0.25 to 0.75‰ (Fig. 5.2.). The direct causes for these small amplitude changes are more complex to reveal, due to additional factors that have to be considered. Furthermore, the minimal changes within the $\delta^{18}O$ can be triggered by the effect of an individual factor. For example, a change of 0.75‰ in $\delta^{18}O$ can be reached by a 3.5°C change of the cave temperature or by a 1.3°C change of the air temperature, whereas the latter is more likely. The positive correlation between temperatures and $\delta^{18}O$ in precipitation indicates that higher (lower) temperatures lead to higher (lower) $\delta^{18}O$ in precipitation. Additional possible factors controlling the short-term variation in the $\delta^{18}O$ of stalagmites are the seasonality of precipitation, the amount of precipitation, changes in storm tracks and possible alteration of the signal within the karst system. The amount effect and storm track changes have minor influence on the $\delta^{18}O$ signal

of Sofular stalagmites. The short-term changes in $\delta^{18}O$ of stalagmites induced by interactions within the karst system are difficult to estimate. From the quantifiable short-term factors, the $\delta^{18}O$ of Sofular stalagmites is mainly controlled by changes in seasonality of precipitation and air temperatures on centennial to decadal time scales (Fleitmann et al., 2009). If for example the amount of precipitation increases in the summer months at the expense of winter precipitation, the resulting stalagmite $\delta^{18}O$ increases as summer rain is isotopically heavier than winter rain (see chapter 3.3 for further details; Clark and Fritz, 1997).

The temporal resolution of the stalagmite determines which short-term effects can be revealed and which effects are smoothed out within the karst aquifer. The resolution of a stalagmite mainly depends on sampling intervals and growth rate, the latter is controlled by the drip rate and saturation of cave drip waters with respect to Calcium (Richards and Dorale, 2003). The isotopic record of stalagmite So-17A has a mean resolution of approximately 28 years. This resolution does mainly allow a minimal reconstruction of stable isotope events on multi-decadal to centennial time scale. Therefore, climatic changes below a reoccurrence level of about 20 years can most likely not be detected in the So-17A. Though, long-term changes in seasonality of precipitation can be detected. Finally, information that could have been extracted from the $\delta^{18}O$ isotope profiles of So-17A will be discussed under the following paragraphs of the discussion.

5.12 $\delta^{13}C$

The $\delta^{13}C$ record of So-17A can also be integrated into the stacked Sofular cave isotopic record of the last 600 ka (Fig. 5.1.). Over all, the $\delta^{13}C$ record shows higher variability than the $\delta^{18}O$ record. The $\delta^{13}C$ of So-17A fluctuates in a range of -7 to -10‰. This range of variability is quite small, compared to glacial periods (eg. MIS 2) and other interglacial periods (eg. MIS 1) reaching values up to -3‰ and down to -11.5‰ respectively. Similar values as in So-17A were recorded at the age of 215 to 180 ka BP during the MIS 7 (chronology from Imbrie et al., 1984). Furthermore, the period of 580 to 535 ka BP (~MIS 14/15) was also characterized by a quite similar range of variation of $\delta^{13}C$.

Long-term changes

The first-order changes in the $\delta^{13}C$ of So-17A are in a range of 3‰ from -10‰ to -7‰ (Fig. 5.3.). The long-term changes in the $\delta^{13}C$ record are not that pronounced compared to the long-term variation in the $\delta^{18}O$ record. The $\delta^{13}C$ of So-17A follows the general course of the long-term climate changes ($\delta^{18}O$) during the MIS 5, in a dampened way.

5.1 PALEOCLIMATIC INTERPRETATION OF THE δ13C AND δ18O PROFILES

The $\delta^{13}C$ of DIC in groundwater have various sources. The CO_2 originates from the soil, atmosphere and dissolution of the karstic bedrock (Fairchild et al., 2006b); all of these steps are explained in detail in chapter 3.33. The $\delta^{13}C$ profiles of stalagmites from Sofular cave are mainly controlled by the type of vegetation, the density of vegetation and the soil microbial activity above the cave (Fleitmann et al., 2009); all of these factors are climate-controlled. Wetter and warmer conditions lead to a higher amount of C3-plants, a higher density of vegetation and a higher soil microbial activity. These conditions lead to a decrease in the $\delta^{13}C$ of stalagmite calcite. A higher abundance of C4-plants, a lower density of vegetation and a reduced soil microbial activity lead to an increase in the $\delta^{13}C$. Very dry conditions lead to a settlement of C4-plants, because they are able to deal with harsh climatic conditions. Furthermore, the soil microbial activity and the vegetation density decrease with extreme (hot/cold) temperatures and drier conditions (further details in chapter 3.33).

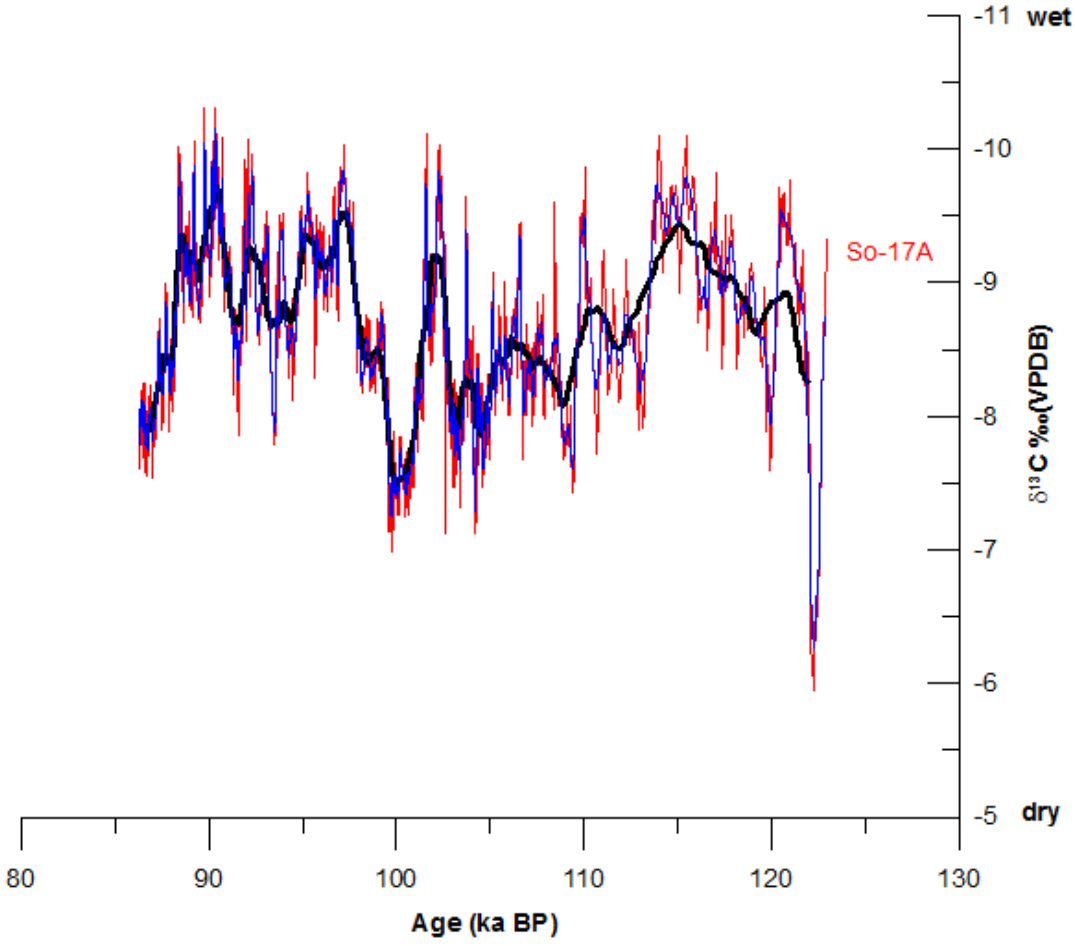

Fig. 5.3. Original $\delta^{13}C$ record of So-17A (red), the long-term changes (moving average = 37 points; possible long-term adaptation time of vegetation ~1000 years; black) and the short-term changes (moving average = 5 points; ~150 years; blue) of the $\delta^{13}C$ record.

The $\delta^{13}C$ in the Sofular stalagmites is characterized by C3 and C4-plant communities with values of -12‰ and -6‰ (VPDB) respectively (Fleitmann et al., 2009).

Short-term changes

The $\delta^{13}C$ short-term changes of So-17A fluctuate in a range of 0.5-2‰ (Fig. 5.3.). Most likely, the short-term variations in $\delta^{13}C$ of Sofular stalagmites reflect minimal adaptations of the vegetation (eg changes in density, microbial activity) above the cave to changing climate conditions. The $\delta^{13}C$ shows higher variability than the $\delta^{18}O$ on shorter time scales. This might reflect the sensitive reaction of vegetation to changes in climate. The comparison of $\delta^{13}C$ with the $\delta^{18}O$ is important to gather additional information about ambiguous $\delta^{18}O$ patterns. The analysis of $\delta^{13}C$ patterns indirectly serves also as a climate indicator (further information in chapters 3.13; 3.33).

5.13 So-6 versus So-17A

As it can be seen in Fig. 5.1., stalagmites So-6 and So-17A of Sofular cave cover quite similar periods. This offers a good opportunity to control the accuracy of the So-17A isotopic record. So-6 covers the time interval from approximately 133 ka BP to 93 ka BP. However, stalagmite growth was interrupted between 127 ka and 120 ka BP as well as between 119 ka and 109 ka BP. This cessation of the stalagmite growth was most likely caused by a dislocation of the drip source or blocking of the fissure feeding stalagmite So-6, because the gap occurred during warm phases and this excludes the possibility of a cold phase hiatus.

For the comparison, the So-17A record was aligned to the So-6 isotopic record, because this record exhibits the highest density of ages and therefore the most accurate dating in the time period from 110 to 105 ka BP.

Overall, the comparison of the $\delta^{18}O$ records of So-6/So-17A (Fig. 5.4; aligned records) shows that the values fluctuate in a quite similar range. The transition from MIS 5d to MIS 5c only differs slightly between the two records. The comparison of the $\delta^{13}C$ records of So-6/ So-17A reveals some contrasts. The $\delta^{13}C$ curve of the stalagmite So-6 follows the course of its $\delta^{18}O$ record and shows lower amplitude variability compared to the $\delta^{13}C$ record of So-17A. The reasons for the differences most likely are stalagmite specific ones. As it was discussed before under paragraph 3.12, the isotopic composition of stalagmites is not only influenced by external forcings but also by cave internal variations. For example, the soil and the build-up of the karst aquifer above the stalagmites control the geochemical properties of water and the water flow behaviour respectively (Fairchild et al., 2006a). These factors induce small-scale changes in the original isotope signal. Moreover, slight differences in the isotopic pattern between stalagmite So-6 and So-17 can also be caused by differences in the quality of the age models.

Conclusively, the comparison shows that a good reproducibility is obtained by the Sofular stalagmites. Therefore, it can be assumed that the Sofular cave environment is relatively stable.

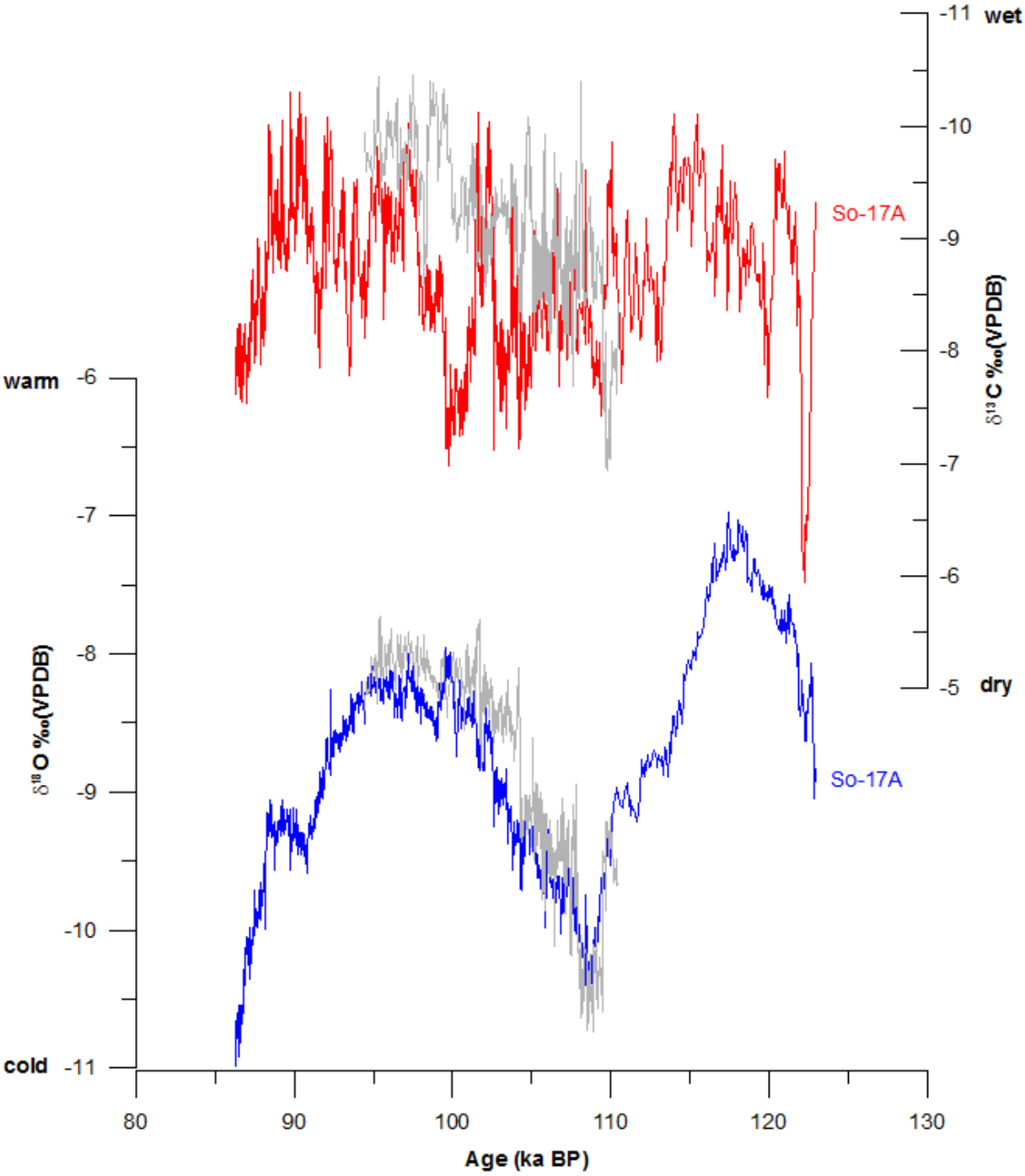

Fig. 5.4. The $\delta^{13}C$ and $\delta^{18}O$ plots of the stalagmites So-6 (grey) and So-17 (blue, red) covering equal periods.

5.2 $\delta^{18}O$ - BLACK SEA HISTORY

As discussed earlier in chapter 2.4., the history of the Black Sea is fairly well reconstructed for the last 30 ka BP. However, information on the hydrological history prior to 30 ka is rather fragmentary and little is known on the exact timing of earlier connection with the Mediterranean Sea, mainly because of the lack of datable climate archives. Therefore, the aim of the project and consequently also of this master thesis is to reconstruct the hydrological history of the Black Sea further back in time.

Phase changes between lake and sea phase have an influence on the isotopic signature of the Black Sea surface waters which are the main control of the long-term changes in the isotope profiles of the Sofular stalagmites, as it was discussed in chapter 5.11. Therefore, it is interesting how the transitions, from lake to sea phases and vice versa, were recorded in the isotopic record of stalagmite So-17A. Additionally, the isotopic record of So-6 was used for the comparison with the isotopic record of So-17A and to look at the transition from the MIS 6 to the MIS 5e.

In order to understand the isotopic signature of Black Sea surface waters, the prevailing processes within the Black Sea during sea phases and lake phases have to be known (Fig. 5.5.).

Climatic transitions to warm phases are often accompanied by sea level rises due to melt water inflow from disintegrating glaciers (eustatic change) and thermal expansion of warming water (thermostatic change; Clark and Huybers, 2009). With rising Black Sea level, the Bosphorus sill is reached after some time and an overflow of Black Sea water into the Mediterranean basin establishes. This process has been demonstrated before during the MIS 1 (Aksu et al., 2002a; Bahr et al., 2008; Kaminski et al., 2002). With some probable delay, the Mediterranean waters also reach the Bosphorus sill, but most likely, the waters cannot immediately penetrate into the Black Sea because of a strong one-layer discharge from the Black Sea through the Bosphorus Strait (Kaminski et al., 2002). With a further sea level rise (model developed by Lane-Serff et al., 1997 for MIS 1) or a decrease in the Black Sea discharge (Kaminski et al., 2002; shown for MIS 1) the Mediterranean waters are enabled to penetrate into the Black Sea. A connection between the two basins is defined by a two-layer flow through the Bosphorus Strait. The Mediterranean waters are characterized by higher temperatures, a higher $\delta^{18}O$ (~1.8‰) and a higher density than Black Sea waters (Özsoy and Ünlüata, 1997). Consequently, the denser waters of the Mediterranean enter the Black Sea basin as a plume and remain mainly at the bottom of the Black Sea (Özsoy and Ünlüata, 1997). The exchange between surface and deep waters within the Black Sea

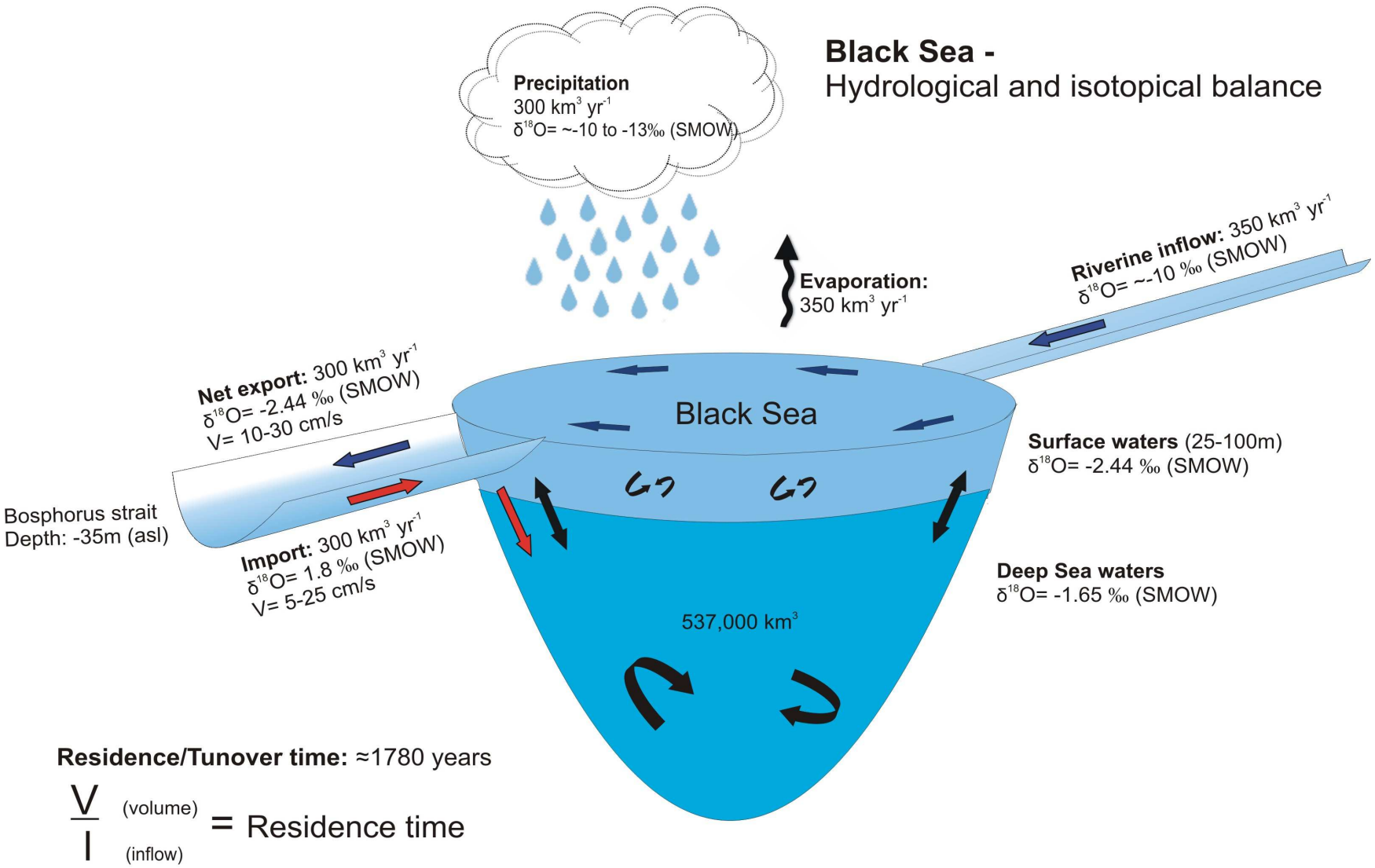

Fig. 5.5. Hydrological and isotopical balance of the Black Sea basin.

is increasingly limited, because of the denser Mediterranean waters at the bottom of the Black Sea. However, a mixing occurs at the boundary between deep waters, surface waters and the mouth of the Bosphorus towards the Black Sea (Özsoy and Ünlüata, 1997). This processes leads to an isotopic signature of the surface waters and the bottom waters of about -2.44‰ and -1.65‰ respectively (Swart, 1991; Fig. 5.5.).

Sea levels decrease during transitions from interglacial to glacial due to the built-up of ice sheets (Mangerud et al., 1991). As a result, the hypothesis can be brought up that the inflow of isotopically heavier Mediterranean waters through the Bosphorus Strait into the Black Sea deep waters decreases and leads to a gradual decrease of $\delta^{18}O$ surface waters. The final disconnection is characterized by the omitted influx of the most positive $\delta^{18}O$ source for Black Sea waters, namely the Mediterranean water inflow. The remaining influxes into the Black Sea system (precipitation, riverine input) are depleted in $\delta^{18}O$ (Swart, 1991; Fig. 5.5.). The disconnection of the Black and Mediterranean Seas induces also a disappearance of the stratification within the Black Sea. A steady adaptation of the Black Sea surface waters to changes in the deep waters takes place (Özsoy and Ünülata, 1997), resulting in a more depleted $\delta^{18}O$ of the Black Sea surface waters compared to connection phases. The time needed by the Black Sea for the adaptation leads to slow transitions in the isotopic signatures of Sofular stalagmites between sea and lake phases. The turnover process lasts for about 2000 years in the Black Sea deep waters (Östlund and Dyrssen, 1986).

The isotopic record of So-17A shows relatively slow transitions between interglacial, stadial and interstadial states. These characteristic shifts are mainly triggered by the adaptation processes, which are described above, leading to new stable state situations of the Black Sea.

A connection between the basins is established by a $\delta^{18}O$ isotopic signature of Sofular stalagmites at about ~-9.8‰ (~Bosphorus sill of -35m) as this was the earliest and most negative $\delta^{18}O$ value of Sofular stalagmites in the MIS 1 connected state (~9.5 ka BP). However, in figures, the transition from lake to sea phase (at a $\delta^{18}O$ level of -9.8‰) has to be marked by a bar. The bar reflects the adaptation of the Black Sea surface waters to changes in the deep waters (personal communication S. Badertscher). This threshold is important to look at when the exchange history between the Black Sea and the Mediterranean Sea is studied. It can be assumed that the threshold (~-9.8‰) and therefore also the Bosphorus sill (~-35m above sea level) remained more or less stable over time. The Black Sea seems to react very sensitively to global sea level changes and our records shows a relatively good coincidence with other proxies reflecting the global sea level (eg. Fig. 5.6). This could be due to the connections of the Black Sea with the global ocean via Bosphorus Strait. Small changes in its

depth may have occurred through removal or accumulation of unconsolidated material. The nearby lying North Anatolian Fault is a horizontal moving geological fault. Therefore, it most likely had no major impacts on the depth of the Bosphorus Strait (personal communication Dominik Fleitmann).

The results obtained from Sofular stalagmites are also compared to a study of Zubakov 1988 discussing the Black Sea history. However, it has to be remarked that the ages of the So-17A are more accurate compared to the ages of the Zubakov sequences. Zubakov established a Pleistocene climatostratigraphic sequence correlating Black Sea oxygen-isotope stages with changes in characteristics and stratigraphy of glacial deposits in loess, alluvial sequences and marine deposits of the Black Sea region (Zubakov, 1988). The study of the deposits allowed drawing conclusions about the origin and the composition of the waters in the Black Sea and Azov Sea respectively. The origin of these waters was either the Mediterranean Sea via Bosphorus Strait or the Caspian Sea via Manych Strait. Phases of salinization went together with invasions of Mediterranean fauna during warm phases. Alternatively, freshening of the Black Sea waters were accompanied by an invasion of Caspian waters and fauna during cold phases (Zubakov, 1988).

The So-17A time series provides the opportunity for studying three transitions between lake and sea phases of the Black Sea. In the following sections, phases of disconnection and reconnection are separately discussed.

Connection / Reconnection

The $\delta^{18}O$ of So-17A registered changes in the isotopic composition of the Black Sea surface waters on a long-term and consequently indicates periods of connection and disconnection of the Mediterranean and the Black Sea during MIS 5. The $\delta^{18}O$ of So-17A was about 1 to 2.8‰ above the critical level of -9.8‰ marking the depth of the Bosphorus sill during MIS 5e (~128 to 115 ka BP). Consequently, a connection was established between the basins at that time. A connection is also assumed, because global sea level was around 2-12m higher than today (Van Andel and Tzedakis, 1996; Waelbroeck et al., 2002; Fig. 5.6.). Zubakov 1988 also suggested a connection between the basins during MIS 5e. The transgression of the StrombusIII/Eltigen registered at about 127-120 ka BP (≈ MIS 5e) is characterized by an inflow of Mediterranean waters into the Black Sea. A connection was indicated by the presence of Mediterranean molluscs (Cardium tuberculatum) in Black Sea sediments (Zubakov, 1988). This sequence coincides roughly with the MIS 5e in the Black Sea isotopic records. Some age differences can occur between the data of Zubakov 1988 and Sofular,

because Zubakov had not the same possibilities in accurate age dating compared to the methods existing today.

One reestablishment of the connection between the Black Sea and the Mediterranean Sea is recorded in the So-17A sequence. This situation can be found at the transition from the MIS 5d (peaked ~107 ka BP) to MIS 5c (peaked ~99 ka BP). The additional incoming solar energy (Berger, 1978) and increasing temperatures triggered melting of ice sheets which were formed during MIS 5d (Mangerud, 1991). As it was discussed before in chapter 3.33 (ice volume effect), the formation of glacier includes mainly light oxygen isotopes. Therefore, the melting of glaciers led most likely to an inflow of depleted oxygen water into the adjacent basins. However, a melt water incursion which has affected the Black Sea surface waters can not be clearly detected in the $\delta^{18}O$ isotopic record of stalagmite So-17A, compared to the melt water signal that was detected by Fleitmann et al. 2009 at ~16.5 ka BP. As a whole, the amount of melt water produced in the MIS 6 and MIS 2 had to be larger than the ones at the end of MIS 5d, resulting in large $\delta^{18}O$ depletions in Black Sea surface waters. The melt water pulse at the end of MIS 6 (~131-130 ka BP) is recorded in stalagmite So-6. The $\delta^{18}O$ of So-6 shows a slight increase marking the transition to MIS 5e about 133.5-133 ka BP (Fig. 5.1.). Afterwards, the melt water leads to a decrease of -1‰ in the $\delta^{18}O$ of So-6 achieving the most negative isotopic value of -14.25‰ (PDB) at 130.95 ka BP. Subsequently, the curve ascends gradually. However, the establishment of the connection at the beginning of the MIS 5e was not recorded in stalagmite So-6 (Fig. 5.1.), due to a hiatus.

During the transition to the MIS 5c, global sea level rose continuously (Fig. 5.6.; Waelbroeck et al., 2002). Globally distributed studies indicate a sea level of around -20m during MIS 5c (Bard et al., 1990; Smart and Richards, 1992; Picket et al., 1985; Waelbroeck et al., 2002; Fig. 5.6.). Sea level rise can be mainly attributed to melt water input from disintegrating ice sheets, volume expansion of warmer water (Clark and Huybers, 2009) and the inflow from other basins. At about 107.5 ka BP, the $\delta^{18}O$ in So-17A reached the critical level of ~-9.8‰ indicating a possible connection between the Black Sea and the Mediterranean Sea. As the $\delta^{18}O$ of So-17A fluctuated around this critical value for another 1 ka, it is difficult to define an exact date for the reconnection. Furthermore, a possible preceding strong discharge of Black Sea waters into the Mediterranean Sea could have also prevented an earlier inflow of Mediterranean waters, as it has already been discussed for the reconnection at the transition from MIS 2 to MIS 1 (Kaminski et al., 2002).

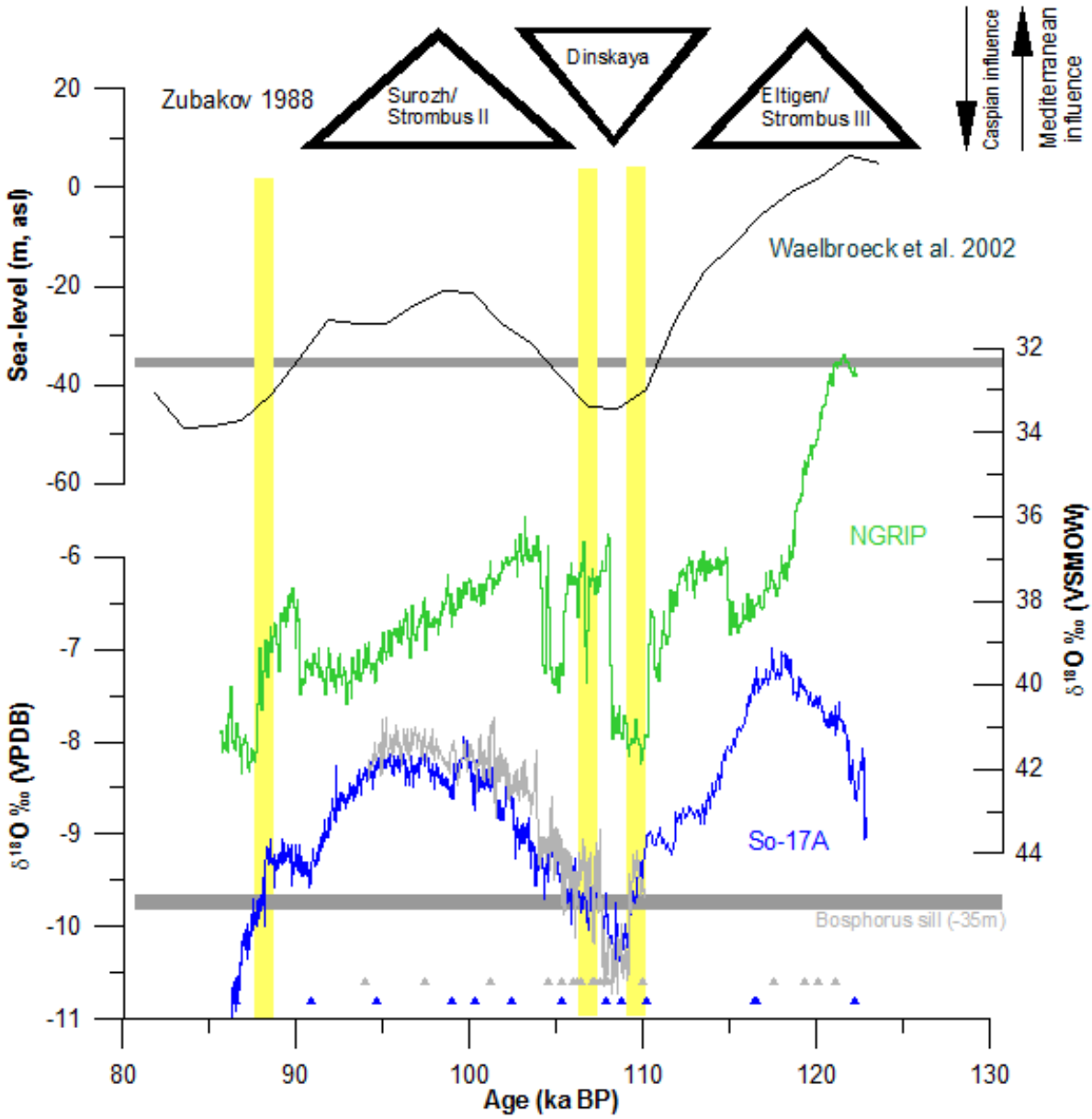

Fig. 5.6. The Black Sea history from 122.96 ka BP to 86.19 ka BP recorded by the $\delta^{18}O$ of the stalagmite So-17A. Additionally plotted are the $\delta^{18}O$ time series of the NGRIP members 2004, the $\delta^{18}O$ of So-6 (grey), the sea level reconstruction of Waelbroeck et al. 2002 and the climatostratigraphic sequence of the Black Sea from Zubakov 1988. The yellow bars indicate the transitions between lake and sea phases, whereas the grey bar stands for the depth of the Bosphorus Strait. The records are aligned as it was discussed in paragraph 5.13.

Zubakov 1988 reconstructed an invasion of Mediterranean mollusc fauna into the Black Sea during the Early Surozh period (≈ MIS 5c). Consequently, this study suggests also a connection during the MIS 5c (Zubakov, 1988). The connection is marked in the Sofular isotopic profiles by an increase in $\delta^{18}O$ (Fig. 5.6.; aligned records). Since 105 ka BP, the isotopic records of Sofular and Greenland begin to differ notably. The oxygen NGRIP record is a proxy for temperature variations in Greenland during the MIS 5 (NGRIP members, 2004). The $\delta^{18}O$ values of So-6/So-17A show a more or less gradual increase, whereas the $\delta^{18}O$ signal of the NGRIP record is characterized by a cold period at about 104 ka BP which is followed by a gradual decrease in temperatures since 102.5 ka BP. However, it is problematic to indicate ages for the NGRIP record as it is not absolutely dated.

Since the reconnection of the Black and Mediterranean Seas, the increase in the $\delta^{18}O$ of So-17A was most likely controlled by long-term changes the Black Sea surface waters. The surface waters adapted to the changes in the Black Sea deep waters (Özsoy and Ünlüata, 1997) which were influenced by the inflow of heavier isotopic water from the Mediterranean Sea (~1.8‰ SMOW) during connection phases. This led to an increase in the $\delta^{18}O$ of the Black Sea surface waters and consequently in the $\delta^{18}O$ of So-17A.

Over all, the sea level reconstruction of Waelbroeck et al. 2002 matches well with the $\delta^{18}O$ profile of So-17A (Waelbroeck et al., 2002; Fig. 5.6.). This good coincidence of the global sea level and the $\delta^{18}O$ record of So-17A could be explained by the connection of the Mediterranean Sea with the global ocean. The increasing global sea level in the period from 105 ka to 100 ka BP could have led to a sea level rise in the Mediterranean Sea and consequently to an increased export of Mediterranean waters into the Black Sea. Thus, Black Sea surface waters could have shown a more positive $\delta^{18}O$ signal. When global sea level reached a stable state about 100 ka BP, the export of Mediterranean waters could have remained stable and therefore also the $\delta^{18}O$ signal. However, the record was slightly adjusted to the So-17A record, because the age-model of the sea level reconstruction is not absolutely dated.

Conclusively, the surface water signal (long-term) predominated over the temperature/precipitation signal (short-term) signal in the $\delta^{18}O$ of So-17A during MIS 5.

Disconnection

The first break-up of the connection between the Mediterranean and the Black Sea captured by the So-17A record took place at the transition from MIS 5e to MIS 5d. The $\delta^{18}O$ of So-17A reached the critical level of -9.8‰ approximately 109.5 ka BP. During the MIS 5d, the $\delta^{18}O$ decreased to a minimal level of -10.5‰. The $\delta^{18}O$ of So-17A fell for about 2 ka below

the bar marking the critical value of -9.8‰. This could be an indication for short stadial conditions; however, the delay in the $\delta^{18}O$ of Sofular stalagmites has to be considered.

A disconnection of the basins most likely results in a decrease of the $\delta^{18}O$ surface waters. This reduction is mainly controlled by the hydrological balance of the Black Sea, as it was discussed earlier in this chapter. The depletion in $\delta^{18}O$ of So-17A during MIS 5d could have been an interaction between the source and the temperature effect. The source effect (chapter 5.2.) of the $\delta^{18}O$ in So-17A can be recognized by a comparison with the NGRIP record. Since these $\delta^{18}O$ ice records primarily register actual temperatures over Greenland, the transitions between different climate states proceed immediately, whereas the So-17A record shows a more gradual transition due to the capture of surface water signals (Fig. 5.6.).

The disconnection during MIS 5d can also be confirmed by other studies. Global sea level was at a level of about -50m during MIS 5d (Van Andel and Tzedakis, 1996). In the study of Zubakov 1988, the Dinskaya (≈ MIS 5d) is characterized by an invasion of Caspian molluscs (Didacna cristata) into the Black Sea. This is clear evidence for a transgression from Caspian Sea waters into the Black Sea (Zubakov, 1988). The stratification within the Mediterranean Sea disappeared, because of the pre-Surozh (before 105 ka BP) regression in the Black Sea (Ostrovsky et al., 1977) and a probable associated decrease in freshwater discharge through the Bosphorus Strait. Additionally, a cold pollen spectrum was found at the coast of the Kerchian Strait at that time (Zubakov, 1988).

The third key event concerning the connection between the Mediterranean and the Black Sea occurred about 91 ka BP. The cooling after the MIS 5c brought the sea level close to the Bosphorus sill. The $\delta^{18}O$ of So-17A indicates that the connection was most likely maintained at that time. The disconnection of the basins took place about 88 ka BP (~9.5‰). The decreasing temperatures could have led to depleted $\delta^{18}O$ values in precipitation and the rivers might have transported isotopic lighter water from the northern regions into the Black Sea basin (isotope effects; further details in chapter 3.33). Furthermore, the water input from the Mediterranean Sea stopped because of the dropping sea level. After a first steep decrease in the $\delta^{18}O$ of So-17A (~88 ka BP) following the aligned Greenland ice core, the $\delta^{18}O$ curve of So-17A proceeds more gradually. This gradual decrease could have been associated with a decrease in the inflow of Mediterranean waters into the Black Sea through the Bosphorus Strait and the adaptation processes within the Black Sea.

All in all, we suggest that the Black Sea was in a lake phase during MIS 5d (from~109.5 to ~107.5 ka BP) and MIS 5b (since ~88 ka BP) and in a sea phase during MIS 5e (to 109.5 ka BP) and 5c (from ~107.5 to 88 ka BP).

5.3 $\delta^{13}C$ – EASTERN MEDITERRANEAN CLIMATE HISTORY

Reconstruction of the climate during MIS 5

There is a lack of well dated and highly resolved climate records covering the MIS 5 in the eastern Mediterranean region. The isotopic data of So-17A can be used to reconstruct climate for this period. As it was discussed in chapter 5.12, the $\delta^{13}C$ of Sofular stalagmites is mainly controlled by type of vegetation, microbial soil activity and density of vegetation above the cave. These factors are themselves influenced by climatic conditions above the cave (temperature, amount of precipitation; Fleitmann et al. 2009). As the $\delta^{18}O$ of Sofular stalagmites is mainly controlled by the Black Sea surface waters on longer time scales, the $\delta^{13}C$ record of So-17A is taken as an indicator for the climate history in the eastern Mediterranean region during MIS 5. However, on short time scales, the $\delta^{18}O$ of Sofular stalagmites is controlled by temperature and seasonality of precipitation and consequently serves as an additional device for the climate reconstruction.

From ~123 to 114 ka BP, the $\delta^{13}C$ of So-17A increases to a value of ~-10‰. This indicates a trend to an enhanced microbial soil activity, an increased density of vegetation and a preferential settlement of C3-plants. These vegetation conditions are most likely triggered by relatively warm and wet climate (see chapter 5.11 for further information), which might have predominated during the MIS 5e. Per definition, the MIS 5e lasted until an age of 115 ka BP (Imbrie et al., 1984). The shifted MIS 5e in the $\delta^{13}C$ record of So-17A could be explained by the additional time required by vegetation to adapt to changes in climate. However, Fleitmann et al. 2009 suggested an adaptation time of about 300 years (Fleitmann et al., 2009). Consequently, the time lag of about 1 ka can not be fully explained by establishment of an equilibrium between vegetation and climate.

The reconstructed climate conditions during MIS 5e can be confirmed by the results of several ice core, marine and continental sediment studies (Van Andel and Tzedakis, 1996). Results of a north-eastern Italy pollen study indicate a dominance of thermophilous trees and shrubs during the MIS 5e (Pini et al., 2009). At about 125 ka BP, Mediterranean vegetation expanded into the southern part of Europe. This community of plants is well adapted to hot summers and high summer insolation (Tzedakis et al., 2003)

From 114 to 114.5 ka BP, the $\delta^{13}C$ of So-17A increased to a level of -8‰ in about 500 years. Afterwards, the values show a long-term increase to ~-7‰, to an age of 103 ka BP. $\delta^{13}C$ values in a range of -7 to -8‰ are most likely an indication for a minor vegetation density, a minor microbial activity and a probable settlement of some more C4-plants above the cave compared to MIS 5e (Fig. 5.1.). These vegetation conditions are mainly induced by relatively

dry and cold/hot climate. However, it can be assumed that cold temperatures prevailed during the MIS 5d. Similar findings about the course of the late MIS 5e were also presented by an European pollen study of Brewer et al. 2008. These findings include a decrease in temperatures and precipitation after the climate optimum phase of the MIS 5e at ~120 ka BP (Brewer et al., 2008). Brewer suggested that this reduction is mainly restricted to locations at higher latitudes. For example, the study of Allen et al. (1999) shows an onset of cooler conditions about 5ka later in the south (Lago di Monticchio; Allen et al., 1999). A transition into MIS 5d at 115 ka BP would better coincide with the long-term changes in $\delta^{13}C$ of So-17A. Tzedakis et al. 2003 suggested with a study in Greece that the cooling phase at the end of the MIS 5e (~120 ka BP) was responsible for the change of the vegetation from taiga into tundra forest. The decrease in temperature was most likely triggered by changes in the orbital parameters leading to a reduction in the northern hemisphere summer insolation (Tzedakis, 2003). The reduction in insolation was mainly caused by a change of the sun's relative position towards the Earth, from a perihelion into an aphelion position (Berger et al., 1993).

In the Baikal Sea region, taiga forest was replaced by cool grass-shrub communities at the transition from MIS 5e to MIS 5d (Tarasov et al., 2007). Further on, the taiga boundary moved farther south. In southern Europe, the main limiting factor of vegetation growth was not temperature, but rather moisture availability (Tzedakis, 2003). One responsible factor triggering the decrease in precipitation could have been the southward shift of the North Atlantic current at about 115 ka BP (Müller and Kukla, 2004), which led to a decrease in moisture transport towards the Mediterranean region (Müller and Kukla, 2004). Between 115 and 110 ka BP, deciduous vegetation prevailed in southern Europe (Müller and Kukla, 2004). After 110 ka BP when full MIS 5d conditions were reached, tree populations disappeared from southern Europe (Tzedakis, 2003). The pollen study of Fauquette et al. 1999 from France shows the dominance of cold biomes during MIS 5d. These cold biomes mainly consisted of cool conifer forest, taiga or cold steppes (Fauquette et al., 1999).

After the MIS 5d, the $\delta^{13}C$ of So-17A changed from a value of ~-7‰ at 103 ka BP to -10.3‰ at 91 ka BP. This is a change of -3.3‰ in $\delta^{13}C$ in a period of 12 ka. Again, this $\delta^{13}C$ signal indicates the predominance of relatively warm and wet climatic conditions during the MIS 5c. The MIS 5c is the first warm phase after the MIS 5e. From the $\delta^{13}C$ of So-17A it cannot be clarified if the MIS 5c reached MIS 5e climatic optimum levels, because the MIS 5e is not fully covered by So-17A. However, mean June insolation at 65°N was about 20 W/m^{-2} lower during MIS 5c compared to MIS 5e (Berger, 1978). A study from Gandouin et al. 2007 shows that temperatures reconstructed with chronomids reached approximately a late MIS 5e-level

in France during the MIS 5c (Gandouin et al., 2007). A milder and wetter MIS 5e is suggested by a pollen record from Lake Urmia, in the North-West of Iran (Djamali et al., 2008). The occurrence of the mesic, thermophilous plant Zelkova carpinifolia is an indication of climatic conditions associated with mild winters and a high amount of spring or summer rainfall. The absence of this pollen during the climate phases following the MIS 5e is interpreted being a sign that MIS 5e optimum conditions have never been reached again (Djamali et al., 2008). Generally, the interstadial phases are marked by a reestablishment of temperate biomes with mixed and sometimes deciduous plant communities (Fauquette et al., 1999).

The increasing amplitude that can be detected in the second part of the $\delta^{18}O$ record of So-17A might have been triggered by the nonlinear responses to changes in insolation which may occur during climatic transition between preferred climate states (Frolgey et al., 1999). Another possibility is that the MIS 5c climate was characterized by a more pronounced seasonality than MIS 5e. A more seasonal climate of MIS 5c indicates also a multiproxy study of Aalbersberg and Litt 1998 for north-western to north-eastern Europe. During MIS 5c, the mean minimum summer temperature remained more or less stable, whereas the mean minimum winter temperatures decreased about 10°C compared to MIS 5e (Aalbersberg and Litt, 1998). Similar conditions can probably also be assumed for the Black Sea region. The relative stability of the warm temperatures could be explained by an influence of the Asian monsoon system (Johnson et al., 2006) on the Black Sea climate system. Interstadial phases are associated with weaker westerly winds and an enhanced summer monsoon (An, 2000), due to a higher northern hemispheric summer radiation (Prell and Kutzbach, 1987). This situation leads to a settlement of the Intertropical Convergence Zone (ITCZ) farther north (Johnson et al., 2006; An, 2000; Kutzbach et al., 1992). Consequently, the Black Sea region could have got into the subsidence zone of the local Hadley cell. The climate in this zone is most likely dry and warm, because of the subsidence of the air (Rodwell and Hoskins, 1996). This led possibly to seasonal changes of precipitation and temperature patterns during MIS 5c. Furthermore, it was suggested that there was also less evaporation during MIS 5c compared to MIS 5e, due to the cooler temperatures (Hodge et al., 2008). This could have possibly led to the improved plant productivity and consequently to slightly more negative $\delta^{13}C$ values during MIS 5c compared to MIS 5e. More negative $\delta^{18}O$ values (eg. 109 ka BP) in the second part of the So-17A record could maybe explained by an increase of the ratio between winter precipitation and summer precipitation due to enhanced summer dryness. The $\delta^{13}C$ of So-17A contemporaneously shows a decrease indicating probably a decreased vegetation density or microbial activity, due to the high temperatures and the lack of moisture during summer.

However, a final solution for the situation leading to higher seasonality in the Black Sea region cannot be provided by this master thesis. Van Andel and Tzedakis 1996 suggested also more continental climate during the MIS 5c compared to the MIS 5e (Van Andel and Tzedakis, 1996).

From about 91 ka BP to 86.19, the $\delta^{13}C$ of So-17A steadily increased from a value of -10.3‰ to -7.6‰. A $\delta^{13}C$ of -7.6‰ indicates again an establishment of cooler and drier conditions during MIS 5b compared to MIS 5c. This overall increase is interrupted by a short decrease in $\delta^{13}C$ at ~88.5 ka BP. This decrease indicates a possible climatic short event characterized by warmer and drier conditions. The same event can also be observed in the NGRIP record of Greenland DO22 (Fig. 5.10.). The occurrence of additional short events will be discussed in chapter 5.4. The $\delta^{13}C$ record shows that the MIS 5b was probably dominated by harsher conditions than the MIS 5d. However, the differences between these two stadials cannot be completely revealed because the MIS 5b is not entirely recorded in stalagmite So-17A.

Conclusively, we suggest that the conditions during the whole MIS 5 were most likely favourable for plant growth as $\delta^{13}C$ of So-17A only varies in a range of 3‰ on long-term scales. This is half of the variance that can be recognized in stalagmite So-1 covering the MIS 2 and MIS 1. In the $\delta^{13}C$ record of So-1, the values vary in a range of ~-6.2 to ~-11.6‰. Consequently, the climatic conditions during MIS 5 were most likely wet and warm enough for plants (mainly C3-plants) to grow (Fig. 5.3). This indicates minimal changes in the plant assemblages and consequently, beneficial climatic conditions for the plants above the cave during the major part of the MIS 5. Besides, possible refugias of thermophilous plants during the cold phases of MIS 5 could have been situated in relative proximity to the cave, due to the southern position of the cave and the moderate climate changes in this period. These conditions could have allowed a fast resettlement of the thermophilous plants in the cave region after a cold phase.

The $\delta^{13}C$ of So-17A remained more or less between -8 to -10‰, therefore the dominance of thermophilous plants can be suggested. During MIS 2, the $\delta^{13}C$ of So-1 rather fluctuated in a range of -6 to -8‰ and C4 plants predominated above the cave (Fankhauser et al., 2008; Fleitmann et al., 2009).

Paleoclimate: MIS 5e versus MIS 1

To get an idea about the anomaly of the current climate change, it is important to have a look at the conditions during the previous interglacial (MIS 5e). The comparison of the MIS 5e and the MIS 1 enables to reveal differences and their possible causes. For this comparison, the MIS 5e is assumed to have extended over a time period from 126 to 110 ka BP in So-17A, because of the shift which is caused by the Black Sea effect. As the same long-term effect is also present in the $\delta^{18}O$ of So-1, this assumption is reasonable. The start of the MIS 1 is set to an age of approximately 11.7 ka BP and is still continuing today (Rasmussen et al., 2006).

The study of Fankhauser et al. 2008 supported the general view of a warm and wet MIS 1 climate in the Eastern Mediterranean (Fankhauser et al., 2008, Mudie et al., 2002; Bar-Matthews et al., 1997; Fleitmann et al., 2009). At a first glance at Fig. 5.7.a, it is noticeable that the MIS 5e (blue) shows generally a higher $\delta^{18}O$ than the MIS 1. The maximal difference between the $\delta^{18}O$ curve of MIS 1 and MIS 5e is around 1‰ during the MIS 5e (~ 118 ka BP) and MIS 1 (~ 4 ka BP) optimum. The onset of the MIS 5e curve shows values approximately 0.5‰ higher than the early MIS 1. The termination of the MIS 5e is marked by its $\delta^{18}O$ falling below the MIS 1 curve. Several reasons can theoretically lie behind these higher $\delta^{18}O$ of the MIS 5e. First, a positive correlation of 0.59‰/°C (Rozanski et al., 1993) exists between temperature and $\delta^{18}O$ in precipitation. Therefore, higher temperatures lead to a higher $\delta^{18}O$. The MIS 5e could have been ~1-2°C warmer than the MIS 1 at 118 and 4 ka BP, respectively, if temperature had been the main control factor of $\delta^{18}O$. Alternatively, an increasing amount of precipitation is negatively correlated with $\delta^{18}O$ of stalagmites. Consequently, higher amounts of precipitation would lead to a decrease in $\delta^{18}O$. Therefore, a wetter MIS 1 or a warmer MIS 5e would both work as possible solutions fitting into the isotopic record. An additional approach could be that the temperatures during the MIS 5e were enormously high. A higher amount of precipitation could have led to an abatement of the differences between the $\delta^{18}O$ of the MIS 1 and MIS 5e. However, the amount effect is not the dominating factor and is only linked with summer precipitation. The study of Zelikson et al. 1998 shows that the MIS 5e temperatures were about 1°C higher than the MIS 1 temperatures (Zelikson et al., 1998). The $\delta^{13}C$ record is an additional tool to solve the indecisive climate situation of the MIS 5e. The $\delta^{13}C$ of the MIS 5e are higher than the MIS 1 during the major part of the interglacial periods. The differences between the $\delta^{13}C$ curves of the interglacials add up to a value of ~2‰ at ~118 and 4 ka BP. These results indicate that the climate during the MIS 5e was most likely drier. To draw a first conclusion, the climate of the MIS 5e was drier and warmer than the MIS 1 during a major part of its duration. The biggest differences can be

recognized at ~118 and 4 ka BP of the MIS 5e and MIS 1 respectively, whereas the early and the late phases are defined by a convergence of the isotopic curves.

The $\delta^{18}O$ curves of the MIS 5e and MIS 1 achieved stable conditions approximately 118 ka BP and 6 ka BP respectively. From that point, the $\delta^{18}O$ of the MIS 1 fluctuated around a -8‰, whereas the curve of MIS 5e began to descend at about 116 ka BP. The decrease in $\delta^{18}O$ of So-17A at the end of MIS 5e (~116 ka BP) is characterized by the decrease in temperatures and the Black Sea effect. The $\delta^{18}O$ of So-17A achieved a MIS 1 level of -8‰ at about 114 ka BP. At the same time, the $\delta^{13}C$ of the MIS 5e record also reached MIS 1-levels (~-9.5‰). Therefore, it can be assumed that climatic/environmental conditions at 115 – 114 ka BP were quite similar to the modern climate conditions in Northern Turkey. This hypothesis can be supported by the fact that deciduous vegetation prevailed in southern Europe during the period from 115 to 110 ka BP (Müller and Kukla, 2004). The modern C3-dominated vegetation ($\delta^{13}C$: -10‰) above Sofular Cave consists of shrubs and trees (Fleitmann et al., 2009) and is therefore probably very similar to the late MIS 5e plant community (Fig. 5.7.b).

After 114 ka BP, the $\delta^{18}O$ of So-17A decreased steadily and the climate changed into the MIS 5b. Conversely, the $\delta^{18}O$ of the MIS 1 still remained at a stable level of -8‰.

For the comparison of the interglacials, it is important to consider the differences in the orbital forcings. Berger et al. 1993 suggested that the MIS 1 never reached an MIS 5e insolation level during the whole period (Berger et al., 1993). This is most likely the main forcing factor leading to higher temperatures registered in the MIS 5e.

In the MIS 1 record, there is no indication for a descent of the $\delta^{18}O$ curve. However, as the long-term changes in the Sofular stalagmites are controlled by the surface waters of the Black Sea, the $\delta^{18}O$ changes could occur with a certain delay. Kukla et al. 2002 found in a study that only small changes in insolation are expected for the next 100 ka (Kukla et al., 2002). Berger and Loutre 2002 came to the conclusion that the MIS 1 may last for another 50 ka (Berger and Loutre, 2002). In the Lake Baikal region, for instance, the MIS 1 forest phase already lasts some thousands of years longer than the forest phase of the MIS 5e (Tarasov et al., 2007).

The termination of the MIS 5e was most likely triggered by the change of the sun from perihelion into aphelion position and was quite similar to modern orbital configuration (Berger et al., 1993). In the case of the MIS 5e, the change into stadial conditions occurred about 13 ka after the start of MIS 5e. If this cycle is chronologically maintained, this principle can also be applied to the MIS 1. Consequently, this shows that at the moment we should be at such a crossing point from interglacial to stadial/glacial conditions (Kukla et al., 1997). However, the earth today receives 40W/m^2 more solar energy than 115 ka BP in northern

Europe (~60°N). Furthermore, the decrease in insolation was twice as large over the course of the MIS 5e compared to the MIS 1 (Risebrobakken et al., 2007). The additional energy which the earth receives today is perhaps one factor which forces the maintaining of the MIS 1 conditions compared to MIS 5e. An additional forcing factor which could also be responsible for the extension of MIS 1 is the settlement and the activities of humans (Risebrobakken et al., 2007). Associated with an increasing greenhouse effect the climate relevant human impacts support the orbital forcings and probably inhibit the change into glacial conditions. Furthermore, it can be recognized in Fig. 5.7 a/b that MIS 1 record shows an increase in $\delta^{18}O$ (red marked) and simultaneously an increase in $\delta^{13}C$ of So-1 in the last few thousand years. This isotopic configuration suggests the occurrence of a little trend towards warmer and drier conditions at the end of MIS 1 record. This trend started about 3.5 ka BP (Fankhauser et al., 2008) and could have been induced by beginning of human settlements and agricultural use above Sofular cave. It remains open whether this trend is maintained over a longer period or forms only a part of a short positive $\delta^{18}O$ excursion. This trend also counteracts the establishment of a new glacial phase in the near future.

Finally, we propose that the climate during MIS 5e was warmer and drier than during MIS 1. The MIS 5e ended after ~114 ka BP, whereas MIS 1 still prevails today.

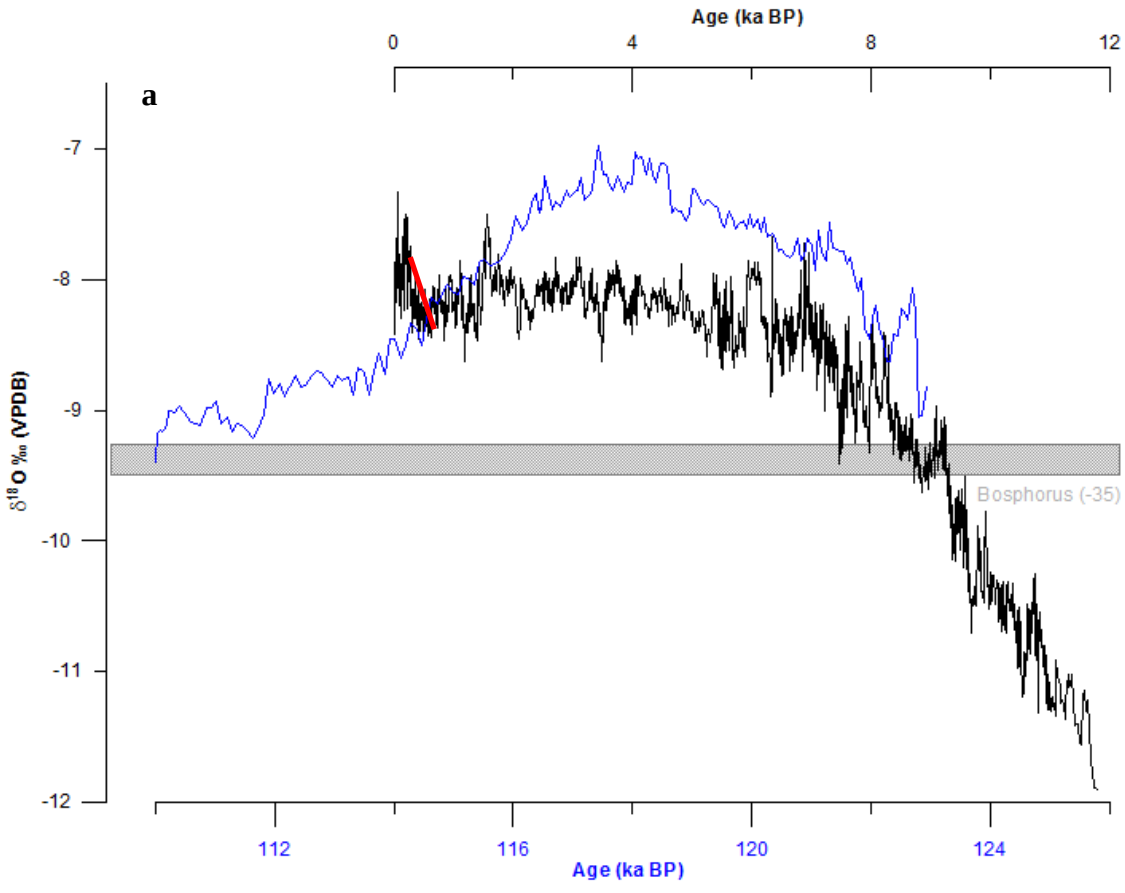

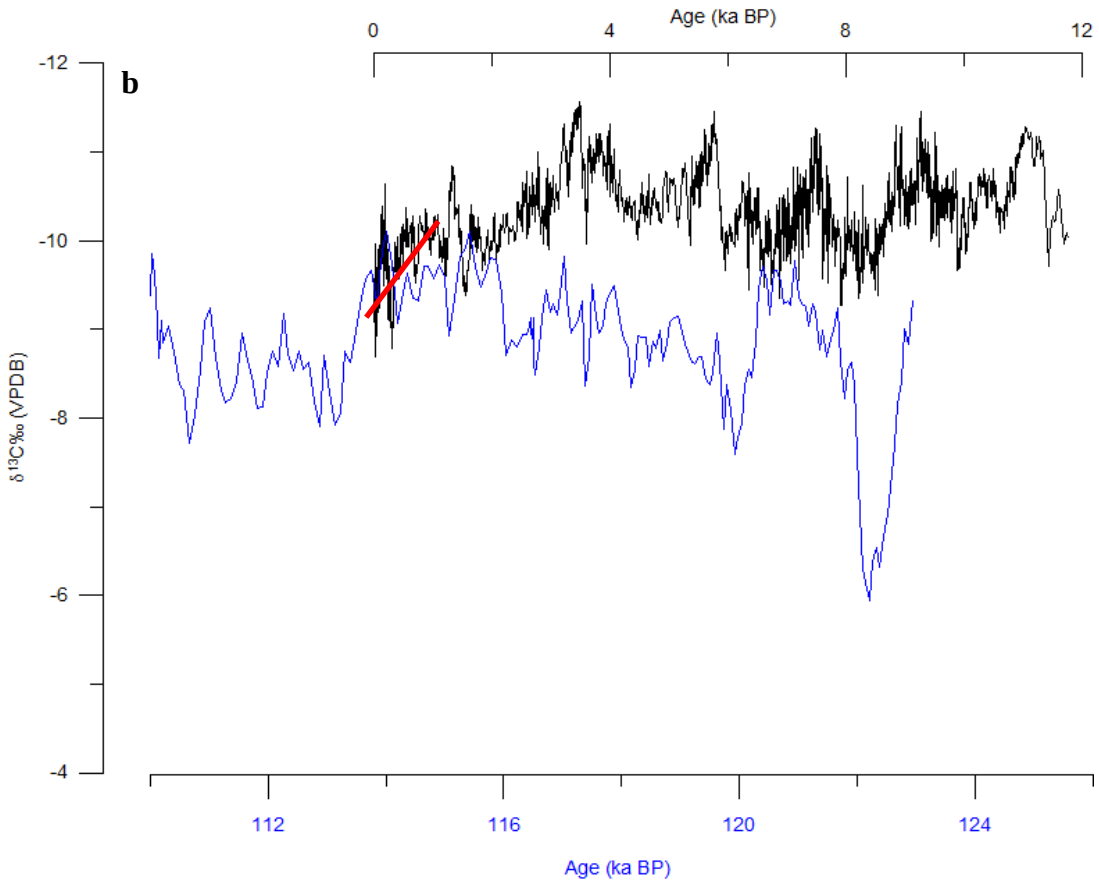

Fig. 5.7. MIS 5e (blue) $\delta^{18}O$ (a) and $\delta^{13}C$ (b) records of So-17A in comparison with MIS 1 (black) $\delta^{18}O$ and $\delta^{13}C$ records of So-1 (So-1 data from Fleitmann et al. 2009). The grey bar marks the sill depth of the Bosphorus Strait.

5.4 MIS 5 CLIMATE VARIABILITY

In the previous sections of this master thesis, the attention was mainly turned to the first-order changes within the isotopic record of So-17A. As it was discussed before, these changes are mainly triggered by changes in the isotopic composition of the Black Sea surface waters and major climate changes. Zooming in from a scale of thousands to hundreds of years, it can be seen that also short-term abrupt events are registered in the isotopic profile of So-17A. The following section is dedicated to the detection of abrupt events and the identification of probable causes.

Prior studies claimed that the MIS 5e climate was relatively stable and uninterrupted (Menke and Tynni, 1984; Frenzel, 1991; Litt et al., 1996). However, it was suggested by a study of Litt et al. 1996 that some climatic fluctuations occurred in MIS 5d-5a (Litt et al., 1996). Later on, some other studies showed evidence for the occurrence of several cold and warm events in the course of the MIS 5 (GRIP members, 1993; Cheddadi et al., 1998; Field et al., 1994; Chapman and Shackleton, 1999 and Boettger et al., 2007). For example, the GRIP members 1993 had their evidence from ice core measurements in Greenland. They suggested the occurrence of high amplitude temperature changes during MIS 5 (GRIP members, 1993). It remains to be seen whether the So-17A record supports the hypothesis of a stable or a variable MIS 5.

Literature about the MIS 5e and the MIS 5d-a shows that abrupt cooling events were mainly recorded in the regions of Greenland and the mid-latitude North Atlantic Sea (GRIP members, 1993; Chapman and Shackleton, 1999). These events mainly happened throughout periods of ice volume maxima (5b, 5d) or during the build up/disintegration of ice sheets (Chapman and Shackleton, 1999).

The climate variability during MIS 5 was higher than expected from the orbital parameters, which were thought to have triggered the major glaciations (Chapman and Shackleton, 1999). Therefore, the cooling events indicate the existence of suborbital forcings not included in the Milankovic theory (Sanchez-Goni et al., 1999). These suborbital forcings are most likely induced by a cooling of North Atlantic surface waters (Sanchez-Goni et al., 1999). Cortijo et al. 1994 brought up the hypothesis that a drop in sea surface temperatures could have been triggered or enhanced by a weakening of the North Atlantic deep water formation due to an inflow of freshwaters. Most likely, the freshwater originated from ice sheets which had melted during warmer phases and from ice rafting events (Cortijo et al., 1994). An interrupt or a dampening of the North Atlantic thermohaline circulation prevents the transport of warmer waters into a northern direction by the north Atlantic drift (Adams et al., 1999). This situation

leads to a cooling in the adjacent regions (Fig. 5.8.) and probably to a built-up of ice sheets (Adams et al., 1999). A further possibility is that the North Atlantic current was displaced to the west (Larsen et al., 1995). This new situation opened the possibility for subarctic water to penetrate southwards (Seidenkrantz et al., 2000) and so did the polar front (Sanchez-Goni et al., 2000).

The North Atlantic Oscillation (NAO) can most likely be excluded as an activator, because a similar NAO index would have led to opposite climate changes in the North Atlantic and the Mediterranean region (Rodwell et al., 1999).

Besides, abrupt changes can also be produced by nonlinear reactions to gradual changes in insolation. This can occur due to the transitions between preferred climate stages (Tzedakis et al., 2003).

The above mentioned cooling events in the North Atlantic were recorded from several proxies in the terrestrial area (Chapman and Shackleton, 1999). Therefore, a detection of these events may also be possible in Sofular stalagmite records.

The propagation of these marine events may be explained by teleconnection phenomena between the Northern Atlantic and continental Europe (Rohling et al., 1998, 2002a), changes in the ice sheet dimensions or general changes in the atmospheric circulation (Chapman and Shackleton, 1999). The teleconnection may be based on the transport of the climatic signal by the westerly wind belt onto the European continent. As it was discussed earlier in this thesis, the predominating wind regime in the Black Sea region is characterized by north-western winds. These winds could bring the climatic signal into the Black Sea region (Fig. 5.8.).

Mayewski 1997 found out that cold periods are characterized by enhanced atmospheric circulations in the northern hemisphere due to the intensification and expansion of the polar vortex (Mayewski, 1997). A strengthening of the atmospheric circulations is associated with an increased occurrence/intensity of polar outbreaks and north-westerlies in the Mediterranean region. Consequently, the polar vortex and the disturbances in the meridional overturning circulation (MOC) are the main factors explaining the synchrony of the marine and continental events (Incarbona et al., 2010). Additional amplifying effects could be global carbon dioxide concentrations, dust content or albedo. These effects are more exactly discussed by Adams et al. 1999. A correlation of marine and terrestrial records would show the marine system to have a great influence on the global climate system (Chapman and Shackleton, 1999).

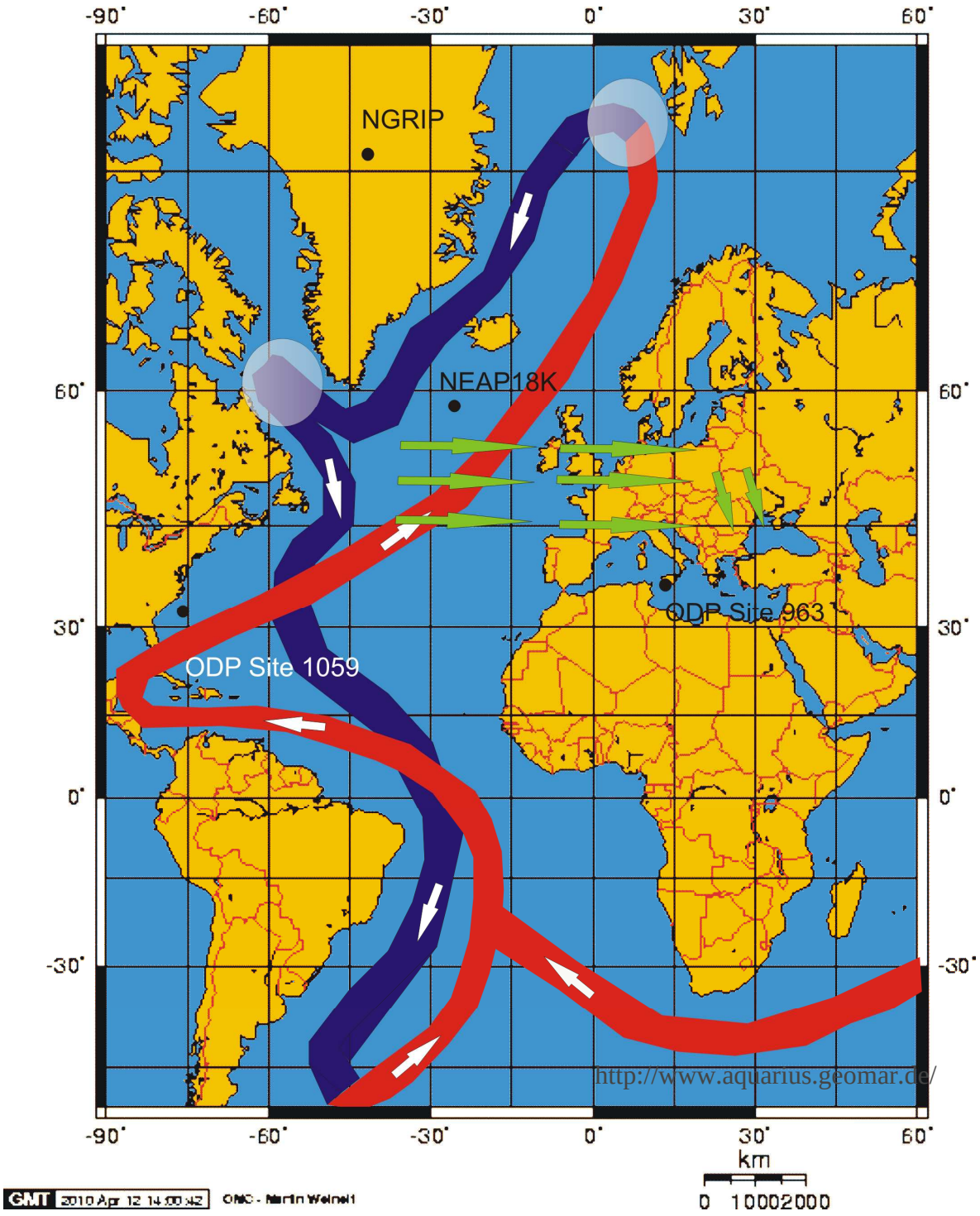

Fig. 5.8. A dampening of the North Atlantic circulation leads to a cooling in the northern regions. The red belt marks the surface warm water circulation. The blue belt shows the route of the cold deep water. The two shaded cycles are the locations of deep water formation working as engines for the circulation. The green arrows indicate the main direction of the winds. Furthermore, the sites ODP 1059 (Heusser and Oppo, 2003), NEAP18K (Chapman and Shackleton, 1999), NGRIP (NGRIP members, 2004) and ODP 963 (Sprovieri et al., 2006) are marked on the map. The studies from these sites served as comparisons to Sofular records.

The ice rafted debris (IRD) events in the North Atlantic were taken as indicators for the abrupt cold events occurring in the Black Sea region (Chapman and Shackleton, 1999; blue bars; Fig. 5.9; Fig. 5.10.). IRD are sediments transported by ice sheets into the ocean. The following melting processes led to the deposition of these sediments on the ocean ground. The occurrence of the mid-MIS 5e cold event was reported by several studies. Each of these cold events is individually discussed in the following part of the chapter. However, it has to be remarked that a correlation of the above mentioned cooling events with the Sofular records is difficult. A dampening and shifting of the signals has to be assumed, because the Black Sea system serves as a source for precipitation. The surface waters maintain their isotopic signature, whereas the ambient cooler temperatures lead to a dampened, cooling signal in the isotopic record. Additionally, it takes the climatic signals some time to propagate from the Northern Atlantic to the Black Sea region. For the detection of these cold events, all the records were aligned to the isotopic record of So-6 to achieve an ideal starting position for the correlation of several abrupt events. The So-6 was taken as an indicator, because its dating resolution is at its highest point from 110 to 105 ka BP. Furthermore, the stalagmites are absolutely dated, whereas the other records are based on correlated age models.

Mid-MIS 5e cold event

Tzedakis et al. 2003 gained evidence for several cold events from results of a combined isotopic and palynological study in Greece. Marine sequences showed a first cold event occurring at about 122 ka BP (Tzedakis et al., 2003; Maslin and Tzedakis, 1996). Additionally, Oppo et al. 2006 studied faunal, isotopic and lithic records from the eastern subpolar North Atlantic. The study also revealed the occurrence of a short cold event approximately 122 ka BP (Oppo et al., 2006). Couchoud et al. 2009 suggested the occurrence of a dry period from 122.4 to 121.6 ka BP in south-western France (Couchoud et al., 2009). Results of a marine study of the Mediterranean Sea also show an increase in the number of cold water species during this period (Sprovieri et al., 2006; Fig. 5.9.).

The isotopic record of So-17A shows a simultaneously occurring event in the $\delta^{13}C$ and the $\delta^{18}O$ record approximately 122 ka BP. The event is marked in the $\delta^{13}C$ curve by a positive excursion of about -3‰ compared to the previous and following values. The achieved value of -6‰ in the $\delta^{13}C$ record indicates the preferential settlement of C4-plants above the cave and therefore the occurrence of rather dry conditions. The same event shows smaller amplitude in the $\delta^{18}O$ record (~-0.5‰). Therefore, a sudden drop in prevailing temperatures

of about 1°C can be suggested. Afterwards, the values change back to previous conditions and continue with the establishment of MIS 5e.

C26 / Late Eemian aridity pulse

The C26 event/ late Eemian aridity pulse (LEAP) was identified by a loess record from Germany indicating high rates of loess deposition about 118 ka BP across Europe (Seelos and Sirocko, 2007). Further on, Chapman and Shackleton 1999 suggested the occurrence of a cooling event approximately 118-119 ka BP in the North Atlantic according to multiproxy data from the North Atlantic deep-sea sediment core NEAP18K. The cold event C26 is absent in the ice rafted debris (IRD) record of the North Atlantic (Chapman and Shackleton, 1999). The reason for this absence is that the MIS 5d ice-sheets were at the beginning of their growth and could not produce any ice-sheet surges (Seelos and Sirocko, 2007). Besides, this event is neither recognizable in the subpolar western North Atlantic record of Oppo and Heusser 2003. Probably, this interruption of the North Atlantic drift mainly had impacts on the climate in southern Europe (Fig. 5.9.). Sirocko et al. 2005 interpreted this cooling to be caused by a southward displacement of the North Atlantic drift which provides the northern Atlantic with warm waters. The reasons for these displacements are not yet understood, however some authors suggest this as a reaction to insolation changes (Khodri et al., 2001; Berger and Loutre, 2002).

A probable cooling event was also recorded in the isotopic profile of stalagmite So-17A at 119 ka BP. The $\delta^{18}O$ of So-17A shows a stabilization of the values, whereas a decrease of about 1.5‰ is recognizable in the $\delta^{13}C$ record of So-17A.

C25

Some of the cold events also occurred during the transition from the MIS 5e to 5d-a (Chapman and Shackleton, 1999). The event C25 was the first cold event after the MIS 5e and occurred about 111.5 ka BP. In the Mediterranean Sea, the event C25 was marked by a decrease of the species G.ruber which occurs mainly in warm water environments (Sprovieri et al., 2006, Fig. 5.9.). A slight negative and positive excursion of the $\delta^{18}O$ (~0.25‰) and $\delta^{13}C$ (~1‰) respectively, can be recognized in So-17A. Therefore, C25 led to a slight decrease in temperatures and precipitation at Sofular cave. This C25 event interrupted the warm event DO25 which was recognized by the NGRIP members (NGRIP members, 2004, Fig. 5.10.). In the So-17A isotopic record, the DO25 event is most likely recorded by the more positive excursion of the $\delta^{18}O$ of So-17A in the time period of 114 ka – 111 ka BP.

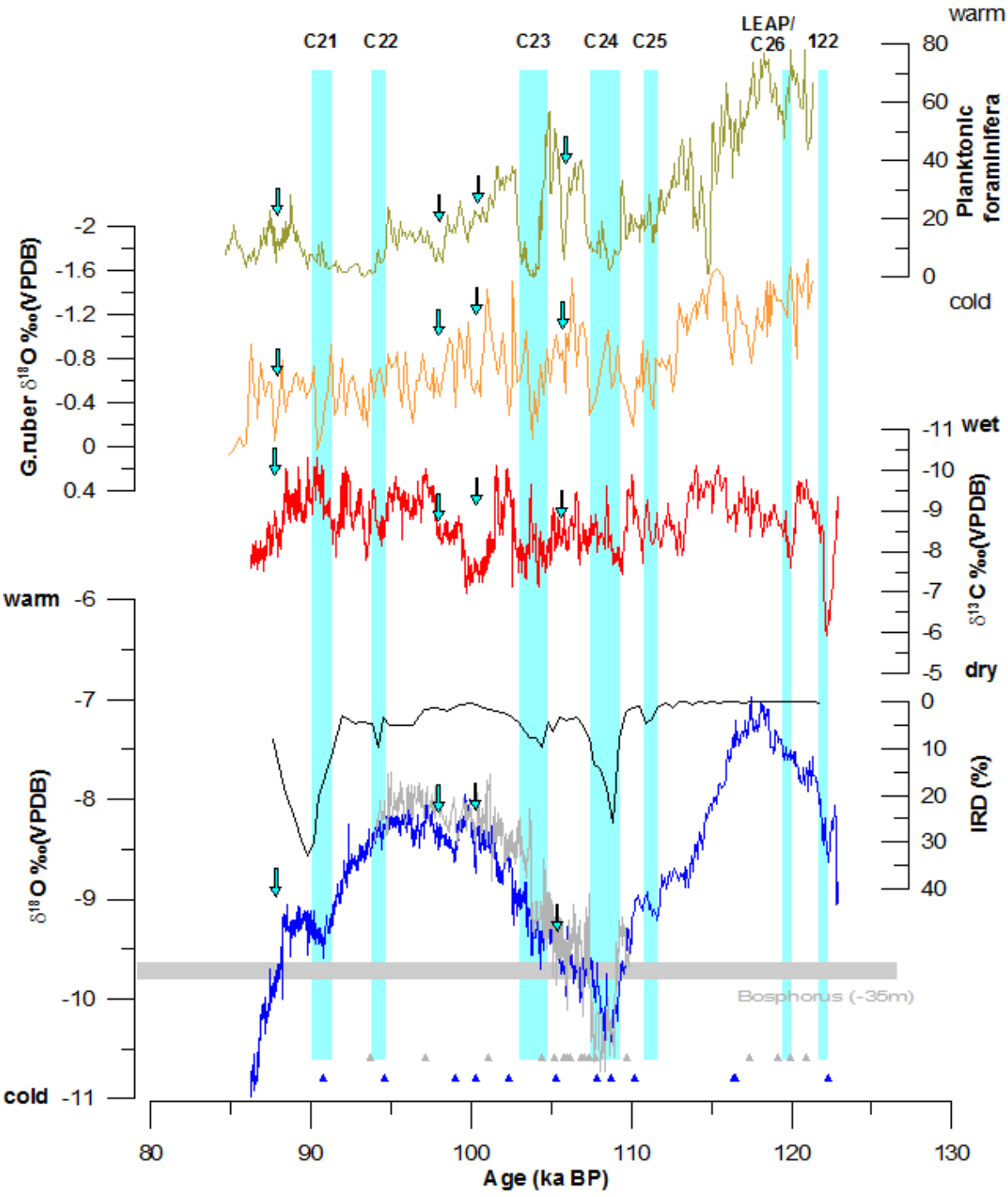

Fig. 5.9. A comparison between several paleoclimatic records over the period from about 123 to 86 ka BP. The following records are displayed: $\delta^{18}O$ (blue) and $\delta^{13}C$ (red) of So-17A, planktionic foraminifera from Sprovieri et al. 2006 (green), IRD record from Chapman and Shackleton 1999 (black), $\delta^{18}O$ of So-6 (grey) and G.ruber record from Heusser and Oppo 2003 (orange). The blue bars indicate the 'C' North Atlantic cooling events, whereas the arrows show the probable occurrence of additional cooling events. The triangles at the bottom of the graph are the U-Th ages of So-17A and So-6.

C24

The cold event C24 is one of the best recognizable events in the IRD sequence of Chapman and Shackleton 1999 and coincidences with MIS 5d around 109 ka BP. In the study of Tzedakis et al. 2003, C24 event was marked by cooling conditions around 110 ka BP in Iberia. This event was triggered by a disruption of the thermohaline circulation in the North Atlantic and a coupled change in the precipitation and temperature regime in Iberia (Tzedakis, 2003). The reason for the disruption of the thermohaline circulation lay in accumulation of sufficient ice to start ice rafting events. The disrupted thermohaline circulation led to a disappearance of tree populations in southern Europe (Tzedakis, 2003).

C24 is marked by a sharp negative excursion in the $\delta^{18}O$ curves of So-17A and So-6 (~-1‰) and by a positive trend in the $\delta^{18}O$ curve of NGRIP (Fig. 5.10.). A drop of -1‰ in $\delta^{18}O$ could be achieved by a temperature decrease of about -2°C. The $\delta^{13}C$ record of So-17A also shows a simultaneous increase in its values. This isotopic profile serves as an indicator for drier and cooler conditions during C24. Therefore, vegetation density and soil microbial activity most likely decreased. The transition from MIS 5d into DO24 is also registered in the $\delta^{18}O$ and $\delta^{13}C$ of So-17A and So-6 at 109 to 108 ka BP. The $\delta^{18}O$ remains on the warm period level, whereas the $\delta^{13}C$ changes back to previous conditions after a short negative excursion. The climate during this warm period was therefore probably warmer but not wetter than the MIS 5d.

C23

The following event C23 is, as C24, marked by an increase in IRD values indicating a possible temperature decrease (Chapman and Shackleton, 1999). Cooling patterns are also shown in the study of the Mediterranean Sea (Sprovieri et al., 2006) and the $\delta^{18}O$ from the subpolar North Atlantic (Heusser and Oppo, 2003)(Fig. 5.9.). The $\delta^{13}C$ records of So-6 and So-17A also show a tendency to drier conditions at about 104 ka BP. The $\delta^{18}O$ records of So-17A and So-6 show a gradual increase in their values. This increase can be explained by an inflow of isotopically enriched waters of the Mediterranean Sea into the Black Sea suppressing the temperature signal in the $\delta^{18}O$ of So-17A.

Drysdale et al. 2007 reconstructed the MIS 5 with evidence from an Italian stalagmite. Before, evidence for cold-events following the MIS 5e came mainly from Greenland ice (NGRIP, 2004), European pollen (Brewer et al., 2008) or North Atlantic marine cores (Chapman and Shackleton, 1999). The improvement of the chronology of these cold-events was the aim of Drysdale. With evidence from stalagmite, Drysdale inferred ages of 105.1±0.9 ka to 102.6 ka BP

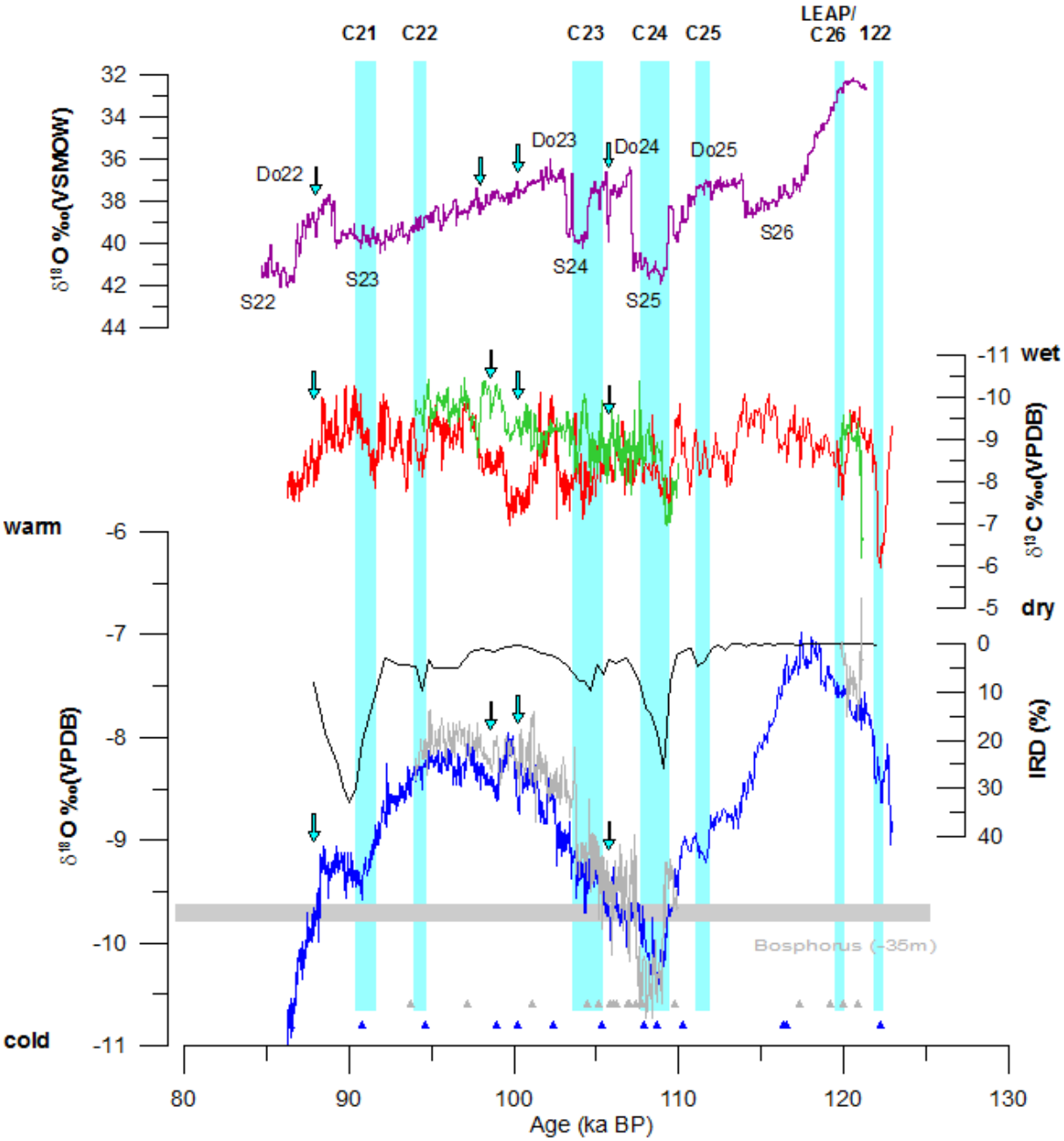

Fig. 5.10. A comparison between several paleoclimatic records over the period from about 123 to 86 ka BP. The following records are displayed: $\delta^{18}O$ (blue) and $\delta^{13}C$ (red) of So-17A, $\delta^{18}O$ (grey) and $\delta^{13}C$ (green) of So-6, IRD record from Chapman and Shackleton 1999 (black) and NGRIP $\delta^{18}O$ record (purple). The blue bars indicate the 'C' North Atlantic cooling events, whereas the arrows show the probable occurrence of additional cooling events. The triangles at the bottom of the graph remark U-Th ages of So-17A and So-6.

for event C23 and 112.0±0.8 ka to 108.8±1 ka for event C24 (Drysdale et al., 2007). These timings are consistent with our results from Sofular stalagmites.

The next warm event (DO23) is followed by a gradual decrease in temperatures in the NGRIP record (NGRIP members, 2004). So-17A and So-6 records show a displaced elevation due to the inert system of the Black Sea explained in chapter 5.2.

C22

MIS 5c was interrupted by the abrupt event C22 at ~104 ka BP. However, the impact of this event on the climate in Sofular is not that intense. A decrease of about -0.15‰ is recorded in the $\delta^{18}O$ of the stalagmites So-6 and So-17A. The $\delta^{13}C$ record of the So-17A indicates a short excursion to drier conditions. Almost no signal can be recognized in the NGRIP record, maybe due to larger impacts in southern Europe.

C21

The C21 event occurred around 91 ka BP and is also detected in the $\delta^{13}C$ and $\delta^{18}O$ of So-17A with an isotopic value of about -9.6 ‰ and -8‰, respectively. The warm event (DO22) is the last event preceding the MIS 5b. Again, the different records from the Northern Atlantic, Mediterranean, Greenland and Sofular cave show that they are in quite a good accordance with this warm event. A sharp cooling event simultaneously occurring in all records then closes this warm event and leads into the MIS 5b.

Additional possible cool events were revealed by the study of Sprovieri et al. 2006. These events occurred ~107.5, ~102, 99.5 and 89.5 ka BP (Fig. 5.10.). In comparison with the Sofular isotopic record, some possible similarities between the different records are recognized. The corresponding cold events are marked by arrows. But finally it can not be clarified whether these arrows show the similar cold events or not.

Warm events

Boettger et al. 2007 mentions at least two warming events occurred during the transition from MIS 5e to 5d. This study was based on geochemical and palynological studies of lacustrine sediments from Germany (Boettger et al., 2007).

The first event was captured at the end of the MIS 5e and in terms of the amplitude comparable with MIS 5c (Boettger et al., 2009). A second short-term warming event took place during MIS 5d (Boettger et al., 2007). Although some possible warm events could be

recognized in the isotopic records of So-17A and So-6, it is difficult to assign some isotopic excursions to these warming events of Boettger. These warming events are mainly thought to be signs of increasing climate instability at the end of interglacial conditions (Boettger et al., 2009).

Overall, it can be seen that IRD events are always associated with cooling events of the North Atlantic. Conversely, marine cooling events do not automatically lead to IRD events (Fig. 5.10.). The inducement of ice sheet discharge by decreasing temperatures seems implausibly; because it takes relatively long time for ice sheets to adapt to new temperatures (Oerlemans, 1993; Lehmann et al., 2002).

Conclusively, seven cold events can be counted during MIS 5 in the $\delta^{18}O$ record of So-17A. Six of them could have been triggered by ice-rafting events in the North Atlantic.

In general, climatic short term changes are better recognizable in the $\delta^{13}C$ record then in the oxygen record in most of the cases. A plausible reason would be that the plants react more sensitive to abrupt climate changes than precipitation above Sofular cave. A reason for that could be that the precipitation is controlled by the Black Sea surface waters on a long-term and this signal is present in the $\delta^{18}O$ record of So-17A as a background effect. Consequently, small changes in climate can lead to major changes within the $\delta^{13}C$ record.

The short-events induced by the ‘C’-events in the North Atlantic can nearly all be detected in the Sofular records, this could be due to their major climatic impacts and the relatively good propagation. The short-term cooling events deduced by Sprovieri et al. 2006 most likely reflect regional effects.

In addition, short-term events occur rather contemporaneously in the aligned records, whereas the long-term events show some shifts. This fact supports the assumption that short-term events are mainly influenced by temperature and precipitation. In contrast, the long-term shifts are mainly controlled by the Black Sea surface waters and consequently by the entire Black Sea basin.

6 CHAPTER SIX – CONCLUSIONS

6.1 CONCLUSION

As a whole, the isotopic $\delta^{18}O$ and $\delta^{13}C$ record of the stalagmite So-17A extends over a period of about 36.77 ka. So17A grew from ~122.25 ka BP to ~86.190 ka BP and allows a climatic reconstruction with an average resolution of 28.2 years. The age-model is built up by thirteen U-Th ages which were evenly drilled over the whole stalagmite.

As it was reconstructed by this thesis and also has been shown by previous studies, the isotopic signature of the Black Sea surface waters predominates the temperature and precipitation signal on a long-term scale within the isotopic records of Sofular stalagmites. This led to the characteristic shifts in the $\delta^{18}O$ record of So-17A compared to the temperature record of the NGRIP members 2004 during climatic transitions.

The $\delta^{18}O$ record shows two positive peaks marking periods of the MIS 5e and MIS 5c. The same structure can also be recognized in the $\delta^{13}C$ record, in a dampened way. Generally, the MIS 5e and the MIS 5c were characterized by warm temperatures and relatively wet climatic conditions. Most likely, the MIS 5c did not achieve MIS 5e optimum climate conditions. The relative stability of the $\delta^{13}C$ during most of the MIS 5 could be explained by quite good climatic conditions for the growth of plants. This means that the climate was mostly moderate with sufficient moisture and without the occurrence of extremely harsh (cold/hot) temperatures. In comparison with MIS 1 conditions, the MIS 5e was warmer and drier. The MIS 5e ended about 114 ka BP in the Black Sea region, whereas the MIS 1 record shows a probable phase of increasing temperatures and decreasing precipitation since 3.5 ka BP. This development does not point to an early end of the MIS 1. Possible reasons for the extension of MIS 1 compared to MIS 5e could be the climate relevant impacts of mankind or distribution of insolation (Risebrobakken et al., 2007).

Three changes between sea and lake phase can be recognized in the So-17A isotopic record characterizing the Black Sea history. Changes into cold phases are associated with a drop in sea level and consequently a break up of the connection between the Black Sea and the Mediterranean Sea (Bosphorus depth = ~-35m). In the So-17A $\delta^{18}O$ record these transitions are marked by a gradual decrease in the $\delta^{18}O$. The gradual descent is mainly produced by the decreasing inflow of the $\delta^{18}O$ enriched Mediterranean waters into the Black Sea. Furthermore, the isotopic signature of the Black Sea surface waters has to adapt to the new conditions in the deep waters, without an inflow of the Mediterranean waters. The residence time of the Black

Sea deep waters is about 2000 years (Östlund and Dyrssen, 1986; chapter 5.2.). The switches into lake phases occurred after the MIS 5e (~109.5 ka BP) and the MIS 5c (~88 ka BP).

Changes into warm phases are coupled with an increase in sea level. When the sea level in the Mediterranean Sea reaches a critical height, the Mediterranean waters flow into the Black Sea basin. This model was developed by Lane-Serff et al. 1997 for the MIS1 reconnection. The inflow of Mediterranean waters lead to an increase in the $\delta^{18}O$ of the Black Sea surface waters. A connection is established with a two-layered exchange between the Black Sea and the Mediterranean Sea through the Bosphorus Strait (~-35m). The isotopic level of ~-9.8‰ within Sofular stalagmites is an indication for such a connection. The reconnection was established ~107.5 ka BP.

The MIS 5e was relatively stable. Higher climate variability was recorded in the MIS 5d-a which included several cold events. The registered cold events were most likely triggered by changes in North Atlantic circulation and were associated with coolings of the sea surface temperatures. These events propagated onto the Eurasian continent. In the isotopic record, these abrupt events are marked by a decrease of -0.25‰ - -0.75‰ in the $\delta^{18}O$ of So-17A and an increase of 0.5‰ - 3‰ in the $\delta^{13}C$. The impact of the cold events on the climate at Sofular cave most likely depends on the magnitude of the cold event and its propagation to the Black Sea region.

6.2 OUTLOOK

First, the MIS 5e is still a quite seldom covered topic in the actual scientific literature. In the eastern Mediterranean region, absolutely dated climate proxies covering the MIS 5e are extremely rare. Therefore, stalagmites from other caves in this region would allow a verification of the results that were revealed by stalagmite So-17A. Furthermore, a comparison would help to distinguish between local, regional and global effects. A first attempt was made by the comparison with the stalagmite So-6 which allowed recognition of local events (stalagmite specific).

Second, stalagmite So-17A could be drilled with a higher resolution. This would probably allow the detection of processes on a shorter time scale and would open the possibility to investigate the impact of teleconnection patterns on the ancient climate in the eastern Mediterranean region.

Last, the composite Sofular record is unique in this region and allows a reconstruction of the Black Sea history back to 600 ka BP. With new stalagmite material, it might possible to fill the remaining temporal gaps.

ACKNOWLEDGEMENTS

I would like to thank…

… first of all, Prof. Dr. Dominik Fleitmann for the perfect supervision of my thesis, for giving me the opportunity to work on this project, for interesting discussions and for the support during the whole year.

… Seraina Badertscher for her patience, support and collegiality, for correcting my thesis, for the fun in the laboratory and for the all the music exchange.

... the group members Dominik Fleitmann, Seraina Badertscher and Ozan Mert Göktürk for their support and interesting discussions.

… Prof. Dr. Markus Leuenberger for the co-supervision of my thesis.

… Sandra Brechbühl and Heidi Vogler for the pleasant working atmosphere in the office.

… Melanie for correcting my English and for her friendship.

… my family for their support during my never-ending story of education and for the distractions at the weekends.

… Jasmine, Fränzi, Megy and Sandra for appreciating my weekends in Nidwalden and for the mental distractions at weekends.

… Heidi for accompanying me through the studies, for cheering me up and for the good times in our WG.

… all the members of the Guugge Chälti-Sägler for the brilliant times at carnival and for the exciting times at the weekends!

REFERENCES

- ADAMS, J., M.A. Maslin, E.Thomas, 1999. Sudden climate transition during the Quaternary. *Progress in physical geography 23*, 1, 1-36.
- AKSU, A.E., R.N. Hiscott, and D.Yasar, 1999. Oscillating Quaternary water levels of the Marmara Sea and vigorous outflow into the Aegean Sea from the Marmara Sea Black Sea drainage corridor. *Marine Geology 153*, 275-302.
- AKSU, A.E., R.N. Hiscott, D. Yasar, F.I. Isler and S. Marsh, 2002a. Seismic stratigraphy of Late Quaternary deposits from the southwestern Black Sea shelf: evidence for non-catastrophic variations in sea level during the last 10 000 year. *Mar. Geol. 190*, 61–94.
- AKSU, A.E., R.N. Hiscott, M.A. Kaminski, P.J. Mudie, H. Gillespie, T. Abrajano and D. Yasar, 2002b. Last glacial-Holocene paleoceanography of the black sea and Marmara sea: stable isotopic, foraminiferal and coccolith evidence. *Mar Geol 190*, 119–149.
- AALBERSBERG, G. and T. Litt, 1998. Multiproxy climate reconstructions for the Eemian and early Weichselian. *Journal of Quaternary Science 13*, 367–390.
- AN, Z.S., 2000. The history and variability of the East Asian paleomonsoon climate. *Quaternary Science Reviews 19 (1–5)*, 171–187.
- BAHR A., F. Lamy, H.W. Arz, C. Major, O. Kwiecien and G. Wefer, 2008. Abrupt changes of temperature and water chemistry in the late Pleistocene and early Holocene Black Sea. *Geochemistry, Geophysics, Geosystems 9,* Q01004.
- BAHR A., H. Arz, F. Lamy and G. Wefer, 2006. Late glacial to Holocene paleoenvironmental evolution of the Black Sea, reconstructed with stable oxygen isotope records obtained on ostracod shells, Earth Planet. *Sci. Lett. 241*, 863–875.
- BAR-MATTHEWS, M., A. Ayalon and A. Kaufman, 1997. Late Quaternary climate in the eastern Mediterranean region-inferences from the stable isotope systematics of speleothems of the Soreq cave (Israel), *Quat. Res. 47*, 155–168.
- BAR-MATTHEWS, M., A. Ayalon, M. Gilmour, A. Matthews, and C.J. Hawkesworth, 2003. Sea-land oxygen isotopic relationships from planktonic foraminifera and speleothems in the Eastern Mediterranean region and their implication for paleorainfall during interglacial intervals. *Geochimica et Cosmochimica Acta 67*, 3181-3199.

- BARD, E., B. Hamelin, and R.G. Fairbanks, 1990. U-Th ages obtained by mass spectrometry in corals from Barbados sea level during the past 130,000 years. *Nature 346*, 456-459.
- BAKER, A., E. Ito, P.L. Smart and R.F. McEwan, 1997. Elevated and variable values of ^{13}C in speleothems in a British cave system. *Chemical Geology 136*, 263–270.
- BERGER A., and M.F. Loutre, 2002. An exceptionally long interglacial ahead. *Science 297*, 1287-1288.
- BERGER, A., M.F Loutre and C. Tricot, 1993. Insolation and earth's orbital periods. *Journal of Geophysical Research 98*, 10341–10362.
- BERGER, A., 1978. *J.Atmos. Sci. 35*, 2362.
- BOETTGER, T., E.Y. Novenko, A.A. Velichko, O.K. Borisova, K.V. Kremenetski, S. Knetsch, F.W. Junge, 2009. Instability of climate and vegetation dynamics in Central and Eastern Europe during the final stage of the Last Interglacial (Eemian, Mikulino) and Early Glaciation. *Quarternary International 207*, 137-144.
- BOETTGER, T., F.W. Junge, S. Knetsch, E.Yu. Novenko, O.K. Borisova and A.A. Velichko, 2007. Indications to short-term climate warming at the very end of the Eemian in terrestrial records of Central and Eastern Europe. In: F. Sirocko, M. Claussen, M.F. Sánchez Goñi and Th. Litt, Editors, The Climate of Past Interglacials, Chapter 17. Series: Development in Paleoenvironmental Research, Springer, 255–264.
- BOURDON, B., S.P. Turner, G.M. Henderson and C.C. Lundstrom, 2003. Introduction to U-series geochemistry. In: B. Bourdon, G.M. Henderson, C.C. Lundstrom and S.P. Turner (Eds.). *Reviews in Mineralogy and Geochemistry, Uranium-Series Geochemistry*, 1-21.
- BOZKURT, E. and S.K. Mittwede, 2001. Introduction to the Geology of Turkey – A synthesis. *International Geology Review 43*, 578-594.
- BREWER, S., J. Guiot, M.F. Sanchez-Goni and S. Klotz, 2008. The climate in Europe during the Eemian: a multi-method approach using pollen data. *Quaternary Science Reviews, 27*, 2303-2315.
- BURNS, S.J., D. Fleitmann, A. Matter, U. Neff, A. Mangini, 2001. Speleothem evidence from Oman for continental pluvial events during interglacial periods. *Geology 29*, 623–626.
- CAGATAY, N., N. Gorur, A. Algan, C.J. Eastoe, A. Tchapalyga, D. Ongan, T.Kuhn and I. Kuscu, 2000. Late Glacial-Holocene palaeoceanography of the Sea of Marmara: timing

of connections with the Mediterranean and the Black Sea. *Marine Geology, 167*, 191-206.

- CHAPMAN, M.R. and N.J. Shackleton, 1999. Global ice-volume fluctuation, North Atlantic ice-rafting events, and deep-ocean circulation changes between 130 and 70 ka. *Geology 27,* 795–798.
- CHEDDADI, R., K. Mamakowa, J. Guiot, J.L. de Beaulieu, M. Reille, V. Andrieu, W. Granoszewski, O. Peyron, 1998. Was the climate of the Eemian stable? A quantitative climate reconstruction from seven European pollen records. *Palaeogeogr Palaeoclimatol Palaeoecol 143,* 73–85.
- CHEN F., W. Siebel, M. Satır, N. Terzioğlu and K. Saka, 2002. Geochronology of the Karadere basement (NW Turkey) and implications for the geological evolution of the Istanbul Zone. *Int. J. Earth Sci. 91,* 469–481.
- CHEPALYGA, A.L., 2007. The late glacial flood in the Ponto-Caspian basin. *In: Yanko-*
- *Hombach, V., Gilbert, A.S., Panin, N., Dolukhanov, P.M. (Eds.), The Black Sea Flood Question: Changes in Coastline, Climate and Human Settlement. Springer, Dordrecht,* 119–148.
- CLARK, I. D and P. Fritz, 1997: Environmental Isotopes in Hydrogeology. Lewis Publishers, Boca Raton.
- CLARK, P. and P. Huybers, 2009. Interglacial and Future Sea Level. *Nature (news and views) 462*, 856- 857.
- CORTIJO, E., J.-C. Duplessy, L. Labeyrie, H. Leclaire, J. Duprat, T.C.E. Van Weering, 1994. Eemian cooling in the Norwegian Sea and North Atlantic ocean preceding continental ice-sheet growth. *Nature 372,* 446–449.
- COUCHOUD, I., D. Genty, D. Hoffmann, R. Drysdale and D. Blamart, 2009. Millennial-scale climate variability during the Last Interglacial recorded in a speleothem from south-western France. *Quaternary Science Reviews 28,* 3263-3274.
- CRAIG, H., 1961. Isotopic variations in meteoric waters. *Science 133*, 1702–1703.
- DJAMALI, M., J.L. de Beaulieu, M. Shah-Hosseini, V. Andrieu-Ponel, P. Ponel, A. Amini, H. Akhani, A.S. Leroy, L. Stevens, H. Alizadeh and S. Brewer, 2008. A late Pleistocene long pollen record from Lake Urmia, NW Iran. *Quat Res 69*, 413–420.
- DANSGAARD, W., 1954. The O^{18}-abundance in fresh water. *Geochimica et Cosmochimica Acta 6*, 241–260.
- DREYBRODT, W. 1999. Chemical kinetics, speleothem growth and climate. *Boreas 28,*

347-356.

- DRYSDALE, R., G. Zanchetta, J.C. Hellstrom, A.E. Fallick, J. McDonald and I. Cartwright, 2007. Stalagmite evidence for the precise timing of North Atlantic cold events during the early last glacial. *Geology 35*, 77-80.
- EDWARDS, R.L., H. Cheng, M.T. Murrell and S.J. Goldstein, 1997. Protactinium-231 dating of carbonates by thermal ionization mass spectrometry: Implications for Quaternary climate change. *Science 276*, 782-786.
- EPSTEIN, S., R. Buchsbaum, H.A. Lowenstam and H.C. Urey, 1953. Revised carbonate-water isotopic temperature scale. Bull. *Geol. Soc. Amer 64*, 1315–1326.
- FAIRCHILD I.J., C.L. Smith, A. Baker, L. Fuller, C. Spötl, D. Mattey and F. McDermott, 2006a. Modification and preservation of environmental signals in speleothems. *Earth-ScienceReviews 75*, 105-153.
- FAIRCHILD, I.J., S. Frisia, A. Borsato. And A.F.Tooth 2006b. Speleothems. *In: Nash, D.J. and S.J. McLaren (ed.), Geochemical Sediments and Landscapes. Blackwells, Oxford,* 200-245.
- FANKHAUSER, H. et al., 2008. Climate Variability Recorded in a 50,000-year old Stalagmite from Northern Turkey. *Master thesis*, Institute of Geological Sciences, University of Bern.
- FAUQUETTE, S., J. Guiot, M. Menut, J.L. de Beaulieu, M. Reille and P. Guenet, 1999. Vegetation and climate since the last interglacial in the Vienne area (France). *Global and Planetary Change 20*, 1–17.
- FETTER, C.W., 1994. Applied Hydrogeology. Prentice-Hall, Englewood Cliffs.
- FIELD, MH, B. Huntley and H. Müller, 1994. Eemian climate fluctuations observed in a European pollen record. *Nature 371*, 779–783.
- FLEITMANN, D., H. Cheng, S. Badertscher, R.L. Edwards, M. Mudelsee, O.M. Gokturk, A. Fankhauser, R. Pickering, C.C. Raible, A. Matter, J. Kramers and O. Tuysuz, 2009. Timing and climatic impact of Greenland interstadials recorded in stalagmites from northern Turkey. *Geophys. Res. Lett. 36*, L19707.
- FLEITMANN, D., S.J. Burns, A. Mangini,, M. Mudelsee, J.D. Kramers, U. Neff, A.A. Al-Subbary, A. Matter, 2007. Holocene ITCZ and Indian monsoon dynamics recorded in stalagmites from Oman and Yemen (Socotra). *Quaternary Science Reviews 26*, 170-188.

- FLEITMANN, D. et al., 2008. White paper on "Speleothem-based climate proxy records". *http://www.ncdc.noaa.gov/paleo/reports/trieste2008/speleothems.pdf* (15.04.2009).
- FRENZEL B, 1991. Das Klima des letzten Interglazials in Europa. *Paleoklimaforschung 1*, 51–78.
- FROGLEY, M.R., P.C. Tzedakis and T.H.E. Heaton, 1999. Climate variability in northwest Greece during the last interglacial. *Science 285*, 1886-1889.
- FRUMKIN, A., D.C. Ford and H.P. Schwarcz, 1999. Continental oxygen isotopic record of the last 170,000 years in Jerusalem. *Quaternary Research 51*, 317–327.
- GANDOUIN, E., P. Ponel, V. Andrieu-Ponel, E. Franquet, J.L. de Beaulieu, M. Reille, F. Guiter, J. Brulhet, É. Lallier-Vergès, D. Keravis, U. von Grafenstein and D. Veres, 2007. Past environment and climate changes at the last Interglacial/Glacial transition (Les Échets, France) inferred from subfossil chironomids (Insecta), *Geosci. 339*, 337–346.
- GASCOYNE, M., 1992. Palaeoclimate determination from cave deposits. *Quaternary Science Reviews 11*, 609– 632.
- GAT, J. R., 1996. Oxygen and hydrogen isotopes in the hydrologic cycle. *Annu. Rev. Earth Planet. Sci. 24*, 225– 262.
- GAT, J.R., 2001. Volume II – atmospheric water. *In: Mook, W.G., (Ed.), Environmental Isotopes in the Hydrological Cycle. IHP-V Technical Documents in Hydrology, 39, UNESCO, Paris.*
- GÖKASAN, E., E. Demirbağ, F.Y. Oktay, B. Ecevitoğlu, M. Şimşek and H. Yüce, 1997. On the origin of the Bosporus. *Marine Geology 140*, 183–199.
- GÖKASAN, E., M. Ergin, M. Ozyalvac., H. Ibrahim Sur, H. Tur, T. Görum, T. Ustaömer, F. Gul Batuk, H. Alp, H. Birkan, A. Turker, E. Gezgin, M. Ozturan, 2008. Factors controlling the morphological evolution of the Canakkale Strait (Dardanelles, Turkey). *Geo-Mar Letters 28*, 107–129.
- GOLDSTEIN S.J. and C.H. Stirling, 2003. Techniques for measuring Uranium-series nuclides: 1992-2002. In: Bourdon B., Henderson G.M., Lundstrom C.C., Turner S.P. (Eds.), Uranium-series geochemistry. *Reviews in Mineralogy and Geochemistry 52*, 23-57.
- GRIP MEMBERS, 1993. Climate instability during the last interglacial period recorded in the GRIP ice core. *Nature 364*, 203-207.

- GROSS, H., 1967. Geochronologie des letzten Interglazials im nördlichen Europa mit besonderer Berticksichtigung der USSR. *Schrifte der Naturwissenschatliche Vereinigung Schleswig-Holsteins,* 37, 111-125.
- GUIOT, J., A. Pons, J.Ll de Beaulieu, and M. Reille, 1989. A 140,000-year continental climate reconstruction from two European pollen records. *Nature* 338, 309-313.
- HARMON, R.S., H.P. Schwarcz, M. Gascoyne, J.W. Hess, and D.C. Ford, 2004. Paleoclimate information from speleothems: The present as a guide to the past. *In: Mylroie, J., and Sasowsky, I.D., eds., Studies of Cave Sediments: Physical and Chemical Records of Paleoclimate*; 199–226.
- HARTING, P., 1874. De bodem van het Eemdal. Verslag Koninklijke Akademie van Wetenschappen, *Afdeling N, II, Deel VIII*, 282-290.
- HENDY, C.H., 1971. The isotopic geochemistry of speleothems-I: The calculations of the effects of different modes of formation on the isotopic composition of speleothems and their applicability as paleoclimate indicators. *Geochimica et Cosmochimica Acta 35*, 801–824.
- HEUSSER, L., and D. Oppo, 2003. Millennial-and orbital-scale climate variability in southeastern United States and in the subtropical Atlantic during Marine Isotope Stage 5: Evidence from pollen and isotopes in ODP Site 1059. *Earth and Planetar Science Lettners 214*, 483–490.
- HILL, C. and P. Forti., 1997. Cave minerals of the world (2nd edition). *National peleological Society,Huntsville, Alabama, U.S.A., ISBN: 1-879961-07-5.*
- HODGE, E., D.A. Richards, P.L. Smart, B. Andreo, D.L. Hoffmann, D.P. Mattey and A. Gonzalez-Ramon, 2008. Effective precipitation in southern Spain (266 to 46 ka) based on a speleothem stable carbon isotope record. *Quaternary Research 69*, 447–457.
- HOEFS, J., 2009. Stable Isotope Geochemistry. Springer Berlin, 6th ed.
- IMBRIE, J. et al., 1984. The orbital theory of Pleistocene climate: support from revised chronology of the marine 18O record. *In: A. Berger, J. Imbrie, J.D. Hays, G. Kukla and B. Saltzman (Editors), Milankovitch and Climate. Reidel, Dordrecht,* 269–305.

  INCARBONA, A, E. Di Stefano, R. Sprovieri, S. Bonomo, N. Pelosi and M. Sprovieri, 2010. Millennial-scale paleoenvironmental changes in the central Mediterranean during the last interglacial: Comparison with European and North Atlantic records. *Geobios 43*, 111-122.

- JEX, C.N., M.J. Leng, H. Sloane, W.J. Eastwood, I.J. Fairchild and L. Thomas, 2009. Calibration of speleothem $\delta^{18}O$ with instrumental climate records from Turkey. *Glob. Planet. Change*, doi:10.1016/j.gloplacha.2009.08.004.
- JOHNSON, K.R., B.L. Ingram, W.D. Sharp, P.Z. Zhang, 2006. East Asian summer monsoon variability during Marine Isotope Stage 5 based on speleothem $\delta^{18}O$ records fromWanxiang Cave, Central China. *Palaeogeogr. Palaeoclimatol. Palaeoecol. 236*, 5–19.
- JONES, I. C., J. L. Banner, and J. D. Humphrey, 2000. Estimating recharge in a tropical karst aquifer. *Water Resour. Res. 36*, 1289– 1299.
- KAMINSKI, M.A., A. Aksu, M. Box, R.N. Hiscott, S. Filipescu and M. Al-Salameen, 2002. Late Glacial to Holocene benthic foraminifera in the Marmara Sea: implications for Black Sea- Mediterranean Sea connections following the last deglaciation. *Marine Geology.190*, 165-202.
- KAUFMAN A and W.S. Broecker, 1965. Comparison of Th^{230} and C^{14} ages for carbonate materials from lakes Lahontan and Bonneville. *Journal of Geophysical Research* 70, 4039-4054.
- KAZMIN, A.S. and A.G. Zatsepin, 2007. Long-term variability of surface temperature in the Black Sea, and its connection with the large-scale atmospheric forcing. *Journal of marine systems 68*, 293-301.
- KHODRI M., Y. Leclainche, G. Ramstein, P. Braconnot, O. Marti, E. Cortijo, 2001. Simulating the amplification of orbital forcing by ocean feedbacks in the last glaciation. *Nature 410*, 570–574.
- KOSAREV, A.N., 2008. Hydrometeorlogical conditions. *In: Kosarev, A.N., A.G. Kostianoy and O. Hutzinger (eds.). The Black Sea environment, Springer-Verlag Berlin Heidelberg*, 135-158.
- KOSTOPOULOU, E. and P.D. Jones, 2007. Comprehensive analysis of the climate variability in the eastern Mediterranean. Part I: map-pattern classification. *Int. J. Climatol. 27*, 1189–1214.
- KÜHL, N. and T. Litt, 2003. Quantitative time series reconstruction of Eemian temperature at three European sites using pollen data. *Vegetation History and Archaeobotany 12*, 205–214.

- KÜHL, N. and T. Litt, 2007. Quantitative time series reconstructions of Holsteinian and Eemian temperatures using botanical data. *In: Sirocko, F., Claussen, M., Sanchez Goni, M.F.., Litt, T. (Eds.), The Climate of Past Interglacials, Elsevier, Amsterdam,* 239-254.
- KUKLA, G., J.F. McManus, D.D. Rousseau and L. Chuine, 1997. How long and how stable was the last interglacial? *Quaternary Science Reviews 16*, 605-612.
- KUKLA, G.J., and 22 others, 2002. Last interglacial climates. *Quaternary Research 58*, 2–13.
- KUTIEL, H. and Y. Benaroch, 2002. North Sea-Caspian Pattern (NCP) – an upper level atmospheric teleconnection affecting the Eastern Mediterranean: Identification and definition. *Theoretical and Applied Climatology 71*, 17-28.
- KUTZBACH, J.E. and T. Webb, 1993. Conceptual basis for understanding Late-Quaternary climates, Chapter 2. *In: Wright, H.E., Jr, J.E. Kutzbach, T. Webb III, W.F. Ruddiman, F.A. Street-Perrott, and P.J. Bartlein (eds.). Global Climates since the Last Glacial Maximum, University of Minnesota Press, Minneapolis*, 5-11.
- KUTZBACH, J.E., P.J. Guetter, P.J. Behling, R. Selinm, 1992. Simulated climatic changes: results of the COHMAP climate-model experiments. *In: Wright Jr., H.E., et al. (Ed.), Global Climates Since the Last Glacial Maximum. Univ. Minnesota Press, Minneapolis*, 24–93.
- LACHNIET, M.S., 2009. Climatic and environmental controls on speleothem oxygen-isotope values. *Quaternary science Reviews 28*, 412-432.
- LAMBECK, K., T.M. Esat and E.K. Potter, 2002. Links between climate and sea level for the past three million years. *Nature 419*, 199–206.
- LANE-SERFF, G. F., E. J. Rohling, H. L. Bryden, and H. Charnock, 1997. Postglacial Connection of the Black Sea to the Mediterranean and its Relation to the Timing of Sapropel Formation. *Paleoceanography*, 12(2), 169–174.
- LAUMANNS, M. and G. Kaufmann, 1988. Drei Höhlen der Region Zonguldak, Schwarzes Meer, Türkei. *Mitt. VDHK, 34* (4)
- LEMKE, W. and J. Harff, 2005. Holocene of Europe. *In: Encyclopedia of environ. microbiol. 71*, 921-929
- LITT, T., F.W. Junge, T. Böttger, 1996. Climate during the Eemian in north-central Europe — a critical review of the palaeobotanical and stable isotope data from central Germany. *Veget Hist Archaebot 5*, 247–256.

- LYKOUDIS, S.P, A.A. Argiriou and E. Dotsika, 2009. Spatially interpolated time series of $\delta^{18}O$ in Eastern Mediterranean precipitation. *Global and Planetary Change*, doi:10.1016/j.gloplacha.2009.09.004.
- MAJOR, C.O., S.L Goldstein, W.B.F Ryan, G. Lericolais, A.M. Piotrowski and I. Hajdas, 2006. The co-evolution of Black Sea level and composition through the last deglaciation and its paleoclimatic significance. *Quaternary Science Reviews 25*, 2031–2047.
- MAJOR, C.O., W.B.F. Ryan, G. Lericolais, G. and I. Hajdas, 2002. Constraints on Black Sea outflow to the Sea of Marmara during the last glacial-interglacial transition. *Marine Geology 190*, 19-34.
- MANGERUD, J., 1991. The Scandinavian ice sheet through the last interglacial/glacial cycle. *In:* Frenzel, B. (ed.), *Klimageschichtliche Probleme der letzten 130,000 Jahre.* Gustav Fischer, Stuttgart, 307-330.
- MANGERUD, M., M. Jakobsson, H. Alexanderson, V. Astakhov, G.K.C. Clarke, M. Henriksen, C. Hjort, G. Krinner, J.-P. Lunkka, P. Moller, A. Muray, O. Nikolskaya, M. Saarnisto and J.I. Svendsen, 2004. Ice-dammed lakes and rerouting of the drainage of northern Eurasia during the Last Glaciation. *Quat. Sci. Rev., 23*, 1331–1332.
- MASLIN, M.A. and C. Tzedakis, 1996. Sultry last interglacial gets sudden chill. *EOS Transactions of the American Geophysical Society 77*, 353–54.
- MAYEWSKI, P.A., E. Rohling, C. Stager, K. Karlén, K. Maasch, L.D. Meeker, E. Meyerson, F. Gasse, S. van Kreveld, K. Holmgren, J. Lee-Thorp, G. Rosqvist, F. Rack, M. Staubwasser and R. Schneider, 2004. Holocene climate variability. *Quaternary Research 62*, 243-255.
- MAYEWSKI, P.A., L.D. Meeker, M.S. Twickler, S. Whitlow, Q. Yang, W.B. Lyons and M. Prentice, 1997. Major features and forcing of high-latitude northern hemisphere atmospheric circulation using a 110,000-year long glaciochemical series. *Journal of Geophysical Research 102*, 26345–26366.
- MCDERMOTT, F., S. Frisia, Y. Huang, A. Longinelli, B. Spiro, T.H.E. Heaton, C.J. Hawkesworth, A. Borsato, E. Keppens, I.J. Fairchild, K. van der Borg, S. Verheyden and E. Selmo, 1999. Holocene climate variability in Europe: evidence from y18O and textural variations in speleothems. *Quaternary Science Reviews 18*, 1021–1038.
- MCDERMOTT, F. 2004. Paleo-climate reconstruction from stable isotope variations in speleothems: a review. *Quaternary Science Reviews. 23*, 901-918.

- MCDERMOTT, F., H.P. Schwarcz and P.J. Rowe, 2006. Isotopes in speleothems. *In: Leng, M.J. (Ed.), Isotopes in Palaeoenvironmental Research. Springer, Dordrecht, The Netherlands,* 185– 226.
- MCHUGH, C.M.G., D. Gurung, L. Giosan, W.B.F. Ryan, Y. Mart, U. Sancar, L. Burckle, N. Çagatay, 2008. The last reconnection of the Marmara Sea (Turkey) to the World Ocean: a paleoceanographic and paleoclimatic perspective. *Mar Geol 255,* 64–82.
- MENKE, B. and R. Tynni, 1984. Das Eeminterglazial und das Weichselfrühglazial von Rederstall/Dithmarschen und ihre Bedeutung für die mitteleuropäische Jungpleistozän-Gliederung. *Geologisches Jahrbuch, Reihe A 76,* 3–120.
- MOORE, G.W., 1954. Speleothem - A new Cave Term. *In: National Speleological Society of the USA News. 10, 6,* 2.
- MUDIE, P.J., A. Rochon, A.E. Aksu, H. Gillespie, 2002. Dinoflagellate cysts, freshwater algae and fungal spores as salinity indicators in Late Quaternary cores from Marmara and Black Seas. *Mar. Geol. 190,* 203-231.
- MÜLLER, U.C. and G.J. Kukla, 2004. North Atlantic Current and European environments during the declining stage of the last Interglacial. *Geology, 32/12,* 1009-1012.
- MÜLLER, U.C., S. Klotz, M.A. Geyh, J. Pross and G.C. Bond, 2005. Cyclic climate fluctuations during the last interglacial in central Europe, *Geology 33,* 449–452.
- NGRIP members, 2004. High-resolution record of Northern Hemisphere climate extending into the last interglacial period, *Nature 431,* 147–151.
- LARSEN, E., H.P. Sejrup, S.J. Johnsen and K.L. Knudsen, 1995. Do Greenland ice cores reflect NW European interglacial climate variations? *Quaternary Research 43,* 125– 132.
- LUDWIG, K.R., K.R. Simmons, B.J. Szabo, I.J. Winograd, J.M. Landwehr, A.C. Riggs and R.J. Hoffman, 1992. Mass-spectrometric ^{230}Th-^{234}U-^{238}U dating of the Devils Hole calcite vein. *Science 258,* 284-287.
- OERLEMANS, J., 1993. Evaluating the role of climatic cooling on production of icebergs and the Heinrich events. *Nature 364,* 783-785.
- OGUZ, T., V.S. Latun, M.A. Latif, V.V. Vladimirov, H.I. Sur, A.A. Markov, E. Özsoy, B.B. Kotovshchikov, V.V. Eremeev, Ü. Ünlüata, 1993. Circulation in the surface and intermediate layers of the Black Sea. *Deep-Sea Res. I40,* 1597-1612.
- OGUZ T., J.W. Dippner and Z. Kaymaz, 2006. Climatic regulation of the Black Sea

hydro-meteorological and ecological properties at interannual-to-decadal time scales. *Journal of Marine Systems 60*, 235–254.

- OPPO, D.W., J.F. McManus and J.L. Cullen, 2006. Evolution and demise of the Last Interglacial warmth in the subpolar North Atlantic. *Quaternary Science Reviews 25*, 3268–3277.
- ÖSTLUND, H. G. and Dyrssen, D., 1986. Renewal rates of the Black Sea deep water. Report on the chemistry of seawater XXXIII. *Department of Analytical and Marine Chemistry, Chalmers University of Technology and Gothenburg University, Göteborg, Sweden.*
- OSTROVSKY, A.B., Y.A. Izmailov, I.P. Balabanov, S.I. Skiba, N.G. Skryabina, K.A. Arslanov, N.A. Gey, and N.I. Suprunova, 1977. New data on stratigraphy and geochronology of Pleistocene marine terraces of the Caucasian Black Sea coast and of the Kerch-Taman region. *In: P.A Kaplin and F.A. Shcherbakov (eds). Pleistocene Paleogeography and Deposits of Southern Seas of the USSR*, Nauka, Moscow (In Russian), 61–68.
- ÖZSOY, E. and Ü. Ünlüata, 1997. Oceanography of the Black Sea: A Review of Some Recent Results. *Earth Sci. Rev. 42(4)*, 231-272.
- PANIN, N., 2007. The Black Sea – Geology, Environment and Archaeology. In: Oaie G. M.Diaconescu, D.Ioane etc. (ed.) Hazard natural: Evenimente tsunami in Marea Neagra, ISBN:978-973-0- 05181-0, 3-10. (http://www.profet.ro/Panin. pdf (15.12.2009))
- PICKET, J.W., C.H. Thompson, R.A. Kelly and D. Roman, 1985. Evidence of high sea level during Isotope Stage 5c in Queensland, Australia. *Quaternary Research 24*, 103-114.
- PINI, R., C. Ravazzi and M. Donegana, 2009. Pollen stratigraphy, vegetation and climate history of the last 215 ka in the Azzano Decimo core (plain of Friuli, northeastern Italy). *Quaternary Science Reviews 28*, 1268–1290.
- POULSON, T.L., and W.B. White, 1969. The cave environment. *Science 165*, 971–981.
- PRELL, W.L., and J.F. Kutzbach, 1987, Monsoon variability over the past 150,000 years. *Journal of Geophysical Research 92*, 8411–8425.
- RAICICH F., N. Pinardi and A. Navarra, 2003. Teleconnections between Indian monsoon and Sahel rainfalland the Mediterranean. *International Journal of Climatology 23*, 173-186.

- RASMUSSEN, J.B.T., V.J. Polyak, Y. Asmerom, 2006. Evidence for Pacific-modulated precipitation variability during the late Holocene from the southwestern USA. *Geophys. Res. Lett., 33*, L08701.
- REHKÄMPER, M., M. Schönbächler and C.H. Stirling, 2001. Multiple collector ICP-MS: introduction to instrumentation, measurement techniques and analytical capabilities. *Geostand. and Geoanalytical Res. 25*, 23–40.
- REVESZ, K.M., J.M. Landwehr, and J. Keybl, 2001. Measurement of delta C-13 and delta O-18 isotopic ratios of $CaCO_3$ using a Thermoquest Finnigan GasBench II Delta Plus XL continuous flow isotope ratio mass spectrometer with application to Devils Hole /core DH-11 calcite. *U.S. Geological Survey Open-File Report 01-257*, 17.
- RICHARDS, D.A., S.H. Bottrell, R.A. Cliff, P.J. Rowe and K.D. Ströhle, 1998, U-Pb dating of a Quaternary-aged speleothem. *Geochimica Cosmochmica Acta, 62,* 3683-3688.
- RICHARDS, D.A. and J.A. Dorale, 2003. Uranium-series chronology and environmental applications of speleothems. *Reviews in Mineralogy and Geochemistry 52*, 407– 460.
- RISEBROBAKKEN, B.R., T. Dokken, O.H. Ottera, E. Jansen, Y. Gao and H. Drange, 2007. Inception of the Northern European ice sheet due to contrasting ocean and insolation forcing. *Quaternary Research 67*, 128–1135.
- RODWELL MJ and B. Hoskins, 1996. Monsoons and the dynamic of deserts. *Quarterly Journal of the Royal Meteorological Society 122*, 1385–1404.
- RODWELL, M.J., D.P. Rowell, and C.K. Folland, 1999. Oceanic forcing of the wintertime North Atlantic Oscillation and European climate. *Nature 398,* 320-323.
- ROHLING, E. J., A. Hayes, S. De Rijk, D. Kroon, W.J. Zachariasse, and D. Eisma, 1998b. Abrupt cold spells in the northwest Mediterranean. *Paleoceanography 13*, 316-322.
- ROHLING, E. J., P.A. Mayewski, A. Hayes, R.H. Abu-Zied and J.S.L. Casford, 2002a. Holocene atmosphere-ocean interactions: records from Greenland and the Aegean Sea. *Climate Dynamics 18*, 587-593.
- ROZANSKI, K., L. Araguas-Araguas and R. Gonfiantini, 1993. Isotopic patterns in modem global precipitation. In: P. K. Swart, K. C. Lohmann, J. McKenzie and S. Savin (eds). Climate Change in Continental Isotopic Records, 1-37. *Geophysical Monograph 78,* American Geophysical Union.
- RYAN, W.B.F., et al. 2003. Catastrophic Flooding of the Black Sea. Annual Review of

Earth & Planetary Science 31, 525-554.

- RYAN, W.B.F., Pitman III, W.C., et al., 1997. An abrupt drowning of the Black Sea shelf. Marine Geology, 138, 119–126
- SANCHEZ GONI, M.F., F. Eynaud, J.L. Turon and N.J. Shackleton., 1999. High resolution palynological record off the Iberian margin: Direct land-sea correlation for the Last Interglacial complex. *Earth and Planetary Science Letters171*, 123–137.
- SANCHEZ-GONI, M.F., J.L. Turon, F. Eynaud, N.J. Shackleton and O. Cayre, 2000. Direct land/sea correlation of the Eemian, and its comparison with the Holocene: a high-resolution palynological record off the Iberian margin. *In: Van Kolfschoten, Th. & Gibbard, P.L. (eds.): The Eemian – local sequences, global perspectives. Geologie en Mijnbouw / Netherlands Journal of Geosciences 79*, 345-354.
- SANCHEZ-GONI M.F., 2007. Introduction to climate and vegetation in Europe during MIS 5, *In: Sirocko F., Claussen M., Sanchez-Goni M.F. & Litt T. (eds.) The climate of past interglacials. Elsevier*, 197-205.
- SASOWSKY, I.D. and J. Mylroie, (eds.), 2004. Studies of Cave Sediments. *Kluwer, New York.*
- SCHWARCZ, H. 2007. Speleothems. *In (ed): ELIAS, S.A., Encyclopedia of quaternary science. Elsevier*, 290-300.
- SEELOS, K. and F. Sirocko, 2007. Abrupt cooling events at the very end of the Last Interglacial. *In: Sirocko, F., Claussen, M., Sanchez Goni, M.F., Litt, T. (Eds.), The Climate of Past Interglacials. Developments in Quaternary Science 7*, 207–222.
- SEIDENKRANTZ, M.S., K.L. Knudsen, P. Kristensen, 2000. Marine late Saalian to Eemian environments and climate variability in the Danish shelf area. *Geologie en Mijnbouw 79*, 335– 343.
- SELF, C.A. and C.A. Hill, 2003. How speleothems grow: An introduction to the ontogeny of cave minerals. *Journal of Cave and Karst Studies 65*, 130-151.
- SENSOY, S, 2003. Climate of Turkey, Web Site of Turkish State Meteorological Service (http://213.139.210.130/2003eng/general/climate/climateofturkey.htm, 23.10.2009).
- SENSOY, S., 2004. The mountains influence on Turkey climate. In: *BALWOIS: Conference on water observation and information system for decision support.* (http://www.balwois.com/balwois/administration/full_paper/ffp-1o-239.pdf, 23.10.2009).

- SHACKLETON, N.J., 1969. The last interglacial in the marine and terrestrial record. *Proceedings of the Royal Society of London B 174*, 135–154.
- SHACKLETON, N.J., M.F. Sanchez Goni, D. Pailler, Y. Lancelot, 2003. Marine isotope substage 5e and the Eemian interglacial. *Global and Planetary Change 36*,151–155.
- SIROCKO, K, Seelos, K. Schaber, B. Rein, F. Dreher, M. Diehi, R. Lenne, K. Jager and M. Krbetscher, 2005. A last Eemian aridity pulse in central Europe during the last glacial inception, *Nature 436*, 833–836.
- SMART, P.L. and D.A. Richards, 1992. Age estimates for the late Quaternary high sea-stands. *Quaternary Science Reviews 11*, 687-696.
- SOLOMINA, O., W. Haeberli, C. Kull and G. Wiles, 2008. Historical and Holocene glacier-climate variations: general concepts and overview. *Global and Planetary Change 60*, 1-9.
- SPÖTL, C., 2001/2002. Stabile Isotope in den Geowissenschaften I. Institut für Geologie und Paläontologie, Universität Innsbruck.
- SPÖTL, C., A. Mangini, N. Frank, R. Eichstädter, and S. J. Burns, 2002. Start of the last interglacial period at 135 ka: Evidence from a high Alpine speleothem. *Geology 30*, 815–818.
- SPROVIERI, R., E. Di Stefano, A. Incarbona and D.W. Oppo, 2006. Suborbital climate variability during Marine Isotopic Stage 5 in the central Mediterranean basin: evidence from calcareous plankton record. *Quaternary Science Reviews 25*, 2332–2342.
- STREIF, H.-J., 1991. Zum Ausmasz und Ablauf eustatischer Meeresspiegelschwankungen im stidlichen Nordseegebiet seit Beginn des Letzten Interglazials. *In: Frenzel, B. (ed.), Klimageschichtliche Probleme der letzten 130,000 Jahre. Gustav Fischer, Stuttgart,* 231-250.
- SWART, P. K., 1991. The oxygen and hydrogen isotopic composition of the Black Sea. *Deep Sea Res., 38,* suppl. 2, 761-772.
- TARASOV, P., E. Bezrukova, E. Karabanov, T. Nakagawa, M.Wagner, N. Kulagina, P. Letunova, A. Abzaeva, W. Granoszewski and F. Riedel, 2007. Vegetation and climate dynamics during the Holocene and Eemian interglacials derived from Lake Baikal pollen records. *Palaeogeogr. Palaeocl., 252*, 440–457.
- TURNER, 1982. Kinetic fractionation of carbon-13 during calcium carbonate precipitation. *Geochim. Cosmochim. Acta* ***46***, 1183–1191.

- TÜYSÜZ, O., 1999. Geology of the Cretaceous sedimentary basins of the Western Pontides. *Geological Journal 34*, 75-93.
- TZEDAKIS, P.C., 2003. Timing and duration of Last Interglacial conditions in Europe: a chronicle of a changing chronology. *Quaternary Science Reviews 22*, 763-768.
- TZEDAKIS, P.C., 2007. Last Interglacial pollen records from Europe. *In: Elias, S.A. (ed.) Encyclopaedia of Quaternary Science. Elsevier, Amsterdam*, 2597-2605.
- TZEDAKIS, P.C., M.R. Frogley and T.H.E. Heaton 2003. Last interglacial conditions in southern Europe: evidence from Ioannina, northwest Greece. *Global and Planetary Change 36*, 157-170.
- VAN ANDEL, T.H. and P. C. Tzedakis, 1996. Palaeolithic landscapes of Europe and environs, 150,000–25,000 years ago. *Quaternary Science Reviews 15*, 481–500.
- VAN CALSTEREN, P. and L. Thomas, 2006. Uranium-series dating applications in environmental science. *Earth-science Reviews 75*. 155-175.
- VELICHKO, A.A., E. Y. Novenko, E. M. Zelikson, T. Boettger and F. W. Junge, 2007. Comparative Analysis of Vegetation and Climate Changes during the Eemian Interglacial in Central and Eastern Europe. *In: Sirocco, F., Clause, M., Sanchez Gone, M. F. and Lit, The (eds.). The Climate of Past Interglacials, Developments in Quaternary Science 7. Springer*, 255-264.
- WAELBROECK, C., L. Labeyrie, E. Michel, J.C. Duplessy, J.F. McManus, K. Lambeck, E. Balbon, and M. Labracherie, 2002. Sea level and deep water temperature changes derived from benthonic foraminifera isotopic records. *Quaternary Science Reviews 21*, 5-305.
- WHITE WB, 2007. Cave sediments and paleoclimate. *Journal of cave and karst studies 69,* 76-93.
- WINOGRAD, I.J., J.M. Landwehr, K.R. Ludwig, T.B. Coplen and A.C. Riggs, 1997. Duration and structure of the past four interglaciations, *Quaternary Research 48*, 141–154.
- YANKO-HOMBACH, V., A.S. Gilbert and P. Dolukhanov, 2007. Controversy over the great flood hypotheses in the Black Sea in light of geological, paleontological, and archaeological evidence. *Quaternary International 167-168,* 91-113.
- YILMAZ Y, C. Genç, E.Yigitbas, M. Bozcu, K.Yilmaz, 1995. Geological evolution of the Late Mesozoic continental margin of north western Anatolia. *Tectonophysics 243*,

155–171.

- ZANS, V., 1936. Das letztinterglaziale Portlandia-Meer des Balticums. *Bulletin de la Commission G~ologique Finlande 115*, 231-250.
- ZELIKSON, E.M., O.K. Borisova, C.V. Kremenetsky, and A.A. Velichko, 1998. Phytomass and carbon storage during the Eemian optimum, late Weichselian maximum and Holocene optimum in Eastern Europe. *Global and Planetary Change, 16/17*, 181-195.
- ZUBAKOV VA, 1988. Climatostratigraphic scheme of the Black Sea Pleistocene and its correlation with the oxygen-isotope scale and glacial events. *Quat Res 29*, 1–24.

DATA REFERENCES

- BAR-MATTHEWS, M., et al., 2003. Soreq and Peqiin Caves, Israel Speleothem Stable Isotope Data, IGBP PAGES/World Data Center for Paleoclimatology Data Contribution Series #2003-061. NOAA/NGDC Paleoclimatology Program, Boulder CO, USA.
- CHAPMAN, M.R. and Shackleton, N.J., 1999. Late Quaternary North Atlantic IRD Data, IGBP PAGES/World Data Center A for Paleoclimatology Data Contribution Series #1999-053. NOAA/NGDC Paleoclimatology Program, Boulder CO, USA.
- FLEITMANN, D., et al. 2009. Sofular Cave Turkey, So-6 Stalagmite Stable Isotope Data.
- FLEITMANN, D., et al. 2009. Sofular Cave, Turkey 50KYr Stalagmite Stable Isotope Data. IGBP PAGES/World Data Center for Paleoclimatology Data Contribution Series # 2009-132. NOAA/NCDC Paleoclimatology Program, Boulder CO, USA.
- HEUSSER, L. and D. Oppo, 2004. ODP Site 1059 MIS 5 Pollen and Isotopic data, IGBP PAGES/World Data Center for Paleoclimatology Data Contribution Series # 2004-001. NOAA/NGDC Paleoclimatology Program, Boulder CO, USA.
- NORTH GREENLAND ICE CORE PROJECT MEMBERS, 2004. North Greenland Ice Core Project Oxygen Isotope Data. IGBP PAGES/World Data Center for Paleoclimatology Data Contribution Series # 2004-059. NOAA/NGDC Paleoclimatology Program, Boulder CO, USA.
- SPROVIERI, R. et al. 2006. Central Mediterranean Last Interglacial Planktonic Foraminifera Data. IGBP PAGES/World Data Center for Paleoclimatology Data Contribution Series # 2006-091. NOAA/NCDC Paleoclimatology Program, Boulder CO, USA.
- WAELBROECK, C., L. Labeyrie, E. Michel, J.C. Duplessy, J.F. McManus, K. Lambeck, E. Balbon, and M. Labracherie, 2002. Sea level and deep water temperature changes derived from benthonic foraminifera isotopic records. *Quaternary Science Reviews 21*, 5-305.

Declaration

under Art. 28 Para. 2 RSL 05

Last, first name: Zumbühl, Angela

Matriculation number: 05-124-417

Programme: Master in Climate Sciences

Thesis title: History of the Black Sea recorded in stalagmites from Northern Turkey

Thesis supervisors: Supervisor: Prof. Dr. Dominik Fleitmann

Co-Supervisor: Prof. Dr. Markus Leuenberger

I hereby declare that this submission is my own work and that, to the best of my knowledge and belief, it contains no material previously published or written by another person, except where due acknowledgement has been made in the text. In accordance with academic rules and ethical conduct, I have fully cited and referenced all material and results that are not original to this work. I am well aware of the fact that, on the basis of Article 36 Paragraph 1 Letter o of the University Law of 5 September 1996, the Senate is entitled to deny the title awarded on the basis of this work if proven otherwise.

.....

Place, date

.....

Signature